

COMPARISON OF EPB-TUNNEL BORING MACHINE PERFORMANCE IN
COHESIVE AND FRICTIONAL SOILS

by

Melek Merve Benli

B.S., Civil Engineering, İstanbul University, 2012

Submitted to the Institute for Graduate Studies in
Science and Engineering in partial fulfillment of
the requirements for the degree of
Master of Science

Graduate Program in Civil Engineering
Boğaziçi University

2019

COMPARISON OF EPB-TUNNEL BORING MACHINE PERFORMANCE IN
COHESIVE AND FRICTIONAL SOILS

APPROVED BY:

Prof. Erol Güler
(Thesis Supervisor)

Prof. Cemal Balcı

Prof. Ayşe Edinçliler

DATE OF APPROVAL: 20.06.2019

ACKNOWLEDGEMENTS

I would like to express my most sincere gratitude to my supervisor, Prof. Erol Güler for his continuous support and generous guidance throughout my study.

Also, I extend my sincere thanks to to the members of my Master's thesis examination committee: Prof. Cemal Balcı and Prof. Ayşe Edinçliler for their kind and supportive attitude towards me and valuable comments on this thesis.

I would like to express my deep appreciation and thanks for Mr. Doğan Talu and Mr. Süleyman Ergut for providing TBM data and permitting job-site visits for the thesis. Their generous support was an immense asset in accomplishing this study. Moreover, I also want to thank Mr. Onur Kansu and Azis Shaban for providing TBM data.

Last but not least, I want to thank my family for their continuous support and encouragement throughout my study.

ABSTRACT

COMPARISON OF EPB-TUNNEL BORING MACHINE PERFORMANCE IN COHESIVE AND FRICTIONAL SOILS

Prediction of EPB (Earth Pressure Balance) TBM's performance is a significant issue in tunnel projects in terms of low-cost and target schedule. This study was conducted based on the measurements made in the Sofia Metro Line-3 tunnel in order to determine the effects of the soil type (cohesive and frictional) affecting the EPB TBM excavation performance. The investigated parameters were: cutterhead torque, EPB TBM thrust force, specific energy and instantaneous cutting rate. The studied tunnel section is divided into three zones with respect to geotechnical parameters such as grain size analysis, Atterberg limits and consistency behavior. Data analysis was performed by linking the cutterhead torque, TBM thrust force, instantaneous cutting rate and specific energy with the geotechnical properties of high plasticity clay, low plasticity clay and medium-grained sand. TBM performance analysis reveal the correlation between the operation parameters of the machine and soil type, and thus, main incidents that make an effect on the performance of the machine are determined. Analysis is critical in terms of the information backlog required for such projects that shall be implemented in the future.

ÖZET

KOHEZİF VE SÜRTÜNME Lİ ZEMİNLERDE EPB TÜNEL AÇMA MAKİNESİNİN PERFORMANSININ KARŞILAŞTIRILMASI

Tünel projelerinde düşük maliyeti yakalama ve hedeflenen programa ulaşmada EPB TBM'in performans tahmini büyük önem taşımaktadır. Bu tez çalışmasında, EPB TBM'in kazı performansının zemin tipine (kohezyonlu ve sürtünmeli) etkisi Sofya Metro Hat-3 Projesi'nde yapılan tünel ölçümleri baz alınarak incelenmiştir. İncelenen parametreler: kesici kafa torku, EPB TBM itme kuvveti, spesifik enerji ve net kazı hızıdır. İncelenen tünel kesimi, dane boyu analizi, Atterberg limiti ve kıvam limiti gibi geoteknik parametreler bakımından üç bölgeye ayrılmıştır. Data analizi kesici kafa torkunu, TBM itme kuvvetini, net kazı hızını ve spesifik enerjiyi, yüksek plastisiteli kilin, düşük plastisiteli kilin ve orta daneli kumun geoteknik özellikleri ile birleştirerek gerçekleştirilmiştir. TBM performans analizi, makinenin işletme parametreleri ve zemin tipi arasındaki korelasyonu ortaya çıkarmakta, ve böylece makine performansına etki eden ama etkenler belirlenmektedir. Analiz, gelecekte gerçekleşecek olan bu tarz projelerde gerekli bilgi birikimini sağlamak bakımından önemlidir.

TABLE OF CONTENTS

ACKNOWLEDGEMENTS	iii
ABSTRACT	iv
ÖZET	v
LIST OF FIGURES	x
LIST OF TABLES	xvi
LIST OF SYMBOLS	xviii
LIST OF ACRONYMS/ABBREVIATIONS	xix
1. INTRODUCTION	1
1.1. Objective of the Thesis	2
2. LITERATURE REVIEW	3
3. GENERAL INFORMATION ABOUT TUNNEL BORING MACHINES	5
3.1. History of TBMs	5
3.2. TBM Types	6
3.2.1. Hard Rock TBMs	6
3.2.1.1. Open-Type TBMs	7
3.2.1.2. Single-Shield TBMs	7
3.2.1.3. Double-Shield TBMs	7
3.2.1.4. Single-Shield TBMs Working in Open and Closed Modes (EPB)	8
3.2.2. Soft Ground TBMs	9
3.2.2.1. Slurry Pressure Balance (SPB) TBMs	10
3.2.2.2. Earth Pressure Balance (EPB) TBMs	11
3.2.3. The Principle of Earth Pressure Balance TBM Tunneling	12
4. FACTORS AFFECTING TBM PERFORMANCE	14
4.1. Geotechnical Properties of the Ground	14
4.1.1. Consistency (Atterberg) Limits	14
4.1.2. Permeability	16
4.1.3. Grain Size Distribution	16
4.1.4. Standard Penetration Test (SPT)	19

4.1.5.	Unit Weight	20
4.1.6.	Cohesion and Internal Friction Angle	20
4.2.	Machine Design Parameters	22
4.3.	Machine Operational Parameters	23
4.3.1.	Thrust Force	23
4.3.2.	Torque	25
4.3.3.	Power	25
4.3.4.	RPM	25
4.3.5.	Specific Energy	26
4.4.	Soil Conditioning	26
4.5.	Applied Earth Pressure	29
5.	DESCRIPTION OF THE SOFIA METRO LINE-3 PROJECT AND TUNNEL GEOLOGY	31
5.1.	Project Description	31
5.2.	Geology of the Tunnel Alignment	32
5.2.1.	Layer 4.1: Multicolored Silty Clay (Pliocene)	33
5.2.2.	Layer 4.1a: Multicolored silty clay, structured (Pliocene)	33
5.2.3.	Layer 4.2: Multicolored Silty Clay (Pliocene)	34
5.2.4.	Layer 4.3: Yellow-Brown Silty Sedium-Grained Sands	34
5.2.5.	Layer 4.4: Yellow-Brown Silty Coarse-Grained Sands	34
5.2.6.	Layer 5.1: Grey Silty Clay (Pliocene)	34
5.2.7.	Layer 5.1a: Grey Silty Clay/Clayey Silt, Structured (Pliocene)	35
5.2.8.	Layer 5.2: Grey Silty Fine-Grained Sands	35
5.2.9.	Layer 5.3: Grey Silty Medium-Grained Sands	35
5.2.10.	Layer 5.4: Grey Silty Coarse-Grained Sands	35
5.2.11.	From the TBM Launching Shaft to the Station MC14	36
5.2.11.1.	Geological Description	36
5.2.12.	From the Station MC14 to the Station MC12	37
5.2.12.1.	Geological Description	37
5.2.13.	From the Station MC12 to the Station MC11	37
5.2.13.1.	Geological Description	37
5.2.14.	From the Station MC11 to the Station MC10	38

5.2.14.1. Geological Description	38
5.2.15. From the Station MC10 to the Station MC09	39
5.2.15.1. Geological Description	39
5.2.16. From the Station MC09 to the Station MC08	40
5.2.16.1. Geological Description	40
5.2.17. From the Station MC08 to the Retrieval Shaft	41
5.2.17.1. Geological Description	41
5.3. TBMs Technical Details	42
5.3.1. Main Properties	42
5.3.2. Cutterhead	43
5.3.3. Shield	46
6. ASSESSMENT OF TBM'S PERFORMANCE PARAMETERS	50
6.1. Effects of Observed Parameters on Performance	54
6.1.1. Cutterhead Torque Values During TBM Operation	54
6.1.2. Thrust Force Values During TBM Operation	57
6.1.3. Specific Energy Values During TBM Operation	59
6.1.4. Instantaneous Cutting Rate Values During TBM Operation	61
6.1.5. Applied Earth Pressure Values During TBM Operation	63
6.2. Comparison of Calculated Performance Parameters	64
6.2.1. Comparison of the Torque and Thrust	65
6.2.2. Comparison of the Torque and Penetration	66
6.2.3. Comparison of the Thrust and Penetration	68
6.2.4. Comparison of the Penetration and Specific Energy	69
6.2.5. Comparison of the Consistency Index and Cutterhead Torque	71
6.2.6. Comparison of Instantaneous Cutting Rate and Plastic Limit	71
6.3. Variation of Performance Parameters Under Different Earth Pressures	72
6.3.1. Effects of Observed Parameters Under (0.0-0.5) Bar Earth Pressure	72
6.3.2. Effects of Observed Parameters Under (0.5-1.0) Bar Earth Pressure	73
6.3.3. Effects of Observed Parameters Under (1.0-1.5) Bar Earth Pressure	75
6.3.4. Effects of Observed Parameters Under (1.5-2.0) Bar Earth Pressure	76
6.3.5. Effects of Observed Parameters Under (2.0-3.0) Bar Earth Pressure	78
6.4. Assessment of TBM Advance Rates and Downtime Analysis	79

6.4.1. Achieved Advance Rates 79

6.4.2. Assessment of TBM Performance Measures and Downtime-Breakdown
Analysis 80

7. CONCLUSIONS AND RECOMMENDATIONS 87

REFERENCES 91



LIST OF FIGURES

Figure 3.1.	First tunnel boring machine by Wilson (Maidl <i>et al.</i> , 2008).	6
Figure 3.2.	General overview of EPB TBM.	11
Figure 3.3.	EPB operating principle - Balanced Pressure (Barla and Pelizza, 2000).	13
Figure 4.1.	Consistency Limits of Fine-Grained Soils (Das, 2009).	14
Figure 4.2.	Consistency Selection criteria of grain size for earth pressure balance and slurry tunnel boring (Bilgin <i>et al.</i> , 2014).	17
Figure 4.3.	Attraction of dipolar molecules in diffuse double layer (Das, 2009).	21
Figure 4.4.	Diffuse double layer of Clay (Das, 2009).	21
Figure 4.5.	Diagram of the structures of (a) kaolinite; (b) illite; (c) montmorillonite (Das, 2009).	22
Figure 4.6.	Sketch of a typical disk cutter used in full-scale linear cutting machine (Bilgin <i>et al.</i> , 2014)	24
Figure 4.7.	Application ranges of the EPB shield (Thewes, 2007).	27
Figure 4.8.	Working Modes of EPB TBMs (Bilgin <i>et al.</i> , 2014).	30
Figure 5.1.	Sofia Metro Line-3 Plan View (TC1527-R05-r0 Report on Recommended EPB Pressure).	31

Figure 5.2.	Sofia Metro Line-3 Geometrical Profile (TC1527-R05-r0 Report on Recommended EPB Pressure).	32
Figure 5.3.	Geological profile along the alignment (From the TBM launching shaft to the Station MC14).	36
Figure 5.4.	Geological profile along the alignment (From Station MC14 to the Station MC12).	37
Figure 5.5.	Geological profile along the alignment (From Station MC12 to the Station MC11).	38
Figure 5.6.	Geological profile along the alignment (From Station MC11 to the Station MC10).	39
Figure 5.7.	Geological profile along the alignment (From Station MC10 to the Station MC09).	40
Figure 5.8.	Geological profile along the alignment (From Station MC09 to the Station MC08).	41
Figure 5.9.	Geological profile along the alignment (From Station MC08 to the Retrieval shaft).	42
Figure 5.10.	EPB TBM Cutterhead (S1014-EPB TBM Shield Drawing 4873-006-000-00).	44
Figure 5.11.	EPB TBM Cutterhead used in the Project.	45
Figure 5.12.	Cutterhead during TBM Disassembly.	45
Figure 5.13.	EPB TBM Shield (S-1014, Drawing 4873-000-001-00).	47

Figure 5.14.	EPB TBM Thrust Cylinders (S-1014, Drawing 4873-000-001-00).	47
Figure 5.15.	Tailskin Wire Brush Seal (Herrenknecht AG, Operating Manuel S-1014).	48
Figure 5.16.	Muck System at (EPB Shield Herrenknecht AG, Operating Manuel S-1014).	49
Figure 6.1.	A sample sheet of performance data from TBM data logger (Ring No: 2.070).	51
Figure 6.2.	Plasticity Chart and Atterberg Limits (NAVFAC, 1986a).	53
Figure 6.3.	Classification diagram for critical consistency changes regarding clogging and dispersing (Hollmann and Thewes, 2013).	54
Figure 6.4.	The Mean Cutterhead Torque values along the alignment.	55
Figure 6.5.	Cutterhead Torque Change in High Plasticity Clay Soil.	55
Figure 6.6.	Cutterhead Torque Change in Medium-grained Sand Soil.	56
Figure 6.7.	Cutterhead Torque Change in Low Plasticity Clay Soil.	56
Figure 6.8.	The Mean Thrust Force values along the alignment.	57
Figure 6.9.	Thrust Force Change in High Plasticity Clay Soil.	58
Figure 6.10.	Thrust Force Change in Medium-grained Sand Soil.	58
Figure 6.11.	Thrust Force Change in Low Plasticity Clay Soil.	59

Figure 6.12. The Mean Specific Energy values along the alignment. 60

Figure 6.13. Specific Energy Change in High Plasticity Clay Soil. 60

Figure 6.14. Specific Energy Change in Medium-grained Sand Soil. 61

Figure 6.15. Specific Energy Change in Low Plasticity Clay Soil. 61

Figure 6.16. The Mean Instantaneous Cutting Rate values along the alignment. 62

Figure 6.17. Instantaneous Cutting Rate Change in High Plasticity Clay Soil. . 62

Figure 6.18. Instantaneous Cutting Rate Change in Medium-grained Sand Soil. 63

Figure 6.19. Instantaneous Cutting Rate Change in Low Plasticity Clay Soil. . 63

Figure 6.20. Face pressures along the alignment. 64

Figure 6.21. Mean Overburden and Mean Water Pressure along the alignment. 64

Figure 6.22. Relationship between Torque and Thrust values in High plasticity
clay. 65

Figure 6.23. Relationship between Torque and Thrust values in Medium-grained
sand. 66

Figure 6.24. Relationship between Torque and Thrust values in Low plasticity
clay. 66

Figure 6.25. Relationship between Torque and Penetration values in High plas-
ticity clay. 67

Figure 6.26. Relationship between Torque and Penetration values in Medium-grained sand.	67
Figure 6.27. Relationship between Torque and Penetration values in Low plasticity clay.	68
Figure 6.28. Relationship between Thrust Force and Penetration values in High plasticity clay.	68
Figure 6.29. Relationship between Thrust Force and Penetration values in Medium-grained sand.	69
Figure 6.30. Relationship between Thrust Force and Penetration values in Low plasticity clay.	69
Figure 6.31. Relationship between Penetration and Specific Energy values in High plasticity clay.	70
Figure 6.32. Relationship between Penetration and Specific Energy values in Medium-grained sand.	70
Figure 6.33. Relationship between Penetration and Specific Energy values in Low plasticity clay.	70
Figure 6.34. Relationship between Consistency Index and Cutterhead Torque.	71
Figure 6.35. Relationship between Instantaneous Cutting Rate and Plastic Limit.	71
Figure 6.36. Foam Installation along the (0.0-0.5) Bar Pressure Section	73
Figure 6.37. Foam Installation along the (0.5-1.0) Bar Pressure Section.	74

Figure 6.38. Foam Installation along the (1.0-1.5) Bar Pressure Section.	76
Figure 6.39. Foam Installation along the (1.5-2.0) Bar Pressure Section.	77
Figure 6.40. Foam Installation along the (2.0-3.0) Bar Pressure Section.	79
Figure 6.41. Daily Advance Rate of EPB TBM.	80
Figure 6.42. Distribution of Total Amount of TBM Working Time.	84
Figure 6.43. Distribution of Time for Downtimes and Breakdowns.	84
Figure 6.44. Distribution of Planned Downtimes.	85
Figure 6.45. Distribution of Unplanned Downtimes.	86

LIST OF TABLES

Table 3.1.	General Classification of Soft Ground TBMs (Bilgin, <i>et al.</i> , 2014).	10
Table 4.1.	Unified Soil Classification System (USCS) (American Society for Testing and Materials, 1985).	17
Table 4.2.	(Unified Soil Classification System (USCS) (American Society for Testing and Materials, 1985).	18
Table 4.3.	Relationship between SPT and Soil Density/Consistency (Meyerhof, 1965).	19
Table 4.4.	Required parameters of the earth muck to be used as the support medium (Thewes and Budach, 2010).	29
Table 5.1.	Technical details of EPB TBM.	43
Table 5.2.	Dimensions of the steel construction cutterhead.	44
Table 5.3.	Dimensions of the excavation tools.	46
Table 5.4.	Dimensions of steel construction shield.	46
Table 5.5.	Numbers of cylinders.	47
Table 5.6.	Dimensions of screw conveyor.	49
Table 6.1.	Geotechnical Parameters for Units Forming the Tunnel Alignment.	52
Table 6.2.	Geological Units Forming the Tunnel Alignment.	53

Table 6.3.	Interpreting the Size of a Correlation Coefficient.	65
Table 6.4.	Variations in EPB TBM operational parameters during excavation of (0.0-0.5) bar earth pressure section.	72
Table 6.5.	Variations in EPB TBM operational parameters during excavation of (0.5-1.0) bar earth pressure section.	74
Table 6.6.	Variations in EPB TBM operational parameters during excavation of (1.0-1.5) bar earth pressure section.	75
Table 6.7.	Variations in EPB TBM operational parameters during excavation of (1.5-2.0) bar earth pressure section	77
Table 6.8.	Variations in EPB TBM operational parameters during excavation of (2.0-3.0) bar earth pressure section.	79
Table 6.9.	Average Advance Speed Values Depending on Soil Types	80
Table 6.10.	Unplanned TBM downtimes.	83
Table 6.11.	Planned TBM downtimes.	84
Table 7.1.	Main Operational Values Along the Tunnel Alignment.	88
Table 7.2.	Machine Utilization.	90

LIST OF SYMBOLS

$c(\%)$	Concentration of the foaming agent
F	Total thrust
IC	Consistency index
IP	Plasticity index
k	Permeability
P	Power
SE	Specific energy
T	Torque
W	Natural water content
WL	Liquid limit
WP	Plastic limit

LIST OF ACRONYMS/ABBREVIATIONS

EPB	Earth Pressure Balance
FER	Foam Expansion Ratio
FIR	Foam Injection Ratio
ICR	Instantaneous Cutting Rate
RPM	Rotation Per Minute
SPB	Slurry Pressure Balance
SPT	Standard Penetration Test
TBM	Tunnel Boring Machine
USCS	Unified Soil Classification System

1. INTRODUCTION

Due to the economic development and accelerated population growth in urban regions, faster ways of transport are needed. In order to keep pace with demand and satisfy infrastructural requirements new and larger tunnels are constructed.

Tunnel boring machines are used to replace standard tunnel driving mining methods. Since most tunnel constructions in urban regions are in soft ground, soft ground tunneling studies becomes critical. Earth pressure balance tunnel boring machines (EPB TBMs) are commonly used in soft ground urban tunneling owing to benefits such as minimal environmental effects and greater advance rates compared to conventional tunneling. In addition, they cause minimal ground disturbance, which is very convenient for the above ground structures and produces uniform muck that helps transport excavated material. This makes them appropriate for use in highly urbanized regions, even when it is necessary to cross ground units with changing strength characteristics.

Oftentimes construction management's efficiency is criticized for contractual issues that occur during excavation. The main cause of such issues can be traced back to original planning in most cases. Due to this reason, realistic performance predictions play a pivotal role in terms of effectiveness, low-cost and target schedule.

For this purpose, the performance parameters of the earth pressure balance TBM (e.g. advance rate, cutterhead torque and thrust) should be anticipated for the specified geological circumstances. Using geotechnical properties of the specified soil types, it is possible to describe the scientific relationships between soil parameters and EPB TBM performance.

1.1. Objective of the Thesis

This thesis' aim is to analyze the performance of an earth pressure balance tunnel boring machine (EPB TBM) tunnel construction in cohesive and frictional soils. A case study with data from Sofia Metro Line-3 is employed to develop a methodology of EPB TBM between operational parameters and geotechnical properties. Several parameters that influence TBM operations in soft ground are identified, analyzed and the interactions between soil type and operational parameters are investigated statistically.

To make a statistical analysis of the TBMs operational parameters, a database is created which includes cutterhead torque, thrust force, power, specific energy, advance speed, applied earth pressure, instantaneous cutting rate and geology for each ring through the tunnel alignment.

According to the geological profile, the studied tunnel alignment is grouped in three different soil types, which includes high plasticity clay, low plasticity clay and medium grained sand.

The database created for the analysis includes total number of 3996 rings. The relationships between soil type and EPB-TBM operation parameters (especially thrust force, cutterhead torque, instantaneous cutting rate and specific energy), were investigated in details and some statistical evaluations were made.

2. LITERATURE REVIEW

Based on an extensive literature research, there are restricted studies focused on prediction of EPB TBM performance, especially for soft ground excavations.

Spagnoli *et al.* (2011) defined soil cohesion as is the force that holds together molecules or like particles within a soil and investigated the clogging properties of excavated materials. According to empirical models developed, clays do not responds in the same way. While the Difuse Double Layer model does not work with kaolinite, smectite demonstrates powerful variety in chemical-mechanical characteristics. Mineralogy of clay, particle size of the excavated material and the consistency of the material affects the propensity to clog. It was concluded that, one of the most important method to understand the clogging characteristics of excavated materials is the cone pull-out test.

German Committee for Underground Construction DAUB (2010), established charts based on soil properties such as the fine grain fraction, consistency, permeability and swelling behaviors for EPB TBM application ranges. In addition, German Committee for Underground Construction DAUB (2010) enables with the selection of available techniques of calculation based on the ground conditions expected.

The issues of adhesion and clogging that happened during fine cohesive soil excavation were investigated by Schlick (1989), Thewes (1999, 2004), Thewes and Burger (2004), Ball *et al.* (2009), Thewes and Budach (2010), Feinendegen *et al.* (2011), Zumsteg and Puzrin (2012), Holman and Thewes (2012 and 2013), and Zumsteg *et al.* (2013) they concluded that this problem could be decreased by using of soil conditioning chemicals. The density, water permeability, compressibility and flow behavior were evaluated for soil-foam mixture by Thewes and Budach (2010). It was concluded that, the support medium properties rely heavily on soil's geotechnical characteristics. Zumsteg and Puzrin (2012) isvestigated that, different clay mixture investigations obviously demonstrate the significance of clay mineral type and the impact of added chemicals

on material strength and stickiness.

Herrenknecht and Maidl (1995), investigated the use of soil conditioning in Valencia Metro Line 5 project. They stated that use of soil conditioning decreased the cutterhead and screw conveyor torque about 20%.

By investigating the effects of clogging and foam injection ratio on the EPB TBM performance, Avunduk and Copur (2019) concluded that increasing foam injection ratio did not improve the penetration rate, even if the muck transport issues and stoppages owing to the cleaning of the blocked cutterhead were decreased. According to studies, the foam injection ratio increased in parallel to clogging potential and the average foam injection ratio were evaluated three times greater for high clogging zone than for the low clogging zone.

The high fluctuation of the soil type values is linked to the variation in the geotechnical characteristics of the specified soil section and may also be related to certain operational procedures.

Considering the effect of operational parameters on performance, Avunduk and Copur (2017) examined the soil properties on the excavation performance of an EPB TBM operating in open mode, without face pressure and without foaming application. In terms of geological and geotechnical circumstances, the tunnel alignment was split into three general sections. For high plasticity clays, the cutterhead torque and specific energy were greater and net cutting rate and thrust values were lower. It was stated that the mean field-specific energy values increased with an increasing consistency index and that the cutterhead torque increased in parallel with vane shear strength. Wang *et al.* (2012) proposed a new model in order to enhance the accuracy of the cutterhead torque calculation. It is stated that earth pressure plays a decisive role in determining the cutterhead torque. When the earth pressure increases by 1%, the cutterhead torque would increase by 0,33%. It was concluded that, the thrust force is not an influencing factor of cutterhead torque although they have similar curve shapes, and both of them are determined by numerous excavating parameters.

3. GENERAL INFORMATION ABOUT TUNNEL BORING MACHINES

3.1. History of TBMs

Since ancient times people have excavated the land to remove mines and stones. Excavation activity was always very risky due to the risk of collapse. Depending on the nature of the soil excavation, whether it is hard, loose or water saturated, this is an unchanging risk.

Tunneling evolved rapidly with the construction of the railway network during industrialization at the beginning of the 19th century. In hard rock, this was by drilling and blasting. The first phase in the growth of tunneling mechanization was therefore the development of efficient drills for drilling holes for the explosive. There were also attempts to excavate the rock completely by machine (Maidl *et al.*, 2008).

As early as 1851, American Charles Wilson developed and manufacture a tunnel boring machine, which he first patented for the first time in 1856 (Figure 3.2). The machine had all the features of a modern TBM and can therefore be categorized as the first machine, which worked by boring the tunnel (Maidl *et al.*, 2008).

In 1963, the Japanese firm Sato Kogyo Company Ltd. established earth-pressure balance shields for the first time. After extensive laboratory and field research, Ishikawajima - Harima Heavy Industries (IHI) manufactured a unit in 1966 (Stack, 1995).

In addition to the growth of the shielded TBM, the manufacturers of open gripper TBMs started to investigate opportunities for enhancing their machines so that any needed lining could be installed earlier. The current state of development with large diameter TBMs is the installation of lining components immediately behind the boring shield or partial areas of the shield and the systematic installation of rock anchors (Maidl *et al.*, 2008).

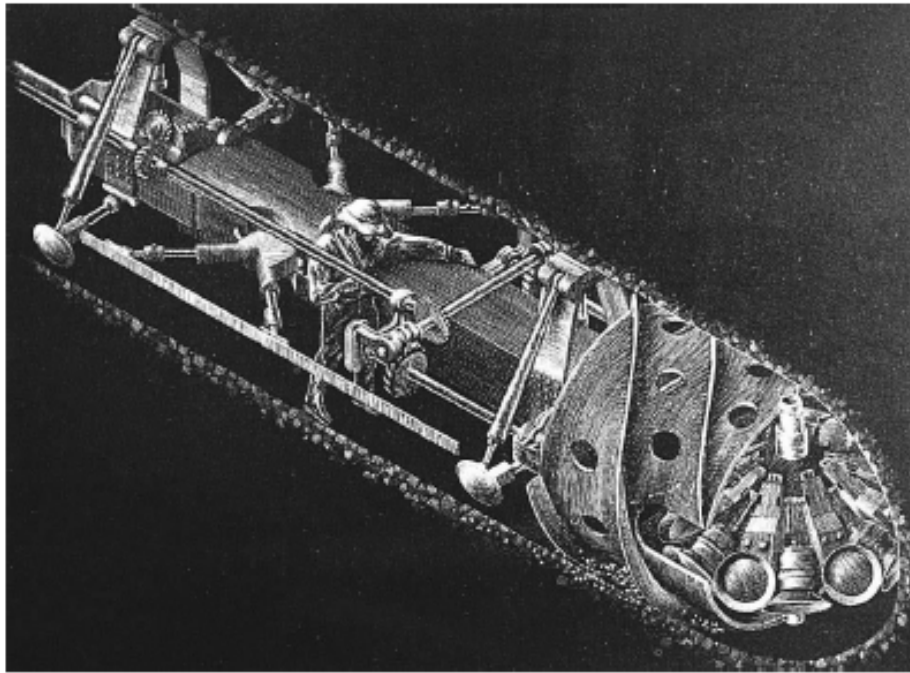


Figure 3.1. First tunnel boring machine by Wilson (Maidl *et al.*, 2008).

Today's TBMs have advanced technologies for controlling and recording the parameters of excavation. In addition, advanced guidance systems are also available to minimize deviation from the route.

3.2. TBM Types

TBM types may be categorized into two main groups: hard rock TBMs and soft ground TBMs.

3.2.1. Hard Rock TBMs

Hard rock TBMs may be classified as open type (open gripper, Kelly beam, or main beam), single shield, and double shield, with TBMs working in open and closed modes (EPB) in some special cases.

3.2.1.1. Open-Type TBMs. Open-type TBMs are particularly appropriate for competent rock formations or geological formations with having little amount of discontinuities and water ingress.

The tunneling performance of open-type TBM relies mainly on the moment it takes to install rock support systems via ring erectors, rock bolts using drilling devices, meshes, shotcrete, steel arch, or any type of transfer support.

3.2.1.2. Single-Shield TBMs. Single-shield TBMs are used in hard rocks where geological discontinuities are common. Important parts of the TBM include shield, hydraulic thrust cylinders, cutterhead. The TBM is advanced by hydraulic thrust cylinders pushing the cutterhead toward the tunnel face. The transfer of high thrust forces through the rolling disk cutters creates fractures in the rock, causing chips to break away from the face. Only segment lining can be used with single-shield TBMs as tunnel support. The shield is supported by hydraulic thrust cylinders on the last segment ring installed. (Bilgin, *et al.*, 2014)

3.2.1.3. Double-Shield TBMs. This type of machine is suitable in hard rock where geological fault and shear zones occur for boring long tunnels. A double-shield TBM consists of a rotating cutterhead, a sliding telescopic shield within the larger outer shield, a gripper shield, and a tail shield.

In this type of TBMs it is possible to use the second shield the gripper assembly on the tail side. It combines the features of gripper and single shield TBM and enables fast excavation even in varying rock formations. In poor ground condition, it works as a single shield machine. When in rocks, grippers are used for forward movement, so segment can be simultaneously installed while excavating. The advantages of this type of TBMs are the flexibility for varying grounds high advancement rates. The increase depends on operation, possibility to have different support measures, e.g., segmental lining, and bolts- shotcrete, possibility of ground treatment and/or probing through the gap between shields.

3.2.1.4. Single-Shield TBMs Working in Open and Closed Modes (EPB). Earth pressure balance tunnel boring machines are TBMs that are mainly used for the excavation of tunnels in soft ground beneath the water table to reduce or prevent surface settlements by applying pressure to the excavation face. However, in some cases where unstable tunnel facing conditions exist only in some parts of the tunnel route, they are designed to work as a single shield in the area where the rock is competent in closed (EPB) mode or in open mode.

The main components of a typical EPB TBM are the cutterhead, the working or excavation chamber, the pressure wall or bulkhead, the screw conveyor, the thrust arms or thrust jacks, the tail sealant or tail brushes mounted on the inside of the tail end of the shield, the concrete segments, and the annulus grout.

An EPB TBM generally has three operation modes: excavation mode, ring build mode, and waiting mode. During the excavation mode, the hydraulic thrust jacks of the EPB TBM push the machine off the installed concrete segments and press the rotating cutterhead, which is equipped with various cutting tools, against the in-situ soil face to scrap off soil. The excavated soil moves through openings in the cutterhead and is collected in the excavation chamber behind the cutterhead. The excavation chamber is kept filled with the excavated soil and pressurized to support the face by counteracting earth and water pressures. The necessary face support pressure is achieved through a combination of excavated soil mass and the thrust applied against through the bulkhead. Furthermore, the mass of soil in the chamber can be regulated by the controlling the intake and outflow of material, through the cutterhead and screw conveyor, respectively. The resulting pressure is normally measured by several earth pressure sensors installed on the bulkhead and kept above a calculated target pressure. A screw conveyor transports the soil from the excavation chamber to a conveyor belt or to muck cars, which take the material out of the tunnel. The pressure within the chamber is controlled by changing the discharge speed of the screw conveyor. While the TBM advances forward, grout is injected out of the tail of the shield into the annulus between the concrete segments and the ground. The annulus between the concrete segments and the surrounding ground is filled with grout to prevent settlements. Tail

shield brushes are installed on the interior of the tail shield and filled with sealant grease to prevent the inflow of grout through the gap between shield and segments into the shield. During the ring building mode, when the TBM is not advancing forward, concrete segments are installed within the tail shield of the machine and form the permanent lining of the tunnel. Waiting mode is enabled whenever excavation or ring building mode is not enabled.

3.2.2. Soft Ground TBMs

Table 3.1 presents a general classification of TBMs used for excavation of soft grounds based on face support types, muck haulage systems, and working modes. Earth pressure balance (EPB) and slurry pressure balance (SPB) are the most commonly used soft ground TBMs. These two types of TBM can function in closed and open working modes to minimize the stability issues.

Earth pressure balance (EPB) and slurry pressure balance (SPB) are the most commonly used soft ground TBMs. These two kinds of TBM can function in closed (with face pressure in unstable grounds) and open (without face pressure in stable grounds) working modes to minimize the stability problems.

Table 3.1. General Classification of Soft Ground TBMs (Bilgin, *et al.*, 2014).

Machine Type	Face Support	Muck Haulage	Mode
Earth pressure balance TBMs (EPB TBMs, auger TBMs)	Pressured muck + one or more of water, foam, polymer, bentonite (processed muck)	Dry muck haulage (rail, conveyor belt, truck)	Closed, open
Slurry pressure balance TBMs (SPB TBMs, hydrosields, bentonite shields)	Pressured water or water + bentonite (or + polymers)	Hydraulic muck haulage (steel pipe)	Closed, open
Compressed air shields (mostly partial face excavation)	Pressured air (against only water ingress, not against earth pressure)	Dry muck haulage (rail, conveyor belt, truck)	Closed, open
Polysields (Mixshields)	Combination of two or more of the above methods	Combined muck haulage (dry and/ or hydraulic)	Closed, open
Blind (extrusion) shields, shields with pressure relieving gate	Mechanical plates	Dry muck haulage (rail, conveyor belt, truck)	Partly open

3.2.2.1. Slurry Pressure Balance (SPB) TBMs. By a special bentonite-water mixture in slurry pressure balance (SPB) TBMs can readily counterbalance the earth pressures in unstable/loose grounds with or without groundwater. For effective pressurization, the pressure chamber should be filled with slurry and muck combination.

In order to ensure the continuity of the system, it is necessary to extract permanently by means of hydraulic pumps (hydraulic transport) the mud loaded with cuttings which is replaced simultaneously by a new sludge flow. A crusher is often used to reduce the size of the cuttings to dimensions compatible with hydraulic trans-

port.

SPB TBMs can be used in open mode without providing any face pressure in stable ground and hard rock conditions.

They are normally used for excavation of gravel, coarse and medium size sands, and silty and/or clayey sands having hydraulic conductivity between 10^{-8} and 10^{-2} m/s (Efnarc 2005).

3.2.2.2. Earth Pressure Balance (EPB) TBMs. The earth/ground and water pressures in unstable (non-self-supporting) cohesive soils, with or without ground water, is counterbalanced with the face pressure given by thrust cylinders to the excavated material (muck, earth) filled fully on the chamber and processed usually by different foaming agents and polymers in earth pressure balance (EPB) TBMs. (Bilgin *et al.*, 2014) The screw conveyor rotational speed and the opening of the screw conveyor discharging gate can be adjusted to control the pressure of the face (excavation chamber). This avoids excessive muck removal leading to instability and settlement, and over pressures leading to compression and heaving of the soil. The screw conveyor's muck discharge rate and rotational speed should be equal to the machine's advance rate, adjusted by thrust cylinders, for adequate face pressure control without stability issues.

The general overview of EPB TBM is showed in Figure 3.3.

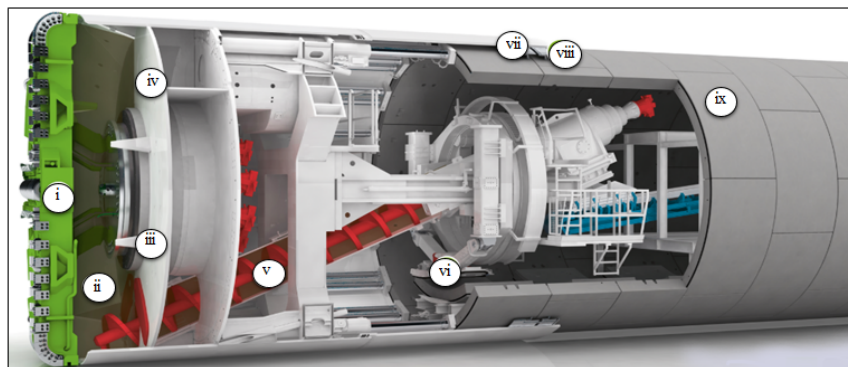


Figure 3.2. General overview of EPB TBM.

- (i) Cutting Wheel: Cutting knives and disc cutters remove the soil from the tunnel face
- (ii) Excavation Chamber: The pliable, plastic soil in the excavation chamber transfers the necessary support pressure at the tunnel face
- (iii) Mixing Arms: Mixing arms at the cutting Wheel and bulkhead mix the soil in the excavation chamber to obtain the required texture
- (iv) Bulkhead: Transfers the thrust force to the soil paste in the excavation chamber where it is controlled using pressure sensors
- (v) Screw Conveyor: The rotation speed determines how much material is removed from the excavation chamber, thus regulating the support pressure
- (vi) Erector: Remote-controlled, movable vacuum manipulator to position the segments during ring building
- (vii) Tailskin: Wire brushes seal the gap between the inside of the tailskin and the outside of the segmental lining
- (viii) Backfilling: The annular gap between excavated surface of the ground and the outside of the tunnel lining is continuously filled with grout
- (ix) Tunnel Lining: Lining of the tunnel with precision precast concrete segments

3.2.3. The Principle of Earth Pressure Balance TBM Tunneling

EPB tunneling is designed to reduce the ground loss ahead, above and behind the TBM as much as possible in order to keep ground movements and surface settlements within acceptable limits. Managing tunnel face support pressure together with regulating the volume of excavation is crucial to ensure the effective operation of an EPB machine. The stability of working face is a key factor in the EPB tunneling.

In the EPB TBM, the excavated material itself is used to support the face of the excavation. The main principle is to counterbalance the earth pressure with the face pressure given by thrust cylinders to the excavated material (muck, earth) filled fully on the chamber and processed usually by different foaming agents and polymers in earth pressure balance (EPB) TBMs (Bilgin *et al.*, 2014).

As seen in Figure 3.3, EPB machine adjusts pressure to balance water and soil pressure in working face by the manners of changing the pressure of thrust cylinders and the rotation speed of screw conveyor.

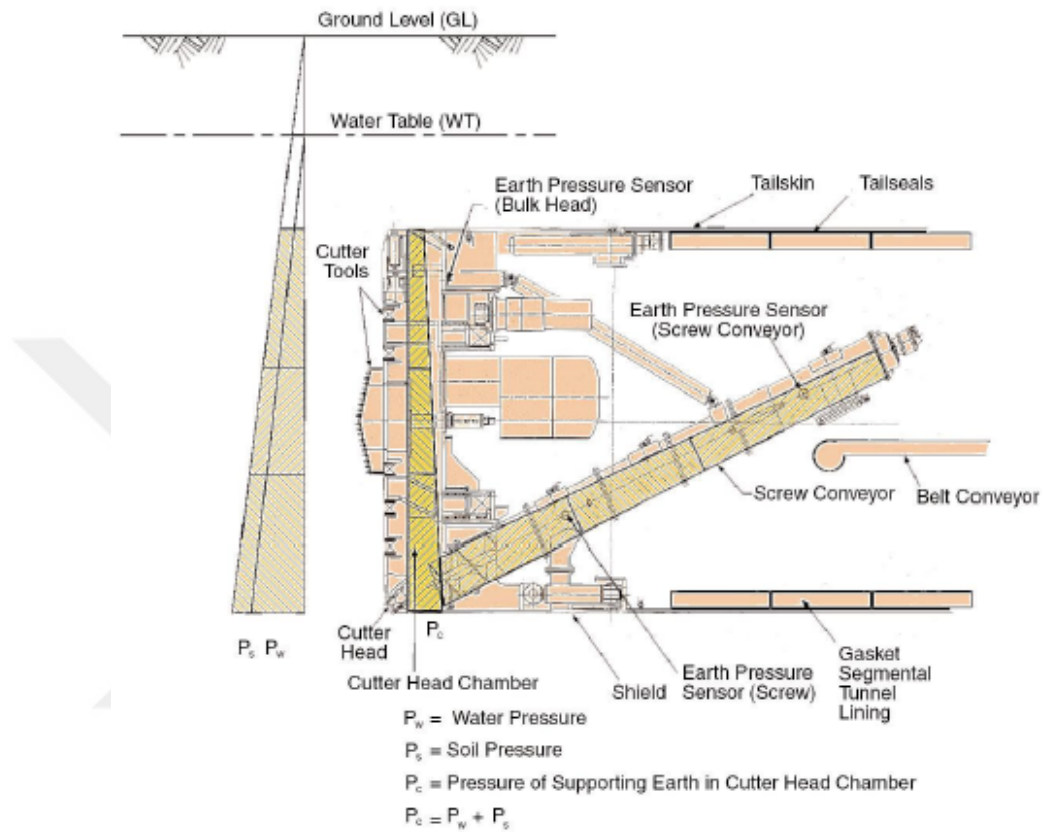


Figure 3.3. EPB operating principle - Balanced Pressure (Barla and Pelizza, 2000).

4. FACTORS AFFECTING TBM PERFORMANCE

The parameters affecting a mechanical excavation system may be categorized into three main groups: geotechnical parameters, machine design parameters and machine operational parameters.

4.1. Geotechnical Properties of the Ground

4.1.1. Consistency (Atterberg) Limits

Atterberg limits, known as consistency limits, are water contents at critical stages of soil behavior. It allows to identify the relations between water and fine-grained soil particles and to assess the plasticity of a soil and its consistency at various moisture contents.

Atterberg limits can be obtained easily with standard testing apparatus.

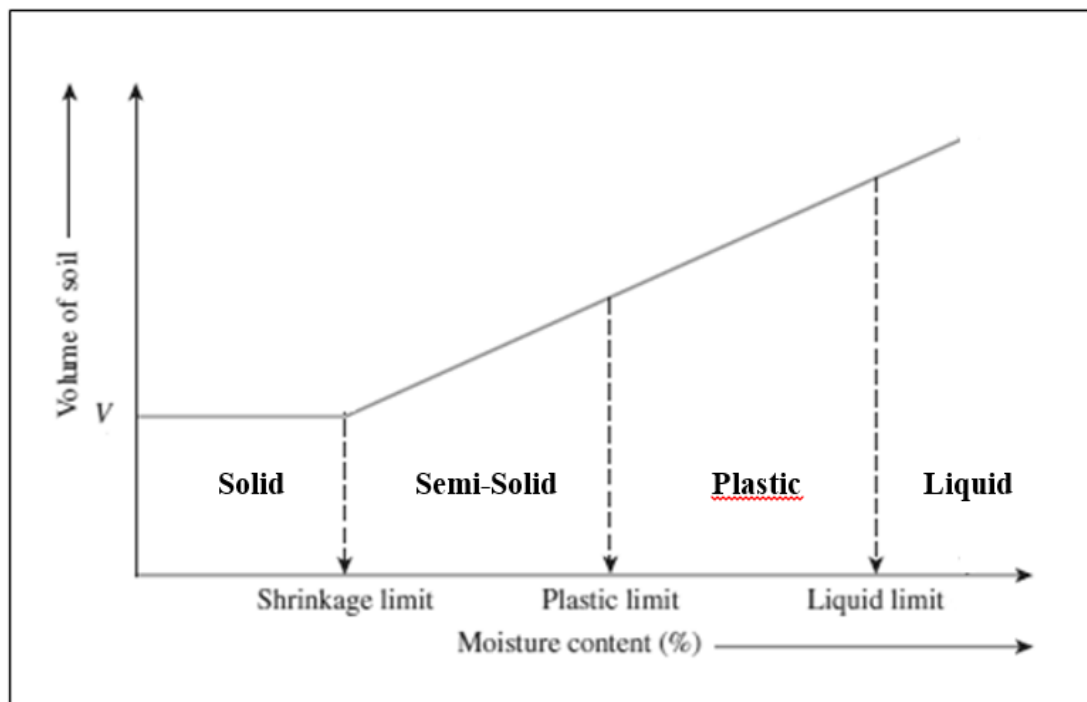


Figure 4.1. Consistency Limits of Fine-Grained Soils (Das, 2009).

Natural moisture content (W) is the value that expresses the natural humidity of the soil. Plastic Limit (W_P) is the moisture content value in which the soil pass from plastic state to semi-solid state. Liquid Limit (W_L) represents the water content limit of clay between flowable and plastic states, while the plastic limit defines the water content limit of clay between plastic and semi-solid states. With the actual water content, the soil consistency can be evaluated easily (Das, 2009).

The plasticity index (I_P) is the difference between the liquid limit and the plastic limit of a soil. As seen in Figure 4.1 the plasticity index, which is important in classifying fine-grained soils, can be calculated by using the Equation 4.1

$$I_P = W_L - W_P \quad (4.1)$$

In the formula I_P shows plasticity index value, whereas W_P is plastic limit value and W_L is liquid limit value.

The consistency index (I_C), indicates the firmness of soil and the changes in water content that allow it to vary from the following states: liquid, very soft, soft, stiff, very stiff, and hard (Terzaghi 1926). At a consistency index of zero (0), soil is equivalent to its liquid limit, and at a consistency index of one (1), soil is equivalent to the plastic limit. The consistency index can be calculated by using the Equation 4.2.

$$I_C = (W_L - W) / (I_P) \quad (4.2)$$

In the formula I_C shows consistency index value, whereas W_L is liquid limit value, W is natural moisture content and I_P is plasticity index value.

Consistency index value between 0.4 and 0.75 is defined as the value that gives the best EPB TBM operation (Maidl, 1995).

4.1.2. Permeability

Permeability is defined as the property of a porous material which permits the passage or seepage of water (or other fluids) through its interconnecting voids.

Permeability or hydraulic conductivity; changes depending on the viscosity of the liquid, the grain size ratio and the soil saturation (Bardet, 1997).

In general, the hydraulic conductivity is high in coarse-grained soils. Therefore, the face pressure is high on such soils. However, deformation control is difficult due to the increase in water content of the soil.

4.1.3. Grain Size Distribution

The grains forming the soils have different size and shape. Mechanical analysis is the determination of the size range of particles present in a soil, expressed as a percentage of the total dry weight. For this aim, sieve analysis is used to find the particle-size distribution of soil.

Data from grain size distribution curves are used to select TBMs and to determine the suitability of using various TBMs. The Standard grain size analysis test determines the relative proportions of different grain sizes as they are distributed among certain size ranges. For grain sizes below 0.074 mm, the hydrometer test is used.

To describe soils by their particle size, several organizations have developed particle-size classifications by sieve analysis and hydrometer tests. Among all, Unified Soil Classification System (USCS) is almost universally accepted and has been adopted. Unified Soil Classification System (USCS) is showed in Table 4.1 and Table 4.2.

Figure 4.1 shows selection requirements for earth pressure balance and slurry mix shield tunnel boring machines based on grain size distribution.

Table 4.1. Unified Soil Classification System (USCS) (American Society for Testing and Materials, 1985).

Prefix	Soil Type	Suffix	Sub-Group
G	Gravel	P	Poorly-graded
S	Sand	W	Well-graded
M	Silt	H	High Plasticity
C	Clay	L	Low Plasticity
O	Organic		

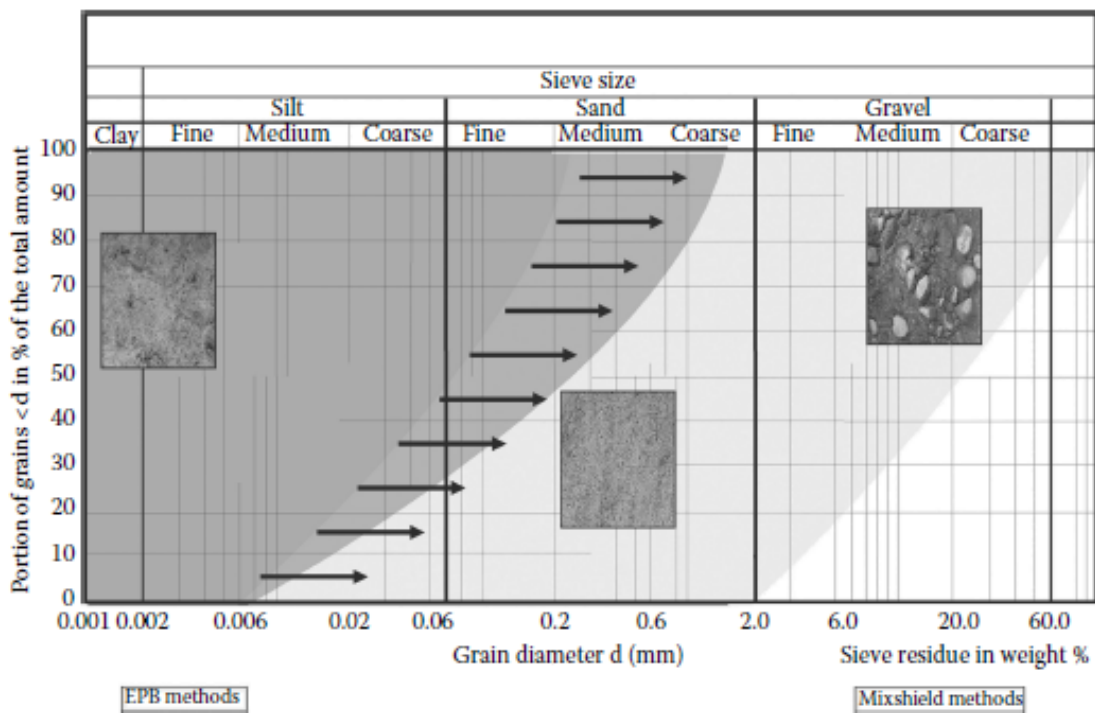


Figure 4.2. Consistency Selection criteria of grain size for earth pressure balance and slurry tunnel boring (Bilgin *et al.*, 2014).

Table 4.2. (Unified Soil Classification System (USCS) (American Society for Testing and Materials, 1985).

Major Division			Group Symbol	Typical Name
Coarse-grained soils	Gravels	Clean Gravels	GW	Well-graded gravels and gravel-sand mixtures, little or fines
		More than 50% of coarse fraction retained on No.4 sieve	GP	Poorly-graded gravels and gravel-sand mixtures, little or no fines
	Sands	Gravels with Fines More than 12% fines	GM	Silty gravels, gravel-sand-silt mixtures
		50% or more of coarse fraction passes on No.4 sieve	GC	Clayey gravels, gravel-sand-clay mixtures
Fine-grained soils	Sands and Silts	Clean Sands	SW	Well-graded sands and gravelly sands, little or no fines.
		Less than 5% fines	SP	Poorly-graded sands and gravelly sands, little or no fines
		Sands with Fines More than 12% fines	SM	Silty sands, and silt-mixtures
	Silty Sands and Silty Clays	Inorganic	ML	Inorganic silts, very fine sands, rock flour, silty or clayey fine sands
			CL	Inorganic clays or low to medium plasticity, gravelly clays, sandy clays, silty clays, lean clays
		Organic	OL	Organic silts and organic silty clays of low plasticity
High organic clays	Inorganic	MH	Inorganic silts, micaceous or diatomaceous fine sands or silts, elastic silts	
		CH	Inorganic clays of high plasticity, fat clays	
	Organic	OH	Organic clays of medium to high plasticity	
		Pt	Peat, muck and other highly organic soils	

4.1.4. Standard Penetration Test (SPT)

Standard Penetration Test (SPT) is a common in situ testing method used to determine the geotechnical properties of the soil. The SPT field test is most conventional test for general characterization of soil. Few correlations are available in literature in terms of SPT N value.

The test is extremely useful for determining the relative density and the angle of shearing resistance of cohesionless soils.

The test is conducted in a bore hole by means of a standard split spoon sampler. Once the drilling is done to the desired depth, the drilling tool is removed and the sampler is placed inside the bore hole.

By means of a drop hammer of 63.5 kg mass falling through a height of 750 mm at the rate of 30 blows per minute, the sampler is driven into the soil. The number of blows of hammer required to drive a depth of 150 mm is counted. Further it is driven by 150 mm and the blows are counted. The number of blows recorded for last two 150 mm intervals are added to give the standard penetration number (N).

Table 4.3. Relationship between SPT and Soil Density/Consistency (Meyerhof, 1965).

Soil	Density/Consistency	N
Sands	Very Loose	0-4
	Loose	4-10
	Medium Dense	10-30
	Dense	30-50
	Very Dense	>50
Cohesive Soils	Very Soft	0-2
	Soft	0-2
	Medium	2-4
	Stiff	4-8
	Very Stiff	15-30
	Hard	>30

4.1.5. Unit Weight

Unit weight is the weight of soil per unit volume. Lower unit weight has given rise to higher void ratio, also higher hydraulic conductivity and higher permeability. In such soils higher water income is expected.

4.1.6. Cohesion and Internal Friction Angle

Fine-grained soil engineering behavior relies primarily on the clay mineralogy of the soil. In order to understand the performance effect of cohesion, the chemo-mechanical behavior of the excavated material should be considered.

The engineering properties and behavior of clays are quite different from other soils. Clay particles have plate-like form which is entirely different shape compared to silt, sand or gravel. Because of the small particle diameter and plate-like shape of clays, the surface area to mass ratio is much greater than in other soils. This ratio is known as the specific surface. The large specific surface provides more contact area between particles, and thus more opportunity for various interparticle forces to develop. It also offers more places for water molecules to attach, thus giving clay a much higher tendency to absorb water.

Clay particles are colloidal in size, so their behavior is regulated primarily by surface forces. It is necessary to consider both the crystal structure of clay minerals and the surface chemistry of clay-water suspensions in order to understand the behavior of clayey soil.

As seen in Figure 4.3, the surface charges of fine-grained soils are negative (anions). These negative surface charges attract cations and the positively charged side of water molecules. Therefore, a thin film of water which is called absorbed water, is bonded to the mineral surfaces.

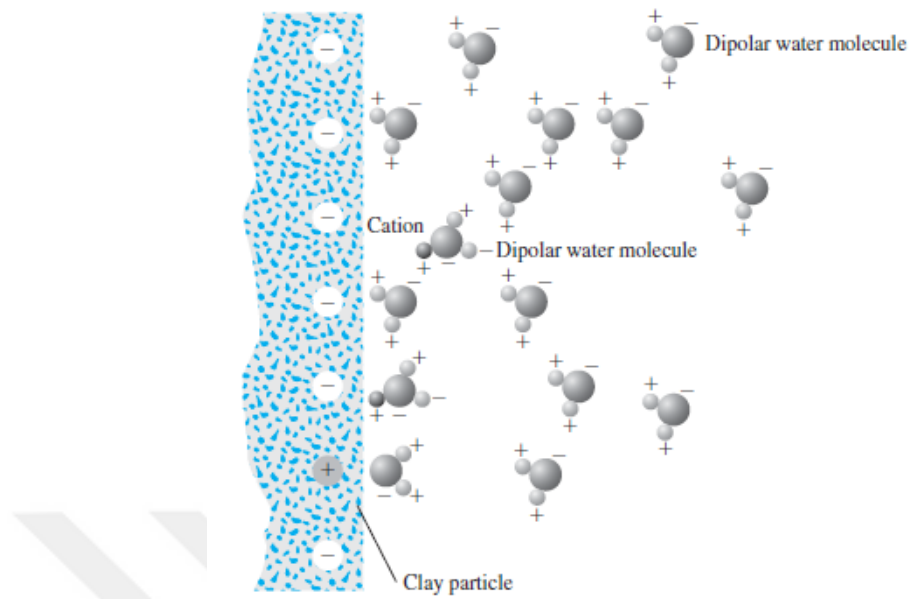


Figure 4.3. Attraction of dipolar molecules in diffuse double layer (Das, 2009).

This thin film of water is known as the diffuse double layer. Figure 4.4 shows that the largest concentration of cations occurs at the mineral surface and decreases exponentially with distance away from the surface.

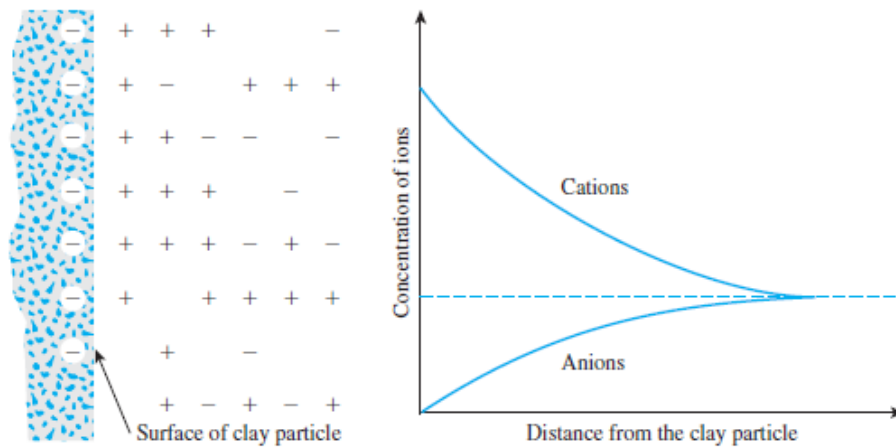


Figure 4.4. Diffuse double layer of Clay (Das, 2009).

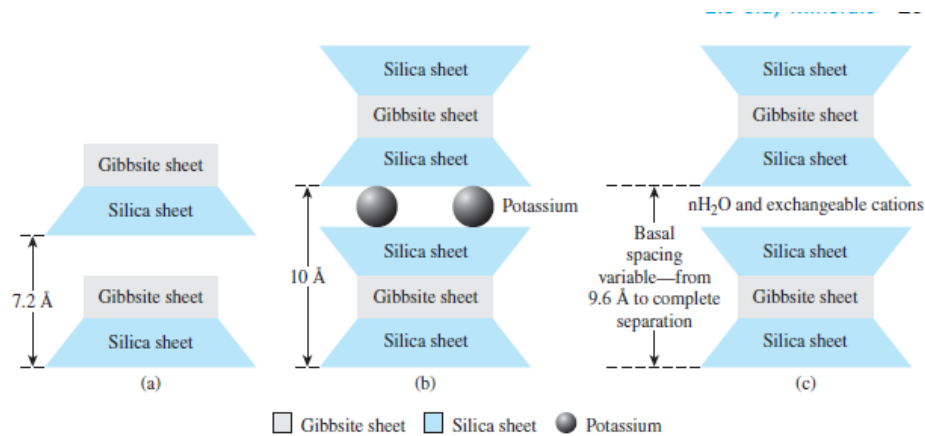


Figure 4.5. Diagram of the structures of (a) kaolinite; (b) illite; (c) montmorillonite (Das, 2009).

There are three main groups of clay minerals: kaolinite, illite and montmorillonite as given in Figure 4.5. Water and moisture cause the swelling (expansion) of clay formations containing high swelling capacity clay minerals such as montmorillonite. Montmorillonite has layers made of two silica sheets and one gibbsite sheet. The bonding of these layers is very weak, so large quantities of water can easily enter and separate them, thus causing the clay to swell. Swelling property can be very inconvenient in terms of TBM operations.

Furthermore, highly cohesive clays show high liquid limits and have the tendency to develop sticky behaviors due to the aforementioned swelling effect of clay particles (Feng, 2004). This may lead to clogging in the cutterhead, working chamber, and screw conveyor of an EPB machine and cause “balling” problems in the pipes and obstruct the shield advance due to friction (Marinos *et al.*, 2008). Responsible for these difficulties are mainly processes that occur at the interfaces/surfaces of the clay minerals of the excavated material (Fernandez-Steeger *et al.*, 2008).

4.2. Machine Design Parameters

TBMs are site specific and designed for optimal performance in given ground conditions. Factors affecting TBM performance depends on the machine design pa-

rameters, thus selection of the convenient machine type.

Once information is available the most important selection for the TBM end user and the manufacturer is the type of face support that will be utilized. The two available methods of pressurized excavation are Earth Pressure Balance (EPB) and Slurry Pressure Balance (SPB).

EPB and SPB machines have their own advantages and disadvantages. Each of which needs to be considered independently for each set of project conditions. Traditionally the EPB machine has been selected for finer grained soils and the SPB for coarser grained soils (Lovat, 2007).

4.3. Machine Operational Parameters

4.3.1. Thrust Force

Thrust force is the force that allows the machine to advance itself parallel to the tunnel axis by reaction force from segment lining. Machine thrust should provide the enough force to efficiently penetrate the tools into the soil surface. The normal force acting perpendicular to the chisels is a function of the thrust force.

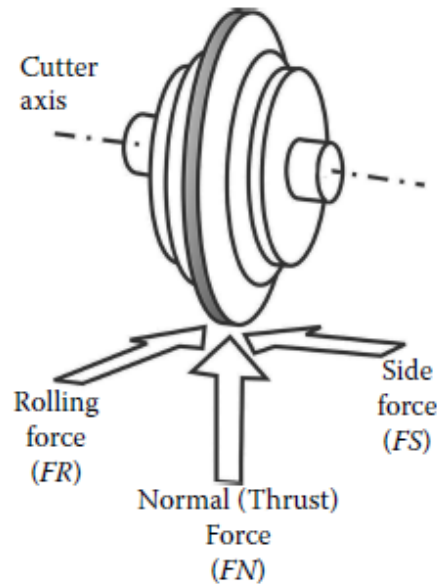


Figure 4.6. Sketch of a typical disk cutter used in full-scale linear cutting machine
(Bilgin *et al.*, 2014)

Total thrust requirement of the soft ground TBMs is suggested as sum of 5 thrust components by (Japan Society of Civil Engineers JSCE, 2007):

$$F = F_1 + F_2 + F_3 + F_4 + F_5 \quad (4.3)$$

where (F) is total thrust (normal) force requirement of the soft ground TBMs, (F1) is thrust force required to overcome friction (adhesion) between shield and ground due to earth pressure, (F2) is thrust force required to overcome the chamber pressure acting on bulkhead, (F3) is thrust force required to overcome the drive force caused by direction changes in curved alignments (If the tunnel is straight; (F3) is taken to be 0), (F4) is thrust force required to overcome the frictional force acting between the segments and the tail seals, and (F5) is thrust force required to overcome the hauling force of trailing (backup) units (If the backup is self-propelled; (F5) is taken to be 0).

4.3.2. Torque

Torque is the rotation moment of the cutting head. Torque capacity must have ability to excavate the soil with chisels, overcome the friction between the cutting head and the excavation face, eliminate the radial forces acting on the TBM (Fernandez, 2007).

Through the estimated maximum torque, the number of driving motor and maximum capacity of a driving motor would be determined.

4.3.3. Power

The total power capacity of the TBM, must meet the torque and the thrust force required by the machine. The power requirement of the TBM can be calculated with Equation 4.4.

$$P = 2\pi \times RPM \times T/60 \quad (4.4)$$

In the formula P shows power, whereas RPM is the number of revolutions per minute of the cutting head, T is the torque capacity.

4.3.4. RPM

RPM is the value that represents the number of rotations of the cutting head per minute. The RPM value is generally inverse with torque (O'Carrol, 2005). The RPM value changes in the same ratio as the required torque value changes according to the characteristics of the geological unit.

As the torque requirement on dense soils increases, the RPM value is reduced to a certain extent so that the machine can maintain the same torque value. On the contrary, due to reason that high torque value is not required for loose soil excavation,

the torque value is reduced and by increasing the RPM value, the advance rate of the machine will be increased within the penetration rate.

4.3.5. Specific Energy

Specific energy is defined as the amount of energy needed to excavate a unit volume of ground (Rostami *et al.*, 1994). The specific energy can be calculated with Equation 4.5.

$$SE = P/ICR \quad (4.5)$$

In the formula SE shows specific energy (kWh/m³), whereas P is the net power consumption (kW), ICR is the instantaneous cutting rate (m³/h). The instantaneous cutting rate was estimated based on the advance speed of the thrust cylinders. Lower specific energy implies higher excavation rates can be achieved by a mechanical miner with a known cutting power or by using a smaller and cheaper excavation machine for excavation.

4.4. Soil Conditioning

The presence of fine particles can be a problem tunneling with EPB TBM because of the sticky characteristics of this type of soil that can lead to the clogging of soil on metallic parts of TBM cutterhead and cutters. A variety of soil conditioners are used in EPB tunneling, including foam, bentonite slurry, and polymers. The injection of foams, polymers and other additives into the tunnel face can significantly modify the characteristics of soft ground, including its plasticity, texture and permeability. Soil conditioning is used to change the properties of the excavated materials to make them more suitable and conveyable for excavation by the TBM.

In EPB TBM technology, the correct use of soil conditioning is essential for a successful and efficient TBM drive and excavation performance. The selection of the

best type and quantity of material for ground conditioning is dependent on the specific geology and the equipment available with the EPB TBM.

For fine-grained soils, as seen in Figure 4.7, the soil may be conditioned by water to improve consistency and by foam to reduce stickiness (Area 1, Figure 4.7). When the excavation is performed through coarser ground, only foam has to be injected as a conditioning agent (Area 2, Figure 4.7). The coarser ground is called the extended application range of the EPB shield. In areas 3 and 4 (Figure 4.7), polymers and foam have to be added into the excavation chamber to provide the required properties of the soil DAUB (German Committee for Underground Construction), (2016).

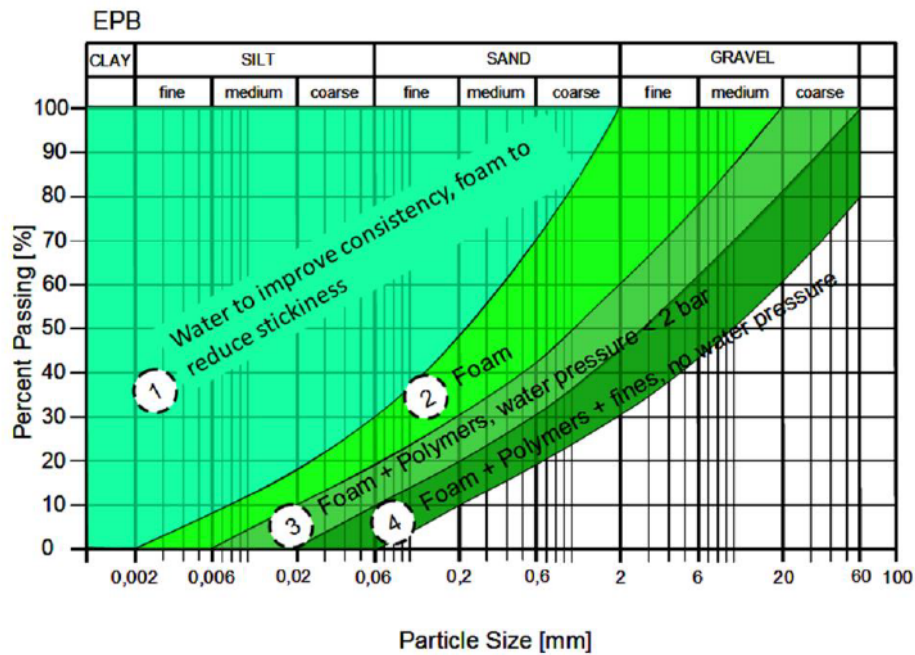


Figure 4.7. Application ranges of the EPB shield (Thewes, 2007).

Soil conditioning is affected by the soil characteristics such as the grain size distribution, the water content, the liquid limit value and the plasticity index of the soil.

Soil conditioners are used to achieve the desired mechanical and hydrological properties of the soil:

- Support pressure transfer at the tunnel face
- Sufficient plasticity
- Low water permeability
- Distinctive resilience properties
- Reduced clogging on the machine
- Reduction of wear
- No deterioration of the driving power

The desired properties achieved by mixing the soil with additives, i.e. by soil conditioning is given in Table 4.4.

Low water permeability is necessary to counteract the water pressure at the face and prevent water drainage and surface settlements. Low internal friction and adhesion ease the material flow from the cutterhead to the belt conveyor and reduce the power draw of the TBM. Increased compressibility and elasticity allow the soil to maintain pressure even during in- and outflow volume fluctuations. Low abrasivity increases the life of cutting tools and all other surfaces in contact with the soil. Soil conditioners can be injected at the face, in the excavation chamber, and in the screw conveyor of the TBM.

Parameters, such as the Foam Expansion Ratio (FER), Foam Injection Ratio (FIR), and Concentration (c) can determine the success of excavation and defined below:

- c (%): Concentration of the foaming agent in water
- FER: To define the quantity of foam generated from a solution and represents the proportion of air to liquid in the foam. It is defined as a ratio and may normally vary between 10 and 30
- FIR: The quantity of foam injected as a proportion of the ground excavated. Dependent on the ground conditions, the FIR may vary considerably between 10 and 80

Table 4.4. Required parameters of the earth muck to be used as the support medium (Thewes and Budach, 2010).

Parameter	Desired property of the support medium	Purpose	Reference
Permeability	$k_i < 10^{-5} \text{ m/s}$	To reduce groundwater inflow in the excavation chamber	Abe <i>et al.</i> -1978
Good consistency for workability	$0.4 < IC < 0.75$	To ensure flow behavior	Maidl -1995
Maintenance of the pressure gradient in the screw conveyor	$0.6 < IC < 0.7$	To enable the pressure difference between excavation chamber and conveyor belt (shield interior)	Maidl -1995
Good compressibility	dependent on the geological conditions of the ground and geometrical dimensions of the shield machine	To achieve homogeneous support	Maidl -1995
Tendency to stick	$IC < 0.5$ or $I_p < 20 \%$	To reduce stickiness	Maidl (1995), Hollmann -2012
Wear effect	$IC < 0.8$	To reduce wear	Maidl -1995

4.5. Applied Earth Pressure

EPB TBM working mechanism is to give a face pressure to counterbalance the earth pressures to provide for stability at face and on surface. EPB TBMs use the excavated soil in a pressurized excavation chamber to apply a support pressure to the tunnel face during excavation.

In terms of applied support pressure, TBM has different working modes. As seen in Figure 4.8; PS is no support pressure, PS,EPB is support pressure in closed mode, PS,CA is support pressure of compressed air.

During open mode, the excavation chamber is almost empty. Therefore, no support is provided to the tunnel face. The excavation can be carried out in open mode if ground conditions ensure a totally stable tunnel face and possible groundwater flow

towards the face or into the excavation chamber does not cause any hydrogeological or shield-operational issues.

In transition mode, EPB shield is operated with a closed but only partially filled excavation chamber. Compressed air pressurized the soil in the excavation chamber, helping to decrease the inflow of groundwater into the excavation chamber. In instances with a stable tunnel face and low risk of over-excavation on the tunnel face, this method is convenient. The transition mode's primary aim is to regulate the flow of water through the face of the tunnel. It is feasible to quickly change this operation to the closed mode.

As for closed mode, the excavation chamber is completely filled with the excavated soil and is pressurized. The applied pressure balances the acting earth and groundwater pressures. In unstable soft soils below the groundwater table, this operation mode is needed.

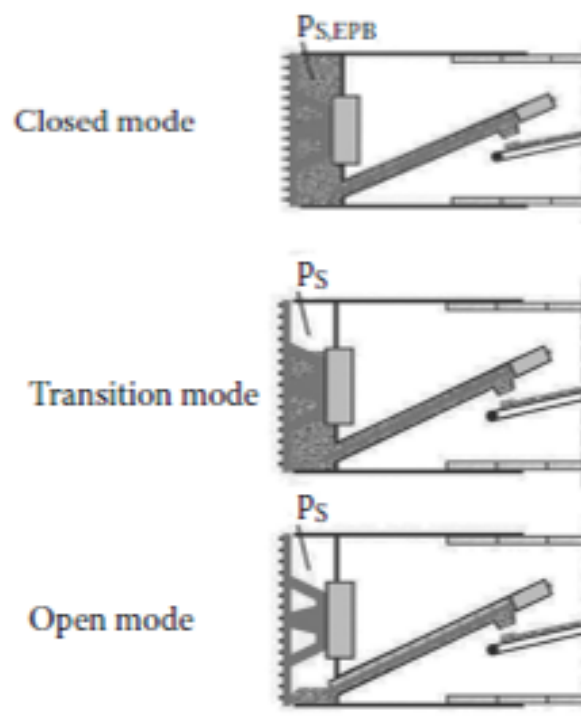


Figure 4.8. Working Modes of EPB TBMs (Bilgin *et al.*, 2014).

5. DESCRIPTION OF THE SOFIA METRO LINE-3 PROJECT AND TUNNEL GEOLOGY

5.1. Project Description

The third metro line project (M3) is aimed to ease the traffic on some of the most congested boulevards in Sofia linking the city's south-western neighborhoods with its eastern districts. The entire third line M3 is 16km long and includes 8 overground and 11 underground stations. The intermediate tunnel stretch of M3 line includes six (6) stations from chainage 5+267 to chainage 11+933.

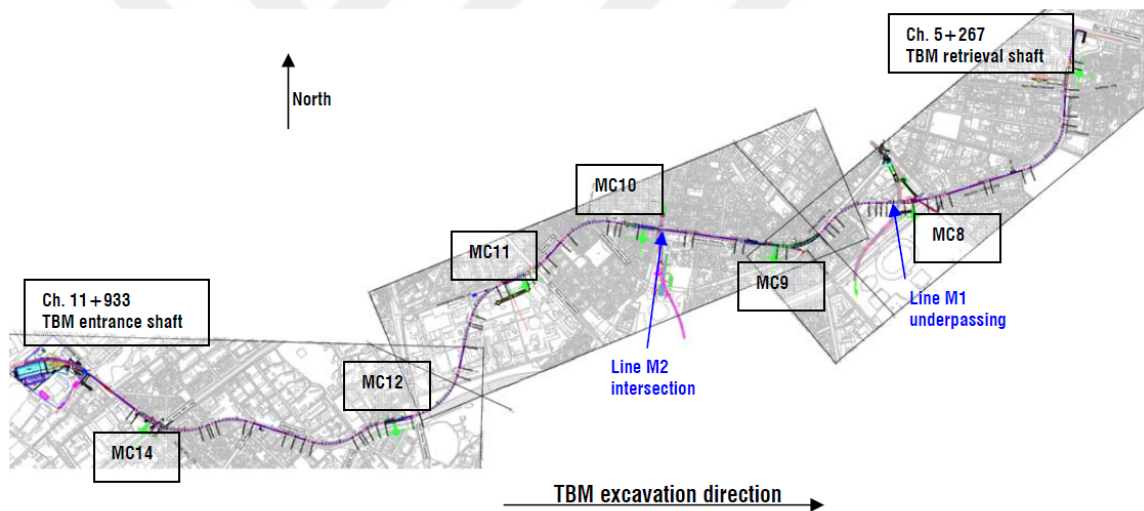


Figure 5.1. Sofia Metro Line-3 Plan View (TC1527-R05-r0 Report on Recommended EPB Pressure).

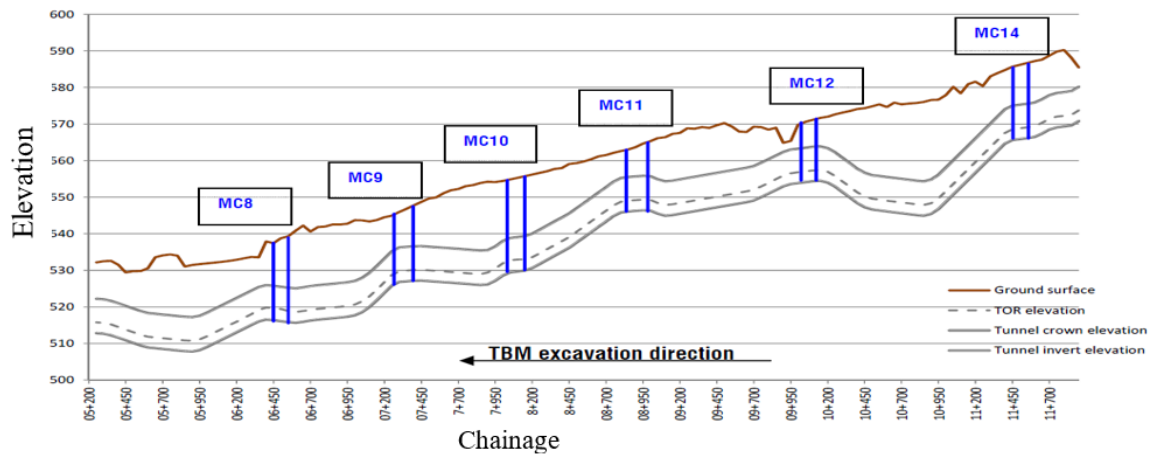


Figure 5.2. Sofia Metro Line-3 Geometrical Profile (TC1527-R05-r0 Report on Recommended EPB Pressure).

Along the entire alignment the mean earth cover at tunnel crown is 13.0 m, ranging from the minimum overburden of 5.2m (after leaving the launching shaft) up to 21.3 m at 10+850.

5.2. Geology of the Tunnel Alignment

The project is situated on the border of Sofia Pliocene basin. Basically it is formed by clayey-sandy material (alternation of clays, sandy clays, sands and gravels), known as Lozenec Formation. The Lozenec Formation consists of irregular alternation in horizontal and vertical direction of clays, sandy clays, very often gravels too. The Pliocene materials have a variable thickness, ranging between 250 meters and 500 meters. On the top of this formation Quaternary deposits formed by brown sandy clays are present (they have a variable thickness between 1.0 m and 7.0 m). (TC1527-R05-r0 Report on Recommended EPB Pressure).

The geological units forming the typical stratigraphic column at the project area are:

- 4.1 - Multicolored silty clay (Pliocene)

- 4.1a - Multicolored silty clay, structured (Pliocene)
- 4.2 - Yellow-brown silty fine-grained sands
- 4.3 - Yellow-brown silty medium-grained sands
- 4.4 - Yellow-brown silty coarse-grained sands
- 5.1 - Grey silty clay (Pliocene)
- 5.1a - Grey silty clay/clayey silt, structured (Pliocene)
- 5.2 - Grey silty fine-grained sands
- 5.3 - Grey silty medium-grained sands
- 5.4 - Grey silty coarse-grained sands

5.2.1. Layer 4.1: Multicolored Silty Clay (Pliocene)

The clay builds the Pre-Quaternary bedrock of the region. Lithographically it belongs to the upper (yellow-brown) horizon of the “Lozenetz formation”. Visually this layer consists of silty-sandy clay to clayey-sandy silt. Its basic color is yellow-brown to rusty, with grey to greenish and black streaks. It includes carbonate inclusions. It is established along the whole alignment as separate layers or thin bands in alternation with the sandy materials.

Layers 4.2, 4.3 and 4.4. Its maximum thickness for single layers of clay is up to 10-14 m in the section between boreholes MC-10, MC-11 and MC-12. In the other part of the alignment the thickness of the single layer is 1.0 m to 4.5-6.0 m.

5.2.2. Layer 4.1a: Multicolored silty clay, structured (Pliocene)

The clay is separated from the main layer based on the aforementioned criteria. In addition there is the increased content of silt and clay fraction, which determines it mainly as clay (Cl) to silty clay (siCl). It is established as separate layers in boreholes MC-4, MC-5, MC-7 and MC-10 with thickness of 2.0 - 4.0 m for each single layer.

5.2.3. Layer 4.2: Multicolored Silty Clay (Pliocene)

The sands are located along different sections of the alignment as layers with increasing depth thickness from 0.5-1.2 m to 5.0-7.0 m. Most often they alternate with the other varieties of the Upper (yellow-brown) complex. The sands are fine-grained, silty, and predominantly yellow-brown, with colour transitions to grey.

5.2.4. Layer 4.3: Yellow-Brown Silty Medium-Grained Sands

The sands in the section are significantly more evenly occurring. They are established in different sections of the alignment as layers with relatively constant thickness from 0.5-1.0 m to 2.0-3.0 m (rarely to 4.5-5.0 m). Analogically to the sands from Layer 4.2, they are also alternating with the other varieties from the Upper (yellow-brown) complex. Visually the sands are described predominantly as medium-grained, clayey, with fine gravels at some places, mainly yellow-brown, with color transitions to grey and greenish.

5.2.5. Layer 4.4: Yellow-Brown Silty Coarse-Grained Sands

This sandy unit is founded along the M3-line section almost rarely. In MC-3 and MC-7 their thickness is from 0.5-1.5 m, and in MC-9 with a thickness to 9.2 m, often with thin bands of fine particle size sands and clays. The sands alternate irregularly with the other varieties from the Upper (yellow-brown) complex. Visually they are described mainly as coarse-grained, unmixed to clayey, with fine gravels, yellow-brown to rusty.

5.2.6. Layer 5.1: Grey Silty Clay (Pliocene)

Lithographically the clay belongs to the Lower (grey-green) horizon of the “Lozetz formation“. Visually it consists of silty-sandy clay to clayey-sandy silt. Its basic color is grey-green to graphite grey. Charred organic intervals are found in this unit. It is established along the whole alignment as separate layers or thin bands in alternation

with the sandy materials of Layers 5.2, 5.3 and 5.4. It is also found as included in the Upper (yellow-brown) horizon of the “Lozenetz formation”. The thickness of the separate layers is about 1.0-3.0 m, as in depth it increases to 10-15 m and more (MC-1, MC-8, MC-12 and MC-13).

5.2.7. Layer 5.1a: Grey Silty Clay/Clayey Silt, Structured (Pliocene)

The clay is separated from the main layer based on the increased plasticity and the void ratio. It is analogical to the one from Layer 5.1-silty and sandy clay (siCl and sasiCl) and sandy to sandy-clayey silt (saSi and saclSi) with irregular transitions. It is established only in boreholes from MC-5 to MC-9, MC-7 and MC-10 with a thickness of single layers from 2.0 - 4.0 m.

5.2.8. Layer 5.2: Grey Silty Fine-Grained Sands

The sands are established in different sections from the alignment as layers with increasing thickness from 1.0-2.0 m to 4.0-8.0 m in depth. They alternate with the other varieties from the Lower (grey-green) complex. The sands are fine-grained, silty, and grey, with charred organic inclusions.

5.2.9. Layer 5.3: Grey Silty Medium-Grained Sands

The sands in the section are established mainly in boreholes MC-2 to MC-5, as well as in MC-8. Their thickness is about 1.0-3.0 m, as in depth in MC-3 it reaches 5.5-6.0 m. They alternate with the other varieties from the Lower (grey-green) complex. The sands are medium-grained, silty, and grey, with slightly charred organics.

5.2.10. Layer 5.4: Grey Silty Coarse-Grained Sands

The sands are established in MC-4, and in MC-5, MC-9 and MC-11 they are in mixed facies with the medium-grained sands from Layer 5.3. Their established thickness inside the section is comparatively permanent about 3.0-5.0 m. There are

often thin bands of fine sands and clays, as well as remains of fauna (shells and snails). Visually they are described mainly as coarse-grained, unmixed, with single fine gravels, grey-green.

5.2.11. From the TBM Launching Shaft to the Station MC14

5.2.11.1. Geological Description. As it can be seen in Figure 5.3, along the initial 200 m long stretch, the tunnel is located within an alternation of clay (layer 2.1) and gravel (layer 2.2) in its upper section, while below the tunnel face consists of fine to medium grained sand (layers 4.2 and 4.3) and fine grey silty clay (layer 5.1). After chainage 11+720, the tunnel face is completely located within grey silty clay with a small lens of grey medium grained sand (layer 5.3) until Station MC14 (station 11+558).

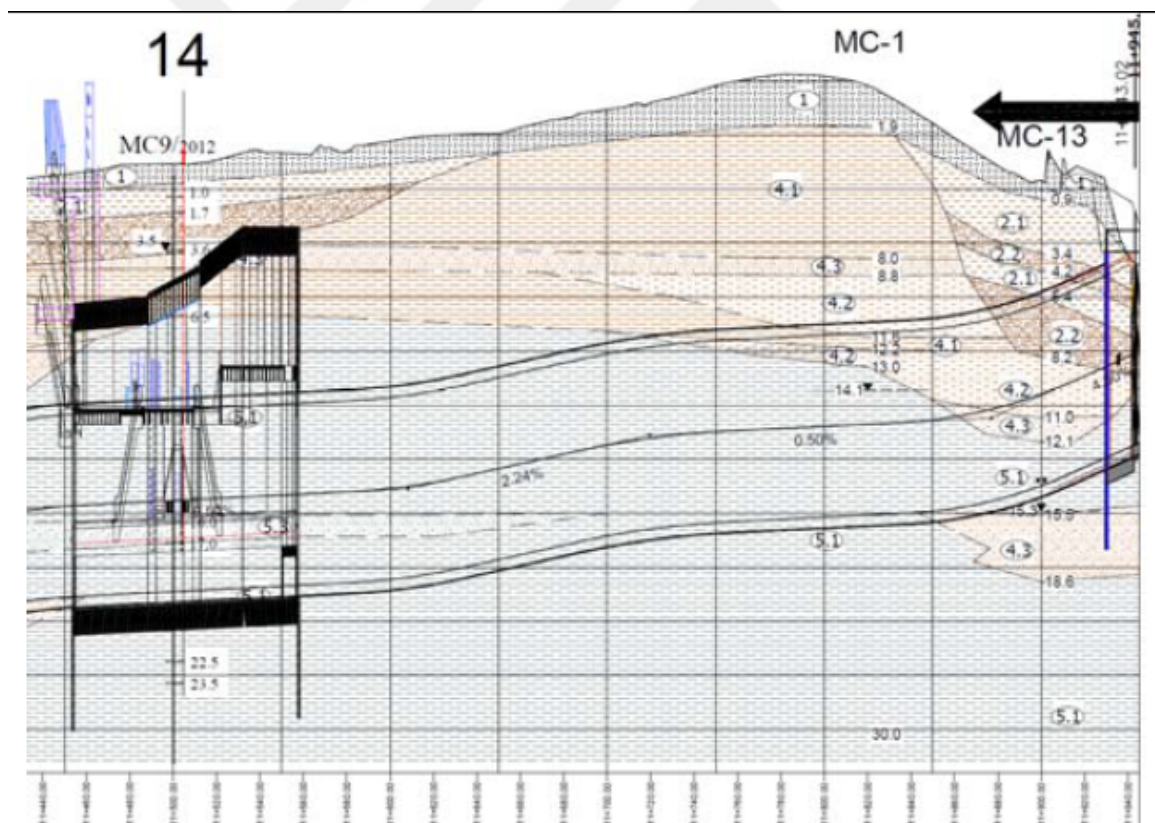


Figure 5.3. Geological profile along the alignment (From the TBM launching shaft to the Station MC14).

5.2.12. From the Station MC14 to the Station MC12

5.2.12.1. Geological Description. Figure 5.4 shows the geological profile along the TBM stretch between Station MC14 and Station MC12, which is characterized by an alternation of grey silty clay (layer 5.1) and grey medium grained sand (layer 5.3). After the initial 235 m, some lens of silty clay (layer 4.1) and silty sand (layer 4.3) are present at the tunnel crown and bottom respectively. Additionally, thick lenses of fine to medium grained grey sand are present on the borehole MC-3. Then from chainage 10+325 up to Station MC12, the tunnel crown is located within fine to medium grained silty sands (layer 4.3-4.4).

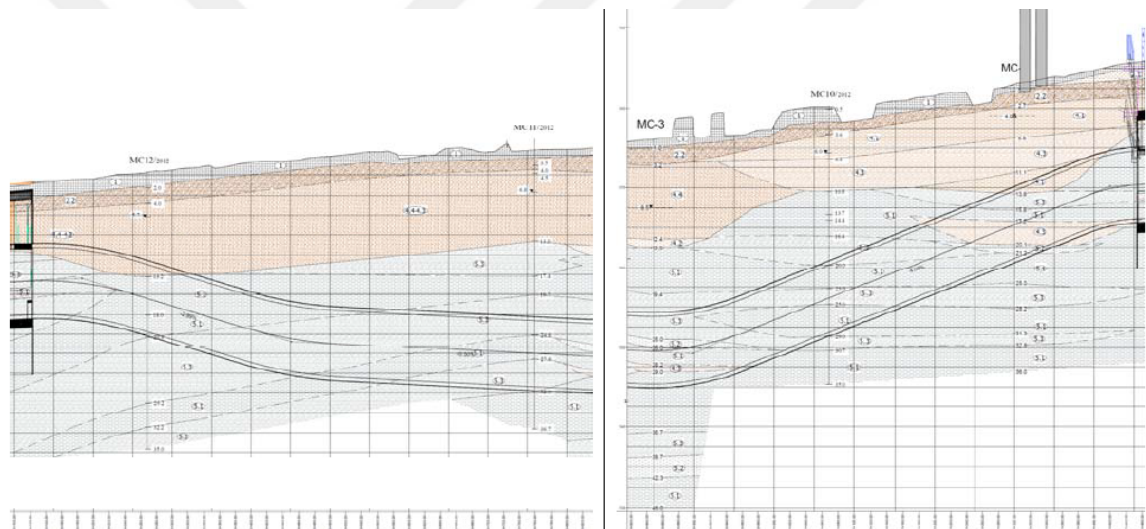


Figure 5.4. Geological profile along the alignment (From Station MC14 to the Station MC12).

5.2.13. From the Station MC12 to the Station MC11

5.2.13.1. Geological Description. As showed in Figure 5.5 the section is completely within alternations of grey silty clay and grey medium sand (layer 5.1 and 5.3). Between chainage 9+900 and 9+500 two graben are identified. At this zone, different units' layers still deposited horizontally as defined below: At the tunnel crown alternation of grey silty clay and grey medium sand (layer 5.1 and 5.3); below silty clay and fine grained sand (layer 4.1 and 4.2).

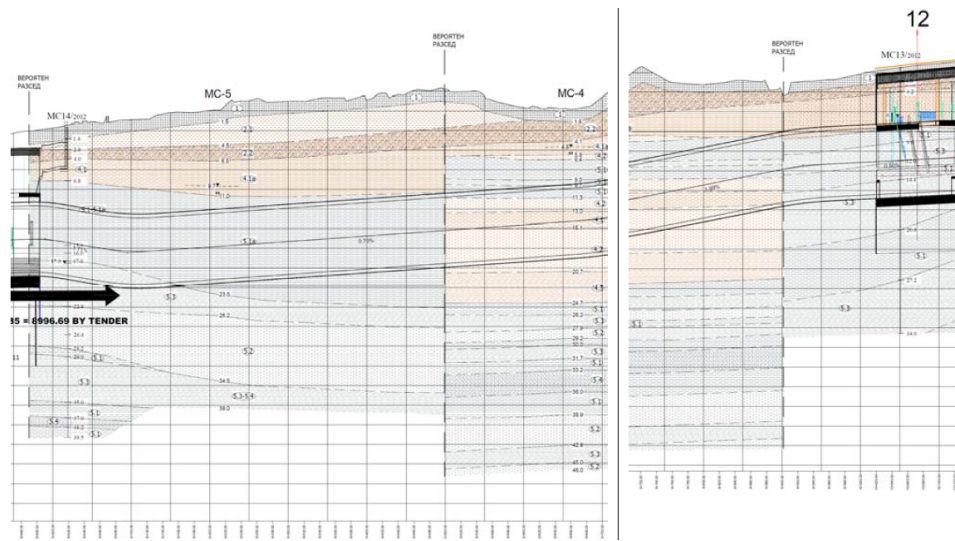


Figure 5.5. Geological profile along the alignment (From Station MC12 to the Station MC11).

5.2.14. From the Station MC11 to the Station MC10

5.2.14.1. Geological Description. The stretch 4 extends from Station MC11 to Station MC10. The initial 54 m there have no geology information, so it was supposed that structured grey silty clay/clayey silt (layer 5.1a) is present. The stretch is characterized by a graben between chainage 8+560 and 8+783 with grey silty clay/clayey silt at the tunnel crown (layer 5.1a) and below silty clay (layer 4.1) and medium silty sand (layer 4.3). The rest of the stretch is characterized by a granular soil (fine to medium sand), with a final section defined by a cohesive soil (grey silty clay; layer 5.1) between chainage 8+245 and Station MC10.

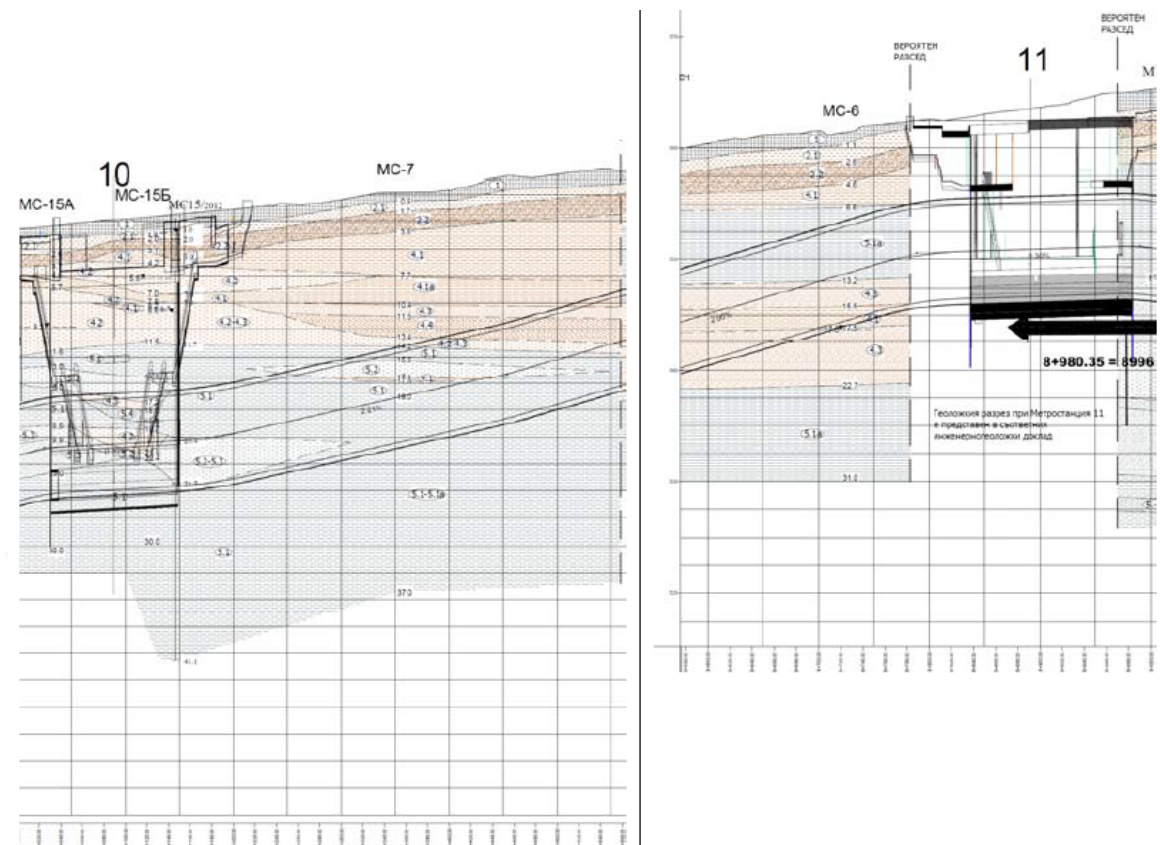


Figure 5.6. Geological profile along the alignment (From Station MC11 to the Station MC10).

5.2.15. From the Station MC10 to the Station MC09

5.2.15.1. Geological Description. The stretch between Station MC10 and Station MC09 have an alternation between granular and cohesive soils at the crown. As it is seen in Figure 5.7, the different unit layers presents are 4.1-5.1 for cohesive soils (clays) and 4.2, 4.3, 5.2 and 5.3 for granular soils (fine to medium sands).

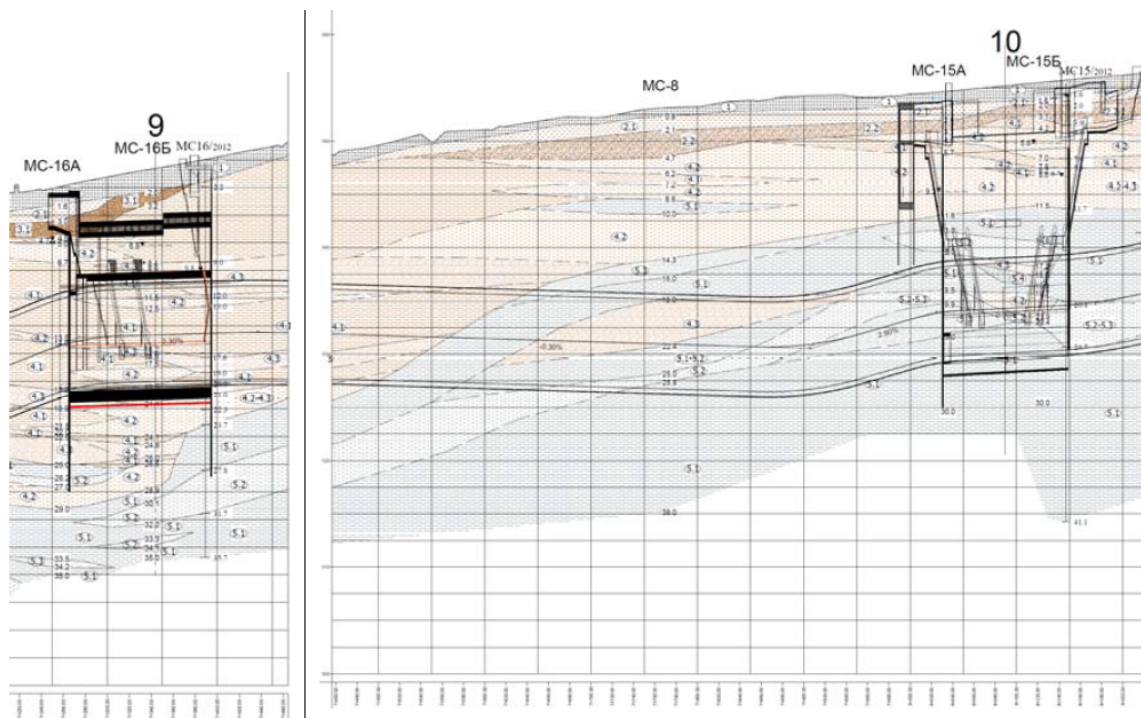


Figure 5.7. Geological profile along the alignment (From Station MC10 to the Station MC09).

5.2.16. From the Station MC09 to the Station MC08

5.2.16.1. Geological Description. As seen in Figure 5.8, along the stretch between Station MC9 and Station MC8, an alternation between silty clay and medium grained sand with some thick lens of grey silty clay define the first 340 m. Then the tunnel section is divided in three layers: silty clay at the tunnel crown, grey silty clay at the bottom and grey fine- grained sands between the two layers since chainage 6+730 till 6+550, where a graben appear. At this point the tunnel section is characterized by alternation of coarse-grained sands and silty clay.

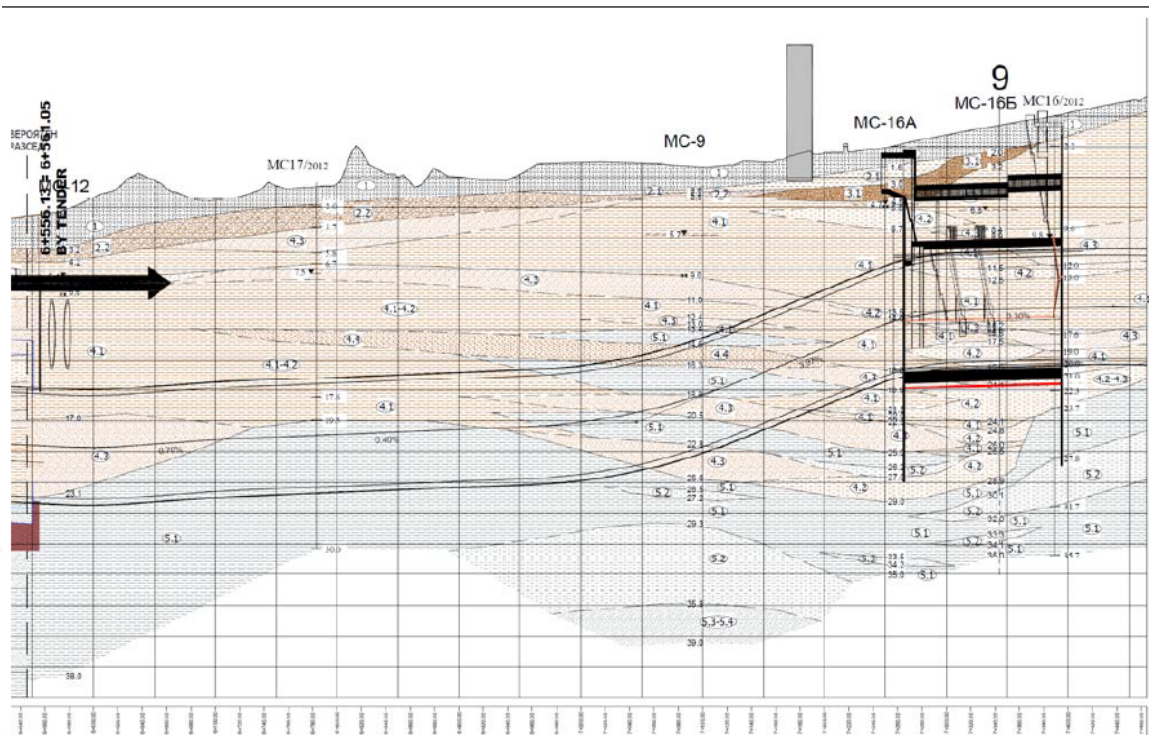


Figure 5.8. Geological profile along the alignment (From Station MC09 to the Station MC08).

5.2.17. From the Station MC08 to the Retrieval Shaft

5.2.17.1. Geological Description. Along the stretch between Station MC8 and Retrieval shaft, the tunnel section has initially a cohesive soil corresponding to a fine to medium grained sand at tunnel crown and below an alternation of clay and medium sand. After the graben, the section is predominantly composed by grey clay and medium grained grey sand with a lens of fine grained grey sand until 5+600, as showed in Figure 5.9.

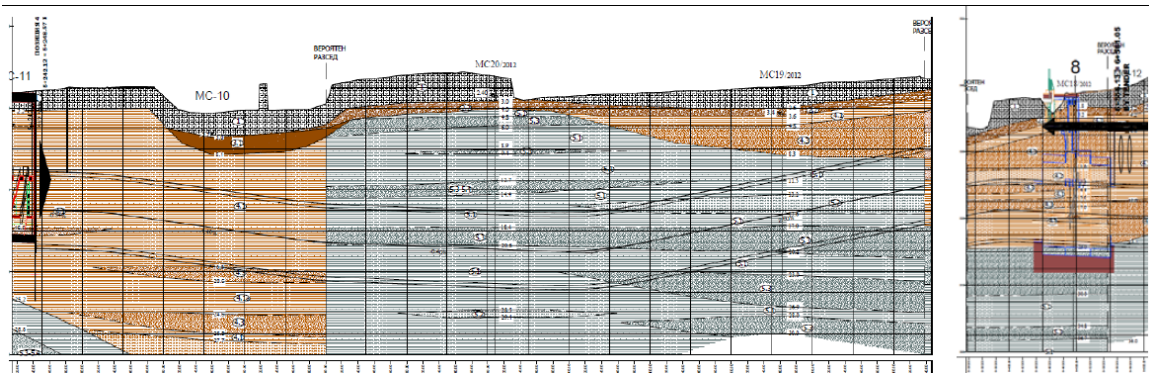


Figure 5.9. Geological profile along the alignment (From Station MC08 to the Retrieval shaft).

At this point another graben occurred and the tunnel section is almost within the silty clay layer, with a lens of medium grained sand at the bottom through 130 m.

5.3. TBMs Technical Details

5.3.1. Main Properties

The TBM that is going to excavate M3 line extension is an Earth Pressure Balance shield (EPB-TBM) that is manufactured by Herrenknecht with serial number S-1014. It is a shield with an excavation diameter of 9.39 meters and it will install a 32 cm thick segmental lining with an inner diameter of 8.43 m.

Table 5.1. Technical details of EPB TBM.

Machine type	Earth Pressure Balance Shield
Installed power	6400 kVA
Length TBM + back-up	approx. 184 m
Weight TBM + back-up	approx. 1120 t
Theoretical thrust speed	80 mm/min
Correction curve radius (min.)	225 m
Height above sea level	595 m
Working pressure (at axis)	4.0 bar
Motors	9
Power	3150 kW
Speed	0 - 3.5 1/min
Torque (nominal)	13697 kNm
Thrust (nominal)	73187 kN
Diameter main drive	4600 mm

The shield has been designed to safely operate up to 4.0bar pressure in the excavation chamber and it is equipped with 5 pressure cells on the bulkhead. (Figure 5.10).

5.3.2. Cutterhead

Cutterhead is the turning part at the front of the TBM which supports the cutting tools. It is located in front of the shield system. Cutterhead consist of different tools such as discs, rippers, buckets and cutting knives which are cutting soft ground and helping excavated material to be collected in working chamber. The disc cutters, which are the key components installed on the cutterhead, are rotating during excavation and increasing friction between excavation face and cutterhead. The excavation diameter is slightly larger than the shield diameter to reduce the frictional forces between the shield and ground and provide easier excavation of the curves. This is provided by usually a few corner cutters placed on the most outer portion of the cutterhead (Bilgin *et al.*, 2014).

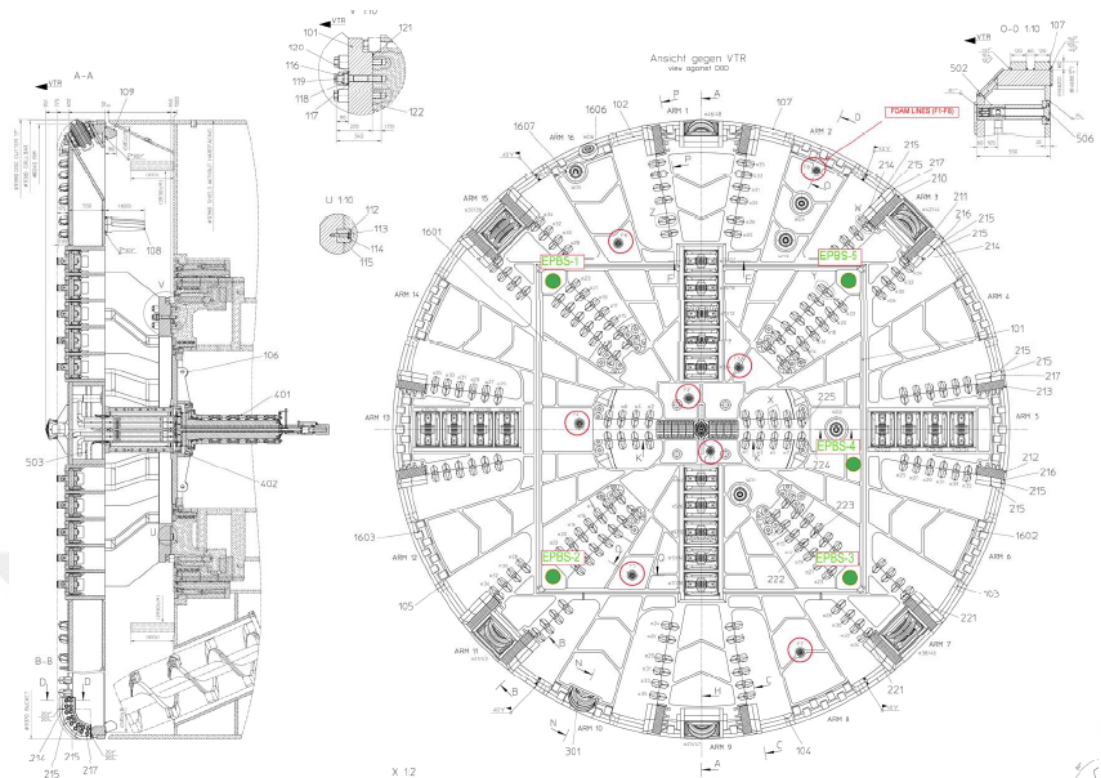


Figure 5.10. EPB TBM Cutterhead (S1014-EPB TBM Shield Drawing 4873-006-000-00).

Table 5.2. Dimensions of the steel construction cutterhead.

Bore Diameter	9390 mm
Weight (with tools)	118.2 t
Wear protection	wear detection plates, protection rings



Figure 5.11. EPB TBM Cutterhead used in the Project.



Figure 5.12. Cutterhead during TBM Disassembly.

The arrangement of cutting tools are designed specifically according to the property of cutting soil. With respect to this arrangement every disc rotates on a different path, not crossing other discs angle.

Table 5.3. Dimensions of the excavation tools.

Disc Cutters (2 rings)	6
Overcutter Roll	1 x threefold disc cutter
Stroke Overcutter	30 mm above bore diameter
Diameter Disc Cutters	17"
Track Pitch	100 mm
Cutting Knives	154
Centre Tool	1
Centre Knife	1
Rippers	18
Buckets	16
Wear Detection	6 sensors

5.3.3. Shield

The steel construction shield consists of three sections; Front Shield, Centre Shield and Tailskin. These sections are connected to each other by articulation jacks (hydraulic cylinders).

The dimensions of the steel construction shield are given in Table 5.4 and Table 5.5.

Table 5.4. Dimensions of steel construction shield.

Diameter front shield	9360 mm
Length front shield	2700 mm
Diameter centre shield	9350 mm
Length centre shield	3510 mm
Diameter tailskin	9340 mm
Length tailskin	4065 mm
Tailskin seal	3 rows of wire brush seals

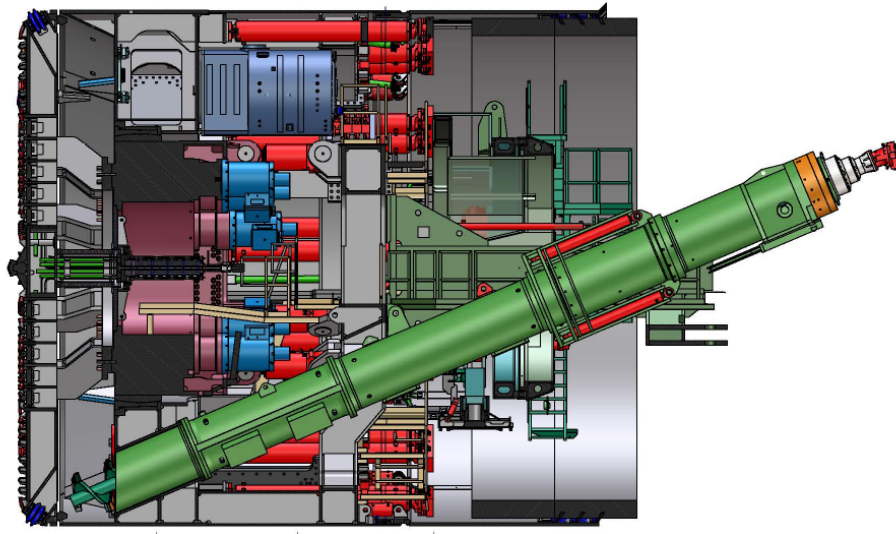


Figure 5.13. EPB TBM Shield (S-1014, Drawing 4873-000-001-00).

Table 5.5. Numbers of cylinders.

Number of tailskin articulation cylinders	2 x 11
Number of thrust cylinders	2 x 13

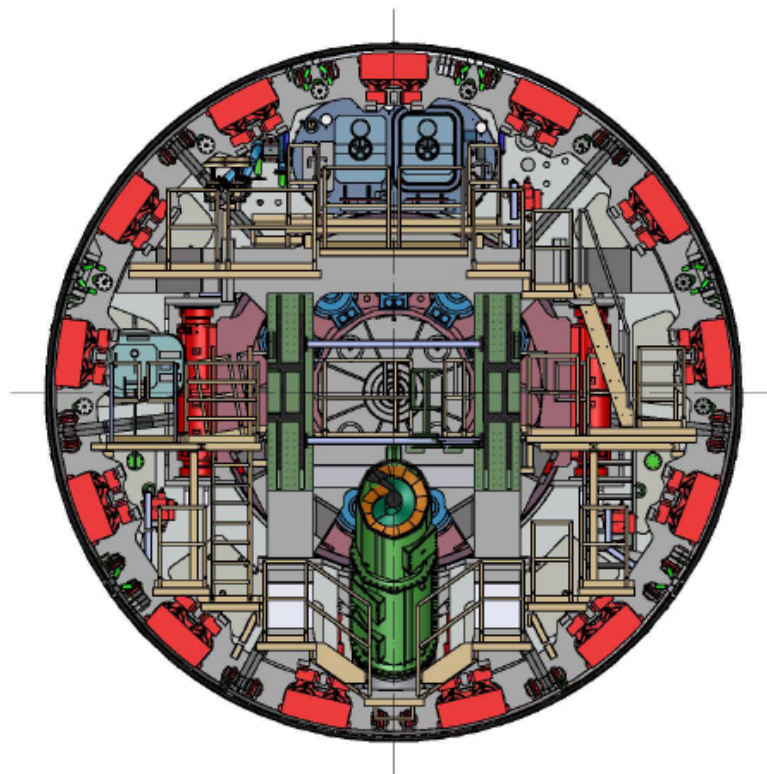


Figure 5.14. EPB TBM Thrust Cylinders (S-1014, Drawing 4873-000-001-00).

The tailskin is equipped with a wire brush seal and a spring sheet ring. The forming chambers between the brushes and the spring sheets are filled with tailskin sealing compound. A certain number of connections is provided for each chamber. Each connection can be opened and closed via a pneumatic ball valve. The installed pressure transducers after each ball valve measure the pressure which is displayed in visualization.

Also, a sufficient supply of the seal with the proper grease is absolutely vital for a long service life and the proper functioning of the wire brush seal.

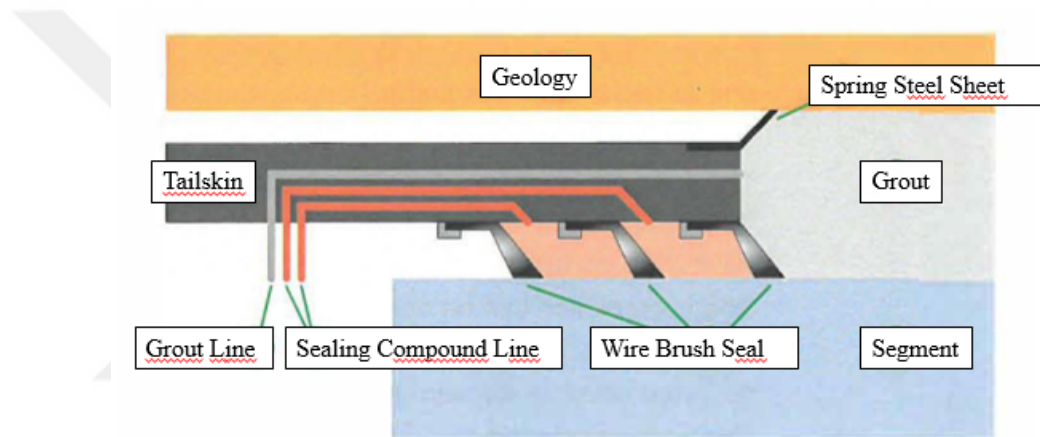


Figure 5.15. Tailskin Wire Brush Seal (Herrenknecht AG, Operating Manuel S-1014).

The conditioned soil within the excavation chamber is transported out to the belt conveyor system by means of a rotating screw conveyor. By changing the rotation speed of screw conveyor, it is possible to control the pressure within the excavation chamber. An earth pressure sensor is installed on the screw conveyor pipe near the screw conveyor discharge gate.

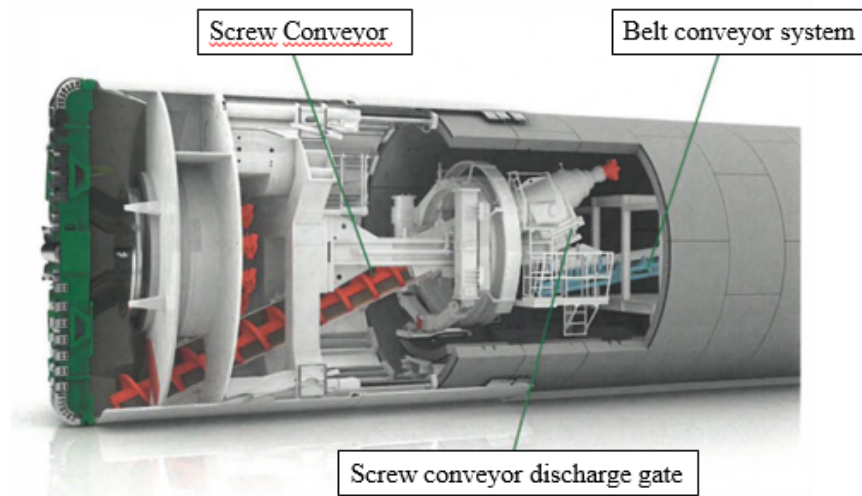


Figure 5.16. Muck System at (EPB Shield Herrenknecht AG, Operating Manuel S-1014).

The muck discharge rate and rotational speed of the screw conveyor should be equivalent to the advance (excavation) rate of the machine, adjusted by thrust cylinders, for proper face pressure control without hazardous stability problems (Bilgin *et al.*, 2014).

Table 5.6. Dimensions of screw conveyor.

Length	16322 mm
Power	400 kW
Speed	0-22 ¹ / _{min}
Torque (nominal)	195 kNm
Telescope stroke	1000 mm

6. ASSESSMENT OF TBM'S PERFORMANCE PARAMETERS

During construction of metro tunnels data logging was undertaken in automatic form for each ring. TBM data logger includes various operational parameters, such as torque (MNm), thrust force (kN), advance speed (mm/min), penetration (rot/mm), grout injection (m³) and earth pressure (bar). A sample sheet of performance data taken from TBM data logger is given in Figure 6.1. By analyzing TBM data logger for each ring and with the help of geotechnical reports and site shift reports, the factors that make an effect on the performance of the TBM is determined.

Types of soils available on the line and tunnel cover thickness were determined by the geological section of the route and suitable soil classification was made, by prepared geotechnical reports, within the scope of soil types that correspond to the tunnel cross-section. The rings from TBM data logger, corresponding to the torque values equals to zero while approaching the stations, were excluded from the statistical analysis. The soil types at tunnel axis and their geotechnical specifications were given in Table 6.1.

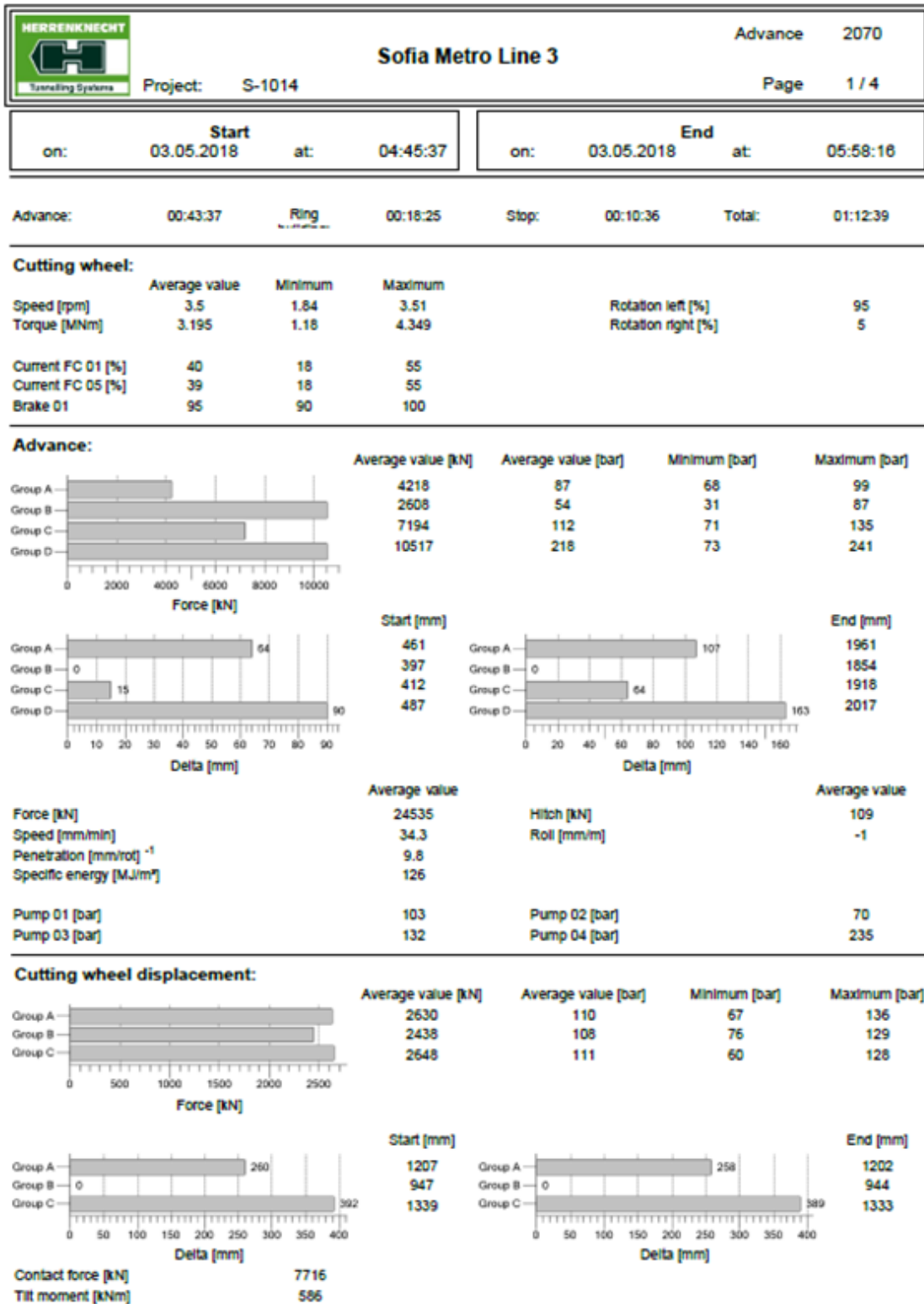


Figure 6.1. A sample sheet of performance data from TBM data logger (Ring No: 2.070).

Table 6.1. Geotechnical Parameters for Units Forming the Tunnel Alignment.

		Grain Size Analysis				Consistency Limits				
		% Gravel	% Sand	% Silt	% Clay	W_n (%)	W_L (%)	W_P (%)	I_P	I_C
4.1	Multicolored silty clay (Pliocene)	2.00	39.00	44.00	15.00	24.72	46.98	20.97	26.01	0.83
4.1a	Multicolored silty clay, structured (Pliocene)	0.09	11.04	60.72	28.15	51.55	85.84	39.31	46.54	0.70
4.3	Yellow-brown silty medium-grained sands	5.00	77.00	15.00	3.00	18.60	30.85	19.14	11.71	1.10
5.1	Grey silty clay (Pliocene)	1.08	28.04	58.65	12.22	30.08	54.57	28.74	25.83	0.93
5.1a	Grey silty clay, structured (Pliocene)	1.00	24.00	59.00	16.00	56.29	77.40	46.05	31.35	0.55
5.3	Grey silty medium-grained sands	4.00	81.00	13.00	2.00	19.11	29.11	20.41	8.70	1.20

Accordingly, 4.1, 4.1a, 5.1 and 5.1a lithologies were classified under “clayey” material class, and 4.3 and 5.3 were comprised of medium-grained sand. As mentioned in the parameters available in Table 6.1, and according to Figure 6.2; soil types having a liquid limit greater than 50% ($W_L > 50\%$) were classified to be “High Plasticity”, and soil types that having a liquid limit less than 50% ($W_L < 50\%$) were classified to be “Low Plasticity”. Accordingly, in Table 6.2 summary of the classification by soil types on the tunnel geology is defined.

Table 6.2. Geological Units Forming the Tunnel Alignment.

Lithology		Determined Soil Type (USCS)	
4.1	Multicolored Silty Clay (Pliocene)	Low Plasticity Clay	CL
4.1a	Multicolored Silty Clay, Structured (Pliocene)	High Plasticity Clay	CH
4.3	Yellow-brown Silty Medium-grained Sand	Medium-grained Sand	SM
5.1	Grey Silty Clay (Pliocene)	High Plasticity Clay	CH
5.1a	Grey Silty Clay/Clayey Silt, Structured (Pliocene)	High Plasticity Clay	CH
5.3	Grey Silty Medium-grained Sand	Medium-grained Sand	SM

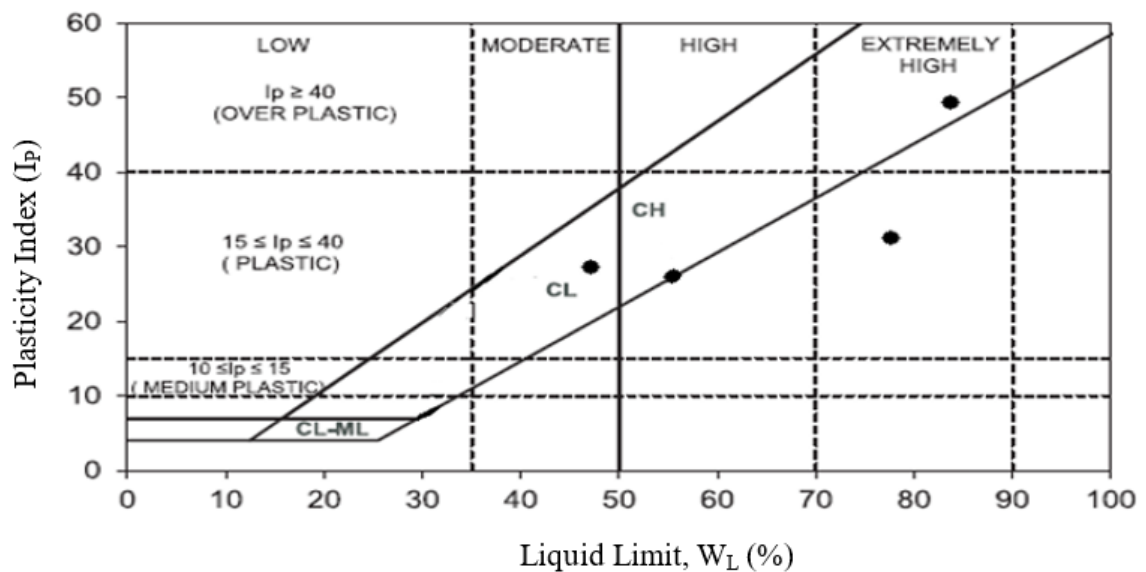


Figure 6.2. Plasticity Chart and Atterberg Limits (NAVFAC, 1986a).

According to Table 6.2, there are three soil types that are defined on the alignment and that are determined as CL, CH and SM on the basis of Unified Soil Classification System. Changes in performance parameters are examined according to aforementioned three types of soil.

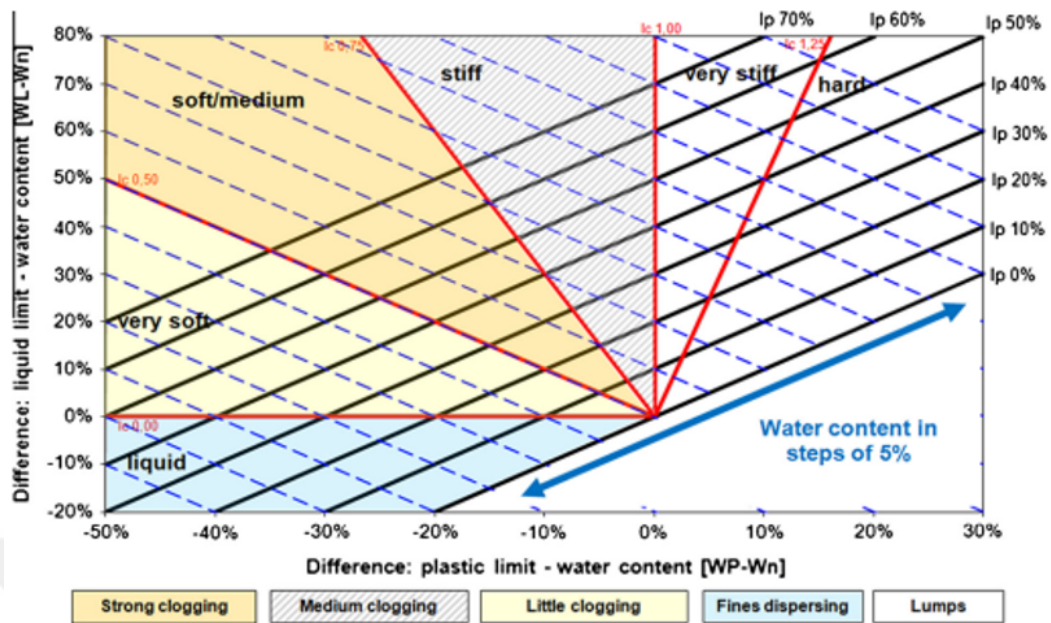


Figure 6.3. Classification diagram for critical consistency changes regarding clogging and dispersing (Hollmann and Thewes,2013).

As seen in Table 6.1 and Figure 6.3, consistency index which varies from 0.55 to 1.20 shows that the soil along the tunnel route could be classified as soft to firm.

Additionally, shift reports include information on the progress, duration of excavations and other works, reasons for stoppage and stoppage times. TBM performance analysis shall reveal the correlation between the operation parameters of the machine and soil type, and thus, main incidents that make an effect on the performance of the machine shall be determined. Analysis is critical in terms of the information backlog required for such projects that shall be implemented in the future.

6.1. Effects of Observed Parameters on Performance

6.1.1. Cutterhead Torque Values During TBM Operation

Figure 6.4 presents the operational torque of cutting head during the construction of tunnel. The mean torque applied during excavation is shown on the plot. The highest cutterhead torque was achieved at 7.43 MNm, while the lowest was achieved at 1.02

MNm. The mean torque value for the entire line was 3.75 MNm. On the basis of the types of soils on Figure 6.5, the EPB TBM torque values generally shows an increase on sandy soil.

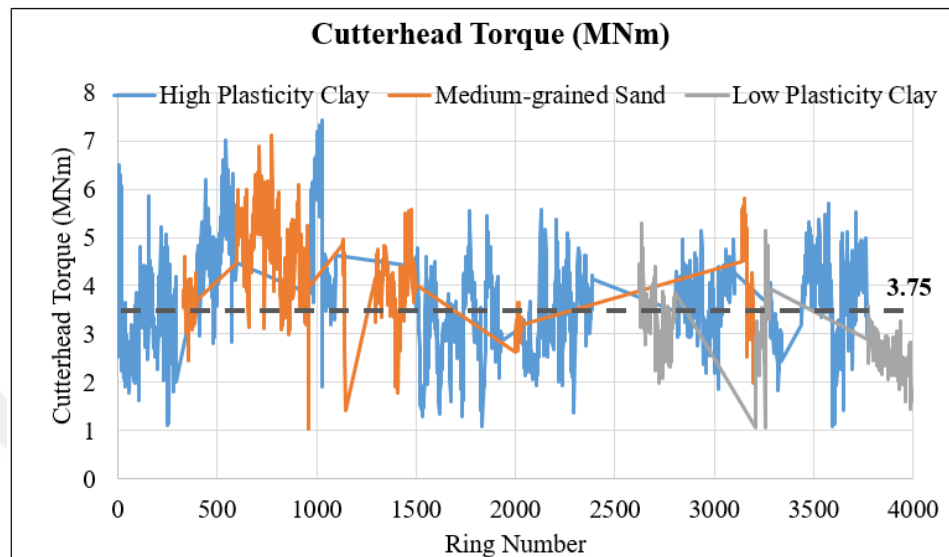


Figure 6.4. The Mean Cutterhead Torque values along the alignment.

Cutterhead torque changes in high plasticity clay, medium-grained sand and low plasticity clay soil types according to the ring number is shown in Figure 6.5, Figure 6.6 and Figure 6.7 respectively. According to Figure 6.5, along the entire tunnel line mean torque value is 3.69 MNm for high plasticity clays.

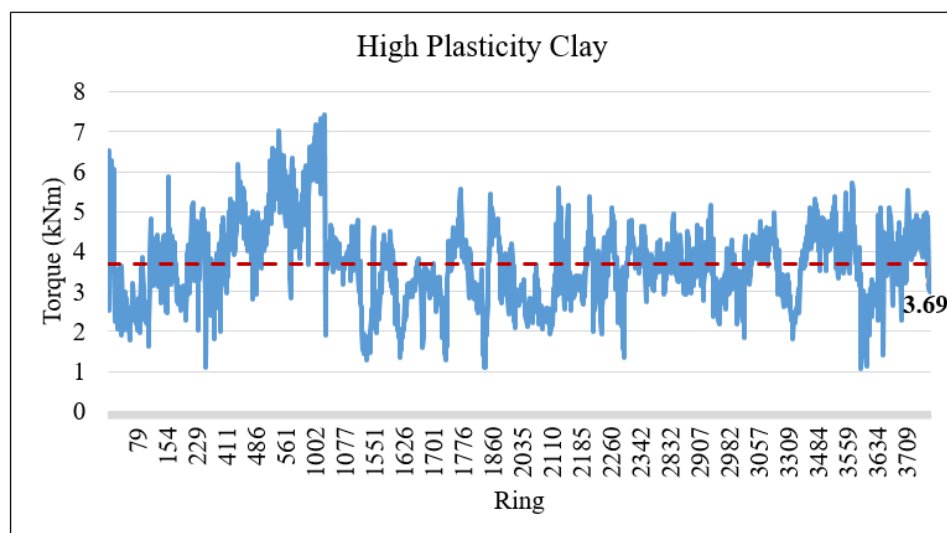


Figure 6.5. Cutterhead Torque Change in High Plasticity Clay Soil.

As seen in Figure 6.6, along the entire tunnel line mean torque value is 4.31 MNm for medium-grained sand.

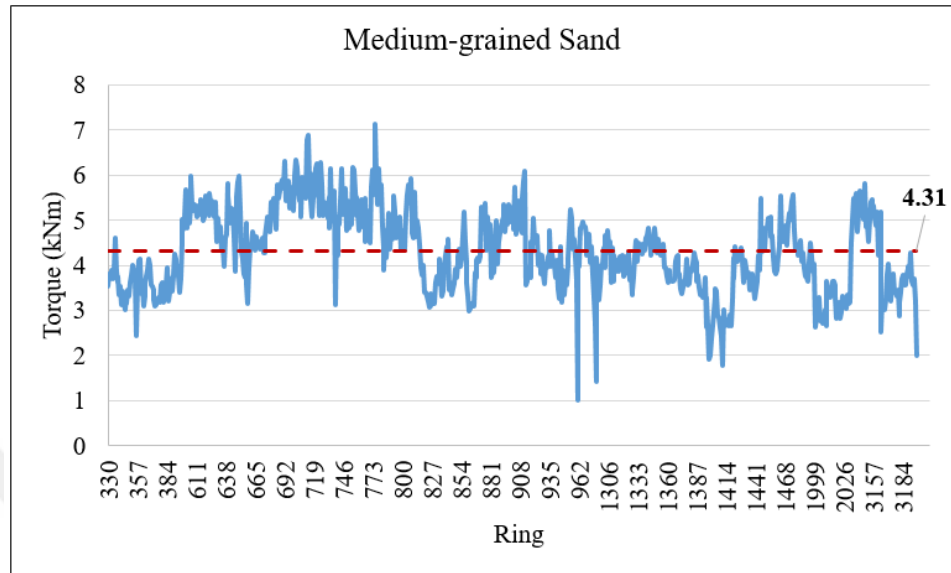


Figure 6.6. Cutterhead Torque Change in Medium-grained Sand Soil.

According to Figure 6.7 the mean cutterhead torque value along the entire line is 2.95 MNm for low plasticity clay.

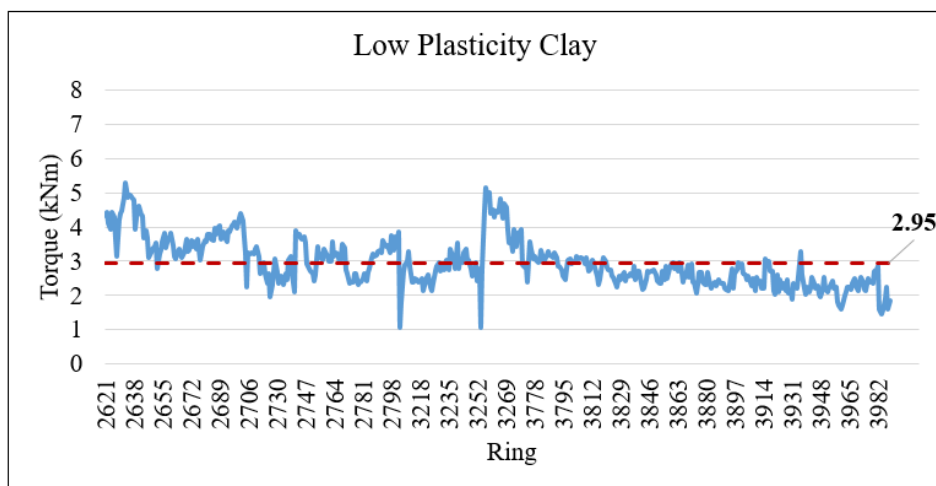


Figure 6.7. Cutterhead Torque Change in Low Plasticity Clay Soil.

6.1.2. Thrust Force Values During TBM Operation

Figure 6.8 presents the operational thrust of TBM during the construction of tunnel. The mean thrust applied during excavation is shown on the plot. The highest thrust force was observed at 47,300 kN, while the lowest was observed at 3,210 kN. The mean thrust value for the entire line was 26,200 kN.

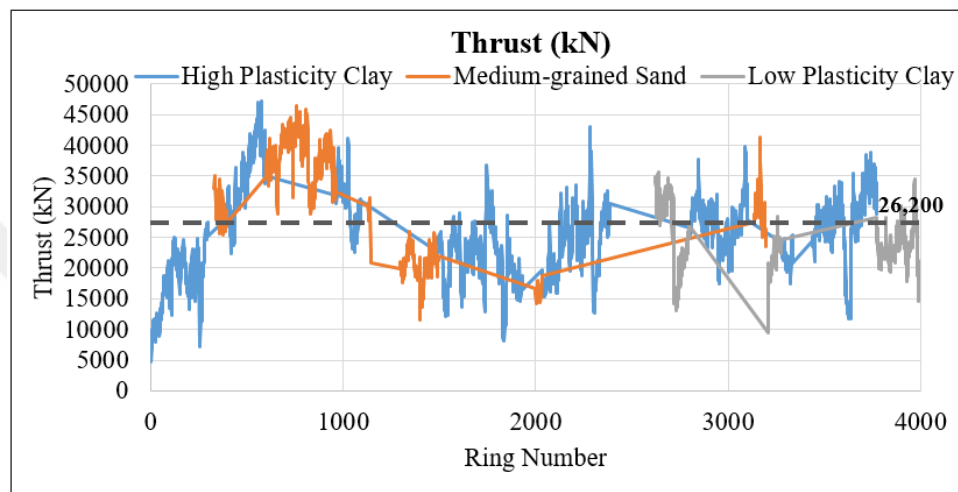


Figure 6.8. The Mean Thrust Force values along the alignment.

According to Figure 6.9, along the entire tunnel line mean thrust force value was 25.300 kN for high plasticity clay. It can be seen from the same Figure 6.9 that the thrust force is also a function of the earth pressure. Where the mean earth pressure was 1.02 bar, the thrust force was relatively lower and where the mean earth pressure was 1.87, the thrust force was relatively higher. In the section where the thrust force circulates around 25.300 kN, the mean earth pressure was around 1.59.

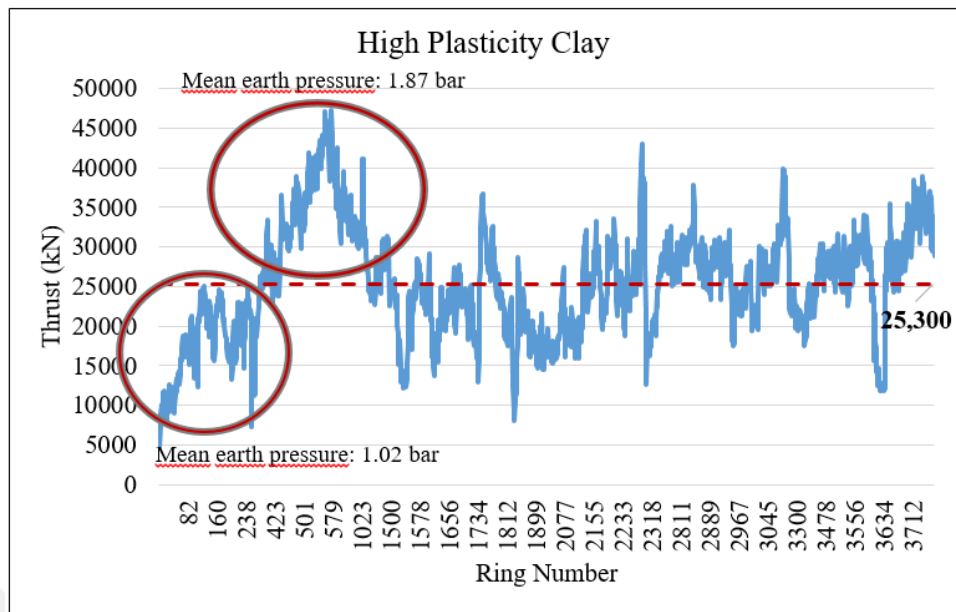


Figure 6.9. Thrust Force Change in High Plasticity Clay Soil.

As seen in Figure 6.10, along the entire tunnel line mean thrust force value is 30.900 kN for medium-grained sand. However, between ring numbers 400 to 1000 we see a clearly higher value when compared to the ring numbers 1300 and 3200. This seems to be related again with the earth pressure. The thrust force was relatively higher when the mean earth pressure was 2.30 bar and the thrust was relatively lower when the mean earth pressure was 1.15 bar.

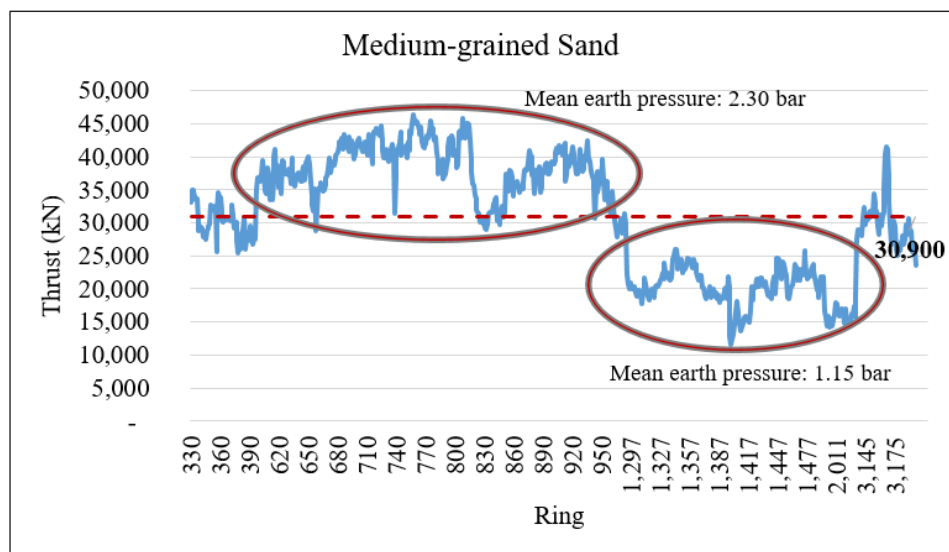


Figure 6.10. Thrust Force Change in Medium-grained Sand Soil.

According to Figure 6.11 the mean thrust force value along the entire line is 24,500 kN for low plasticity clay. The earth pressure also in this section seems to be a major parameter effecting the thrust force.

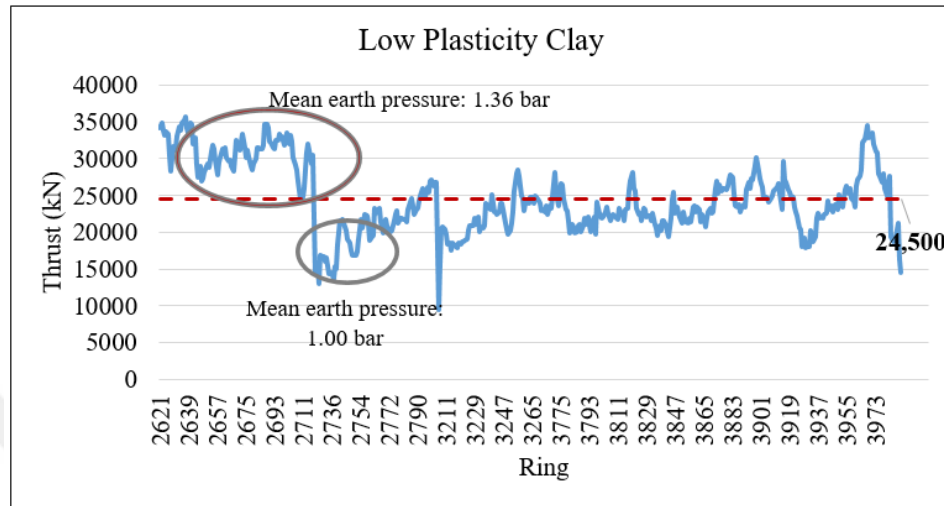


Figure 6.11. Thrust Force Change in Low Plasticity Clay Soil.

6.1.3. Specific Energy Values During TBM Operation

The values calculated from the MJ/m^3 unit on the machine indicators based on the ring on the whole tunnel route are expressed in Figure 6.12. The specific energy was calculated by dividing the net power by net cutting rate in volume per unit time. The net cutting rate was predicted based on the advance speed of the thrust cylinders. The highest specific energy was observed at $123.96 \text{ MJ}/\text{m}^3$, while the lowest was observed at $5.53 \text{ MJ}/\text{m}^3$. The mean specific energy value for the entire line was $26.93 \text{ MJ}/\text{m}^3$.

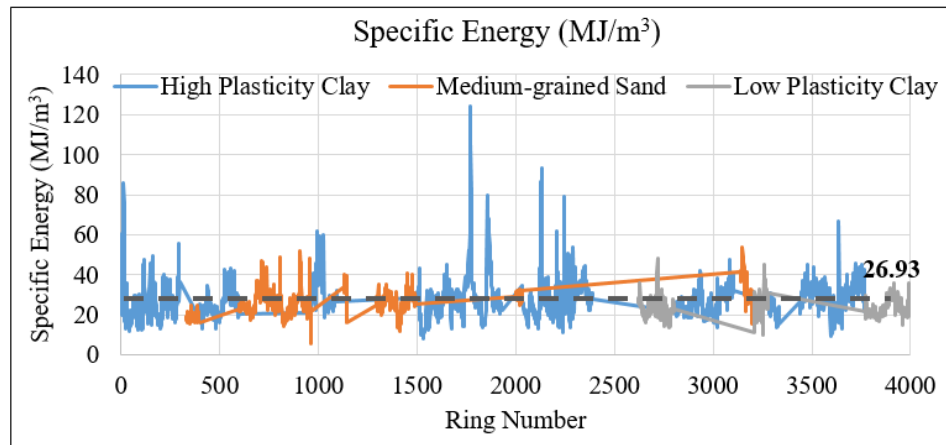


Figure 6.12. The Mean Specific Energy values along the alignment.

As seen in Figure 6.13, along the entire tunnel line mean specific energy value is 27.57 MJ/m³ for high plasticity clays.

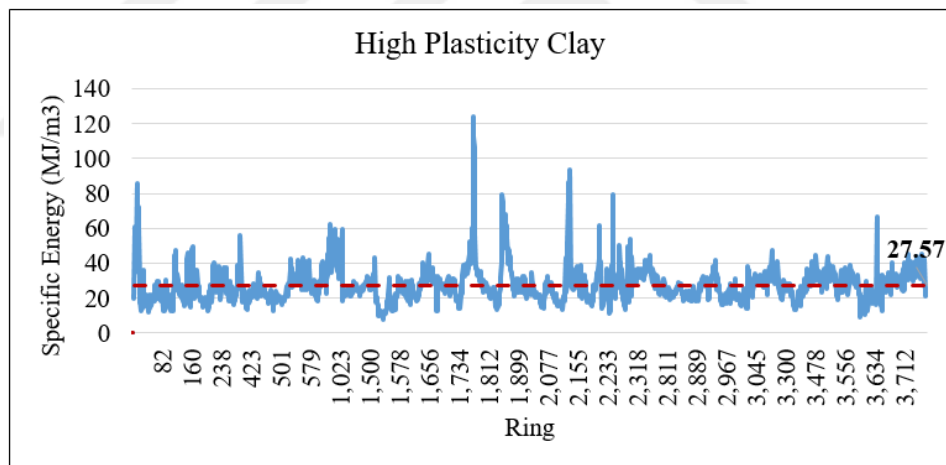


Figure 6.13. Specific Energy Change in High Plasticity Clay Soil.

According to Figure 6.14, along the entire tunnel line mean specific energy value is 26.10 MJ/m³ for medium-grained sand.

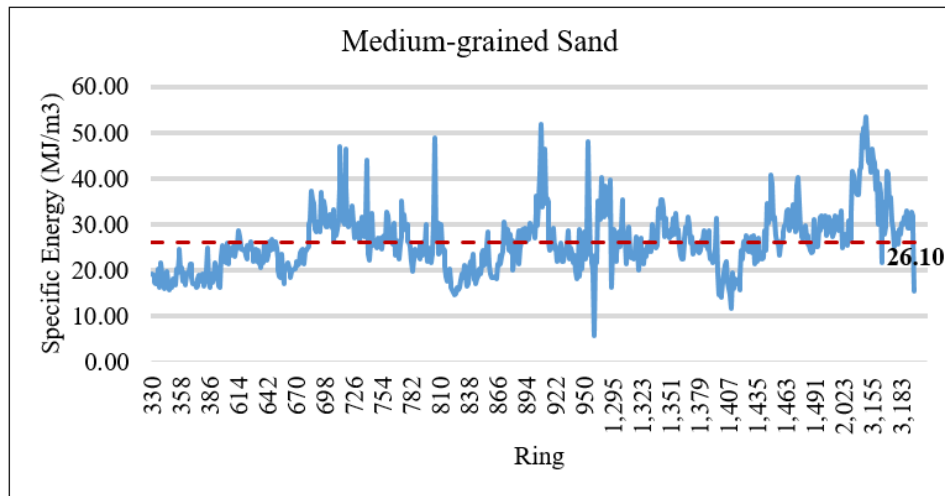


Figure 6.14. Specific Energy Change in Medium-grained Sand Soil.

According to Figure 6.15 the mean specific energy value along the entire line is 23.28 MJ/m³ for low plasticity clay.

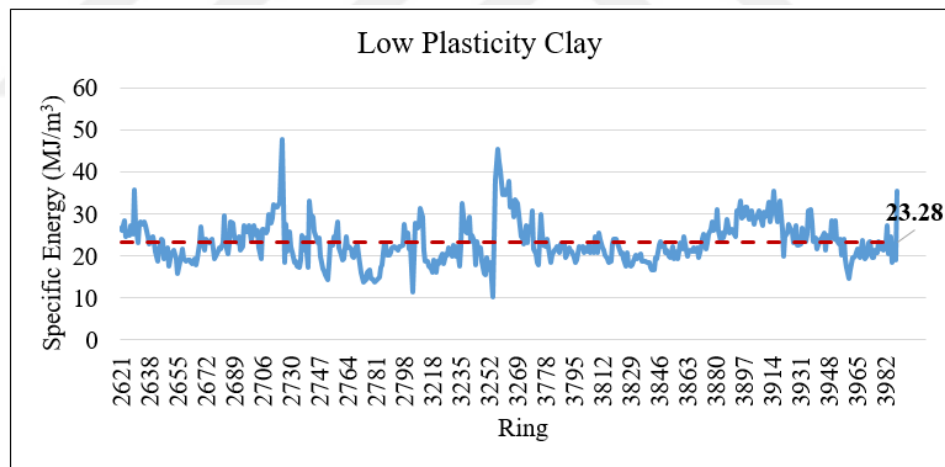


Figure 6.15. Specific Energy Change in Low Plasticity Clay Soil.

6.1.4. Instantaneous Cutting Rate Values During TBM Operation

The instantaneous cutting rate values calculated from the m³/h unit on the machine indicators based on the ring on the whole tunnel route are expressed in Figure 6.16. The highest instantaneous cutting rate was observed at 304 m³/h, while the lowest was observed at 27.8 m³/h. The mean instantaneous cutting rate value for the

entire line was $165.7 \text{ m}^3/\text{h}$.

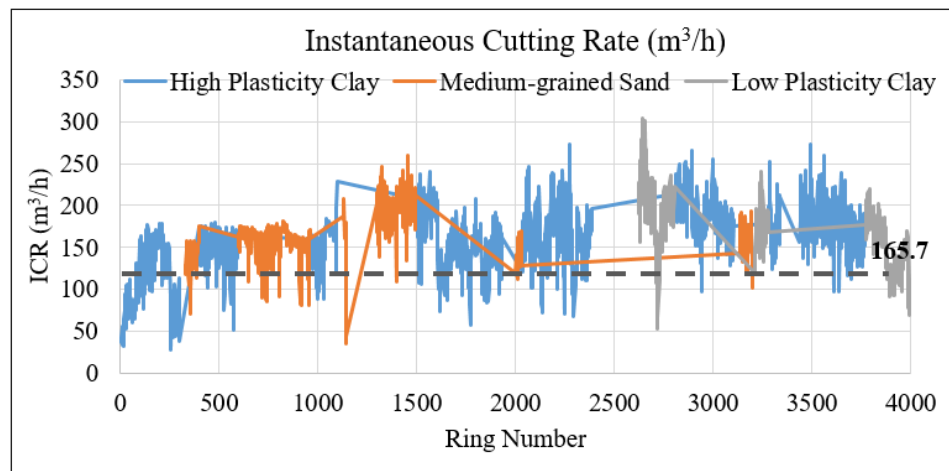


Figure 6.16. The Mean Instantaneous Cutting Rate values along the alignment.

As seen in Figure 6.17, along the entire tunnel line mean instantaneous cutting rate value is $160.5 \text{ m}^3/\text{h}$ for high plasticity clays.

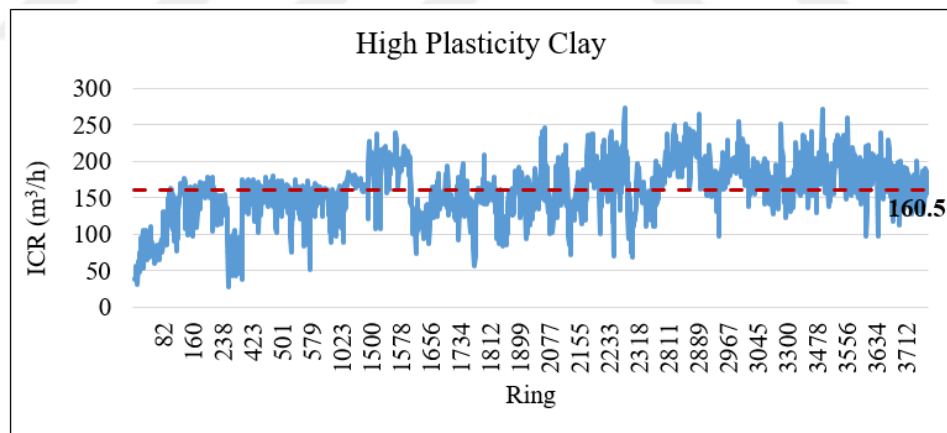


Figure 6.17. Instantaneous Cutting Rate Change in High Plasticity Clay Soil.

Along the entire tunnel line mean instantaneous cutting rate value is $165.8 \text{ m}^3/\text{h}$ for medium-grained sand as expressed in Figure 6.18.

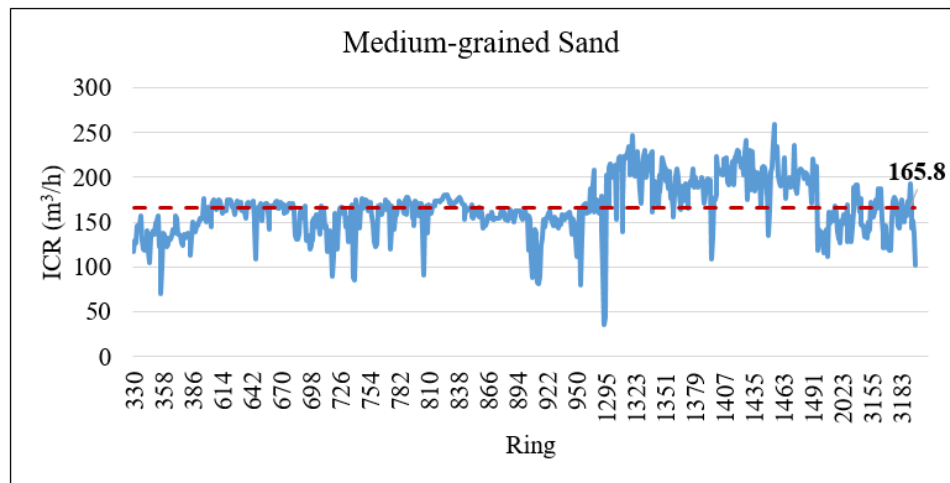


Figure 6.18. Instantaneous Cutting Rate Change in Medium-grained Sand Soil.

According to Figure 6.19 the mean instantaneous cutting rate value along the entire line is 170.9 m³/h for low plasticity clay.

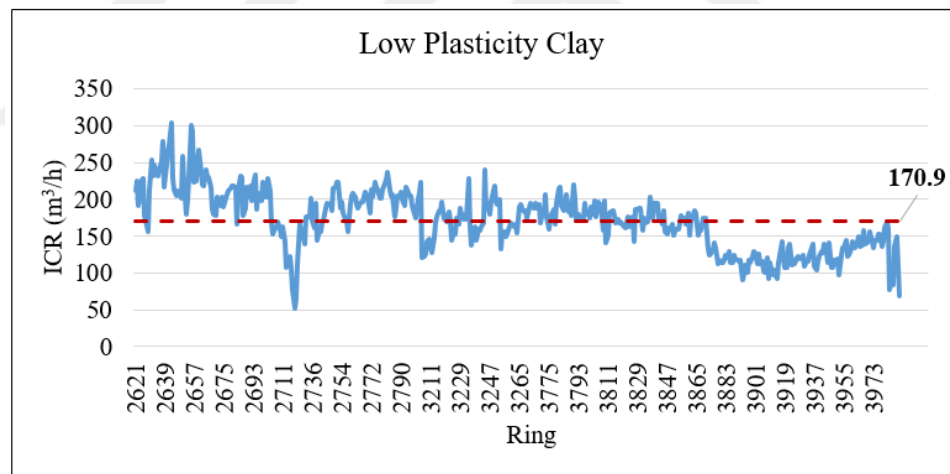


Figure 6.19. Instantaneous Cutting Rate Change in Low Plasticity Clay Soil.

6.1.5. Applied Earth Pressure Values During TBM Operation

EPB TBM is equipped with 5 pressure cells on the bulkhead. During the analysis of face pressures for have better results only 1 sensor (P1) is considered considering the clogging effect of sticky material. The upper load pressure cell “P1” is installed 2,08 m below the shield top. The face pressures logged during construction from P1 sensor is presented in Figure 6.20. The highest earth pressure was applied at 2.74 bar.

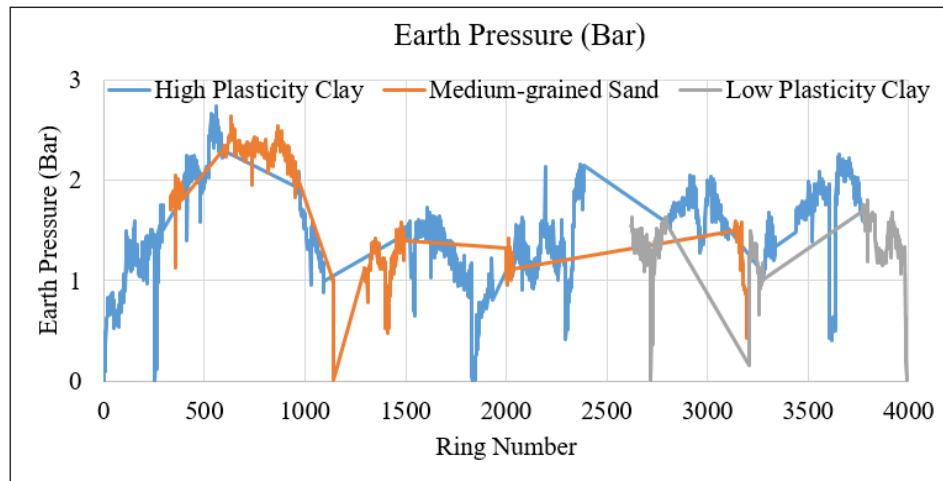


Figure 6.20. Face pressures along the alignment.

As seen in Figure 6.21, the earth cover along the entire alignment is ranging from the minimum overburden of 5,2 m (after leaving the launching shaft) up to 21,3 m at 10+850. As the overburden increases, the earth pressure is also increases in parallel. Between the chainage 10+000.00 and 11+500.00 the overburden reaches to its maximum value. As expected, the earth pressure value also increased slightly for this 1,5 km interval.

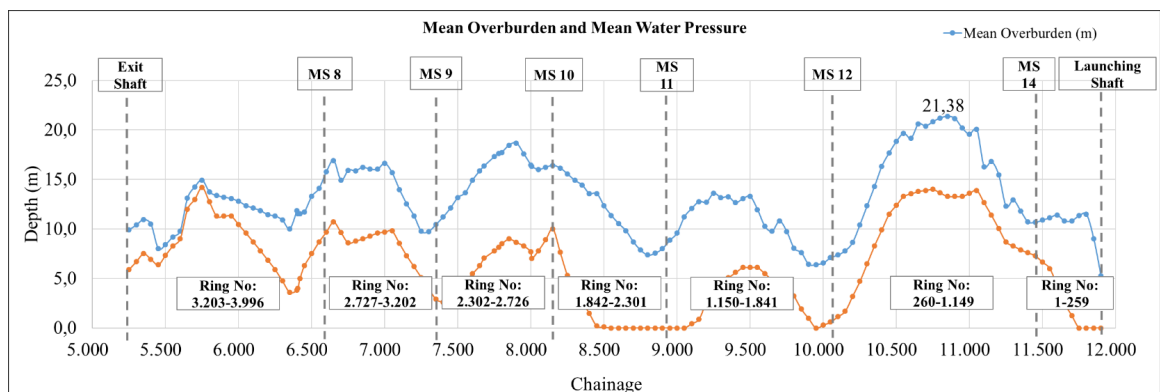


Figure 6.21. Mean Overburden and Mean Water Pressure along the alignment.

6.2. Comparison of Calculated Performance Parameters

Correlation coefficient, R^2 value was calculated with the assistance of Microsoft Office Excell 365 program in order to compare the level of correlation between currently

available TBM operational parameters and relative data. In Table 6.3, you may find the comments that may be made in relation with the correlation coefficient value.

Table 6.3. Interpreting the Size of a Correlation Coefficient.

R^2	Interpretation
<0.25	No Relationship
0.25-0.50	Weak Relationship
0.50-0.65	Moderate Relationship
0.65-0.80	High Relationship
>0.80	Very High Relationship

6.2.1. Comparison of the Torque and Thrust

Cutterhead torque value and thrust force make a direct effect on the power requirement of the machine. Therefore, the correlation between them was observed. As it may be observed in Figure 6.22, there is a low-grade and directly proportional exponential relationship with $R^2=0.43$ between thrust value and torque value on the soil type of High Plasticity Clay.

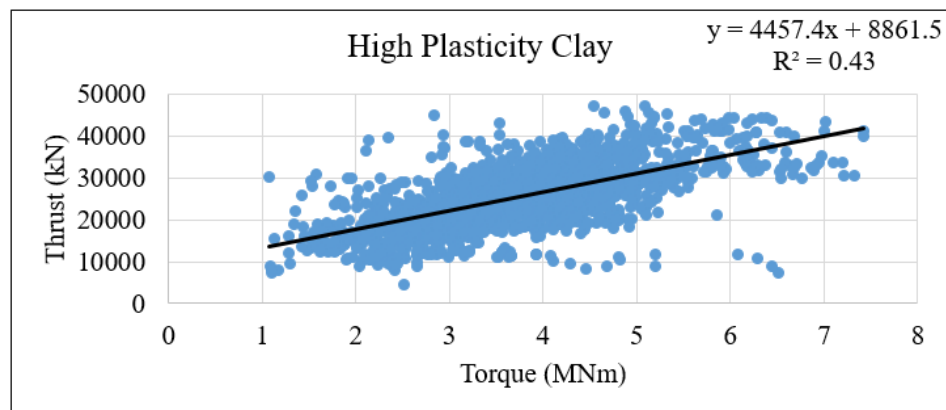


Figure 6.22. Relationship between Torque and Thrust values in High plasticity clay.

As it may be observed in Figure 6.23, there is a low-grade and directly proportional correlation with $R^2=0.41$ between thrust force and cutterhead torque value on medium-grained sand.

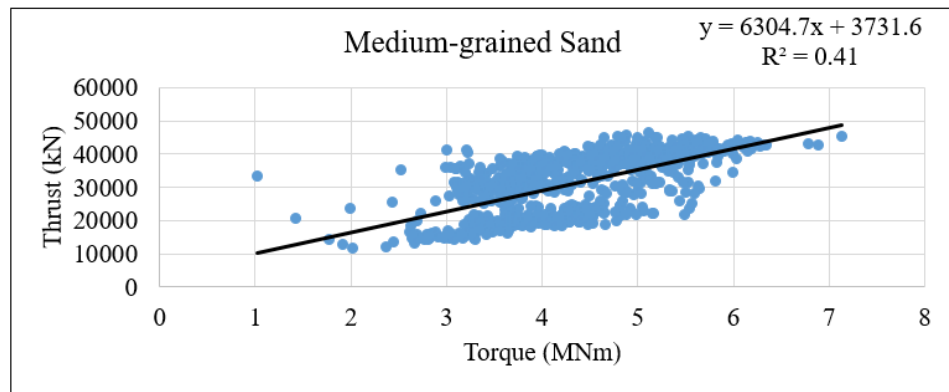


Figure 6.23. Relationship between Torque and Thrust values in Medium-grained sand.

According to Figure 6.24, there is a low-grade and directly proportional correlation with $R^2=0.25$ between thrust and torque value on low plasticity clay.

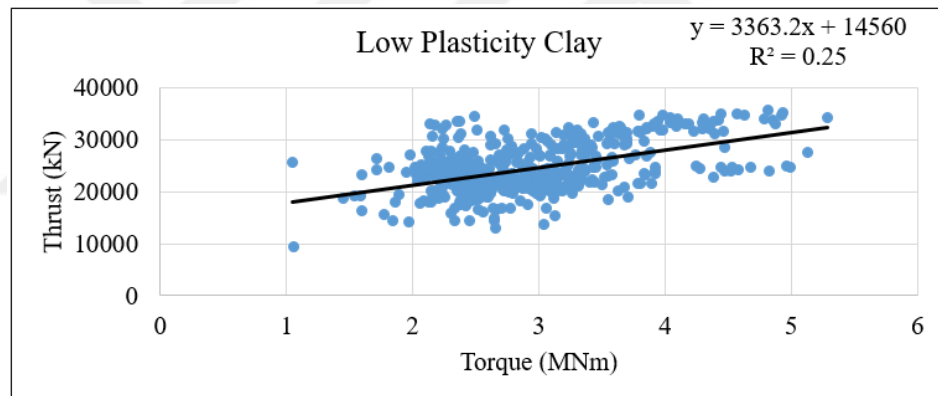


Figure 6.24. Relationship between Torque and Thrust values in Low plasticity clay.

6.2.2. Comparison of the Torque and Penetration

It was considered that the required torque value shall increase with the escalation of penetration value, and the correlation between the two is researched for such purpose. As it may be observed in Figure 6.25, in terms of high plasticity soils, there is no correlation between penetration value and torque value based on the value of $R^2=0.10$.

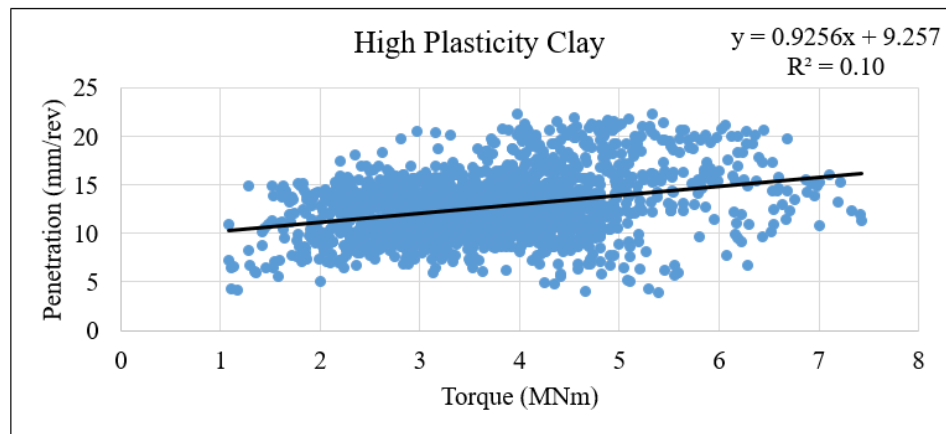


Figure 6.25. Relationship between Torque and Penetration values in High plasticity clay.

As it may be observed in Figure 6.26, in terms of medium-grained sand, there is no correlation between penetration value and torque value based on the value of $R^2=0.13$.

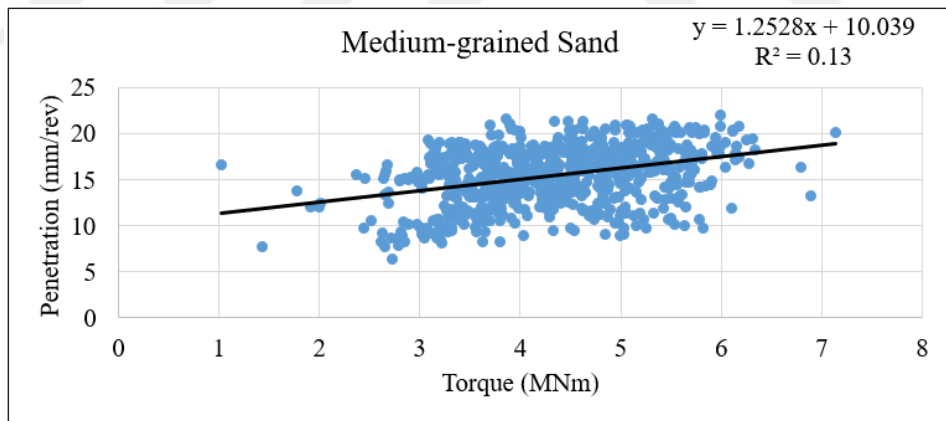


Figure 6.26. Relationship between Torque and Penetration values in Medium-grained sand.

According to Figure 6.27, in terms of low plasticity clay, there is a directly proportional and weak correlation between penetration value and torque value based on the value of $R^2=0.39$ in comparison to other types of soil.

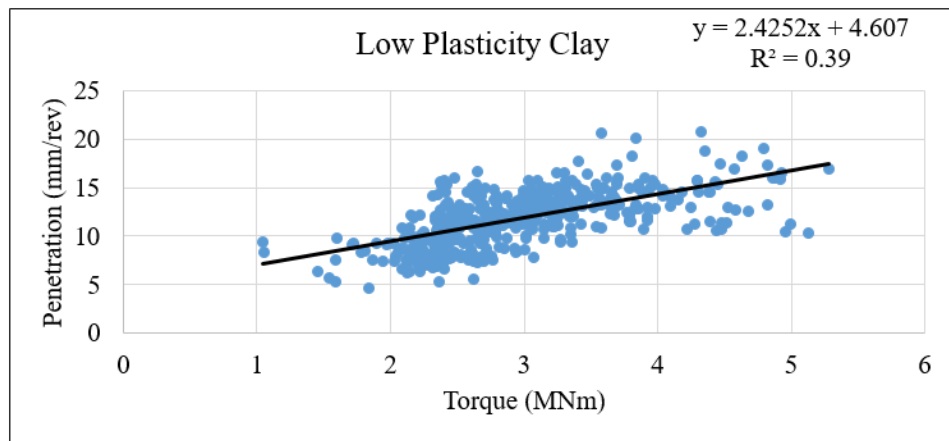


Figure 6.27. Relationship between Torque and Penetration values in Low plasticity clay.

6.2.3. Comparison of the Thrust and Penetration

As it may be observed in Figure 6.28, in terms of high plasticity clay, there is no correlation between penetration value and thrust value based on the value of $R^2=0.08$.

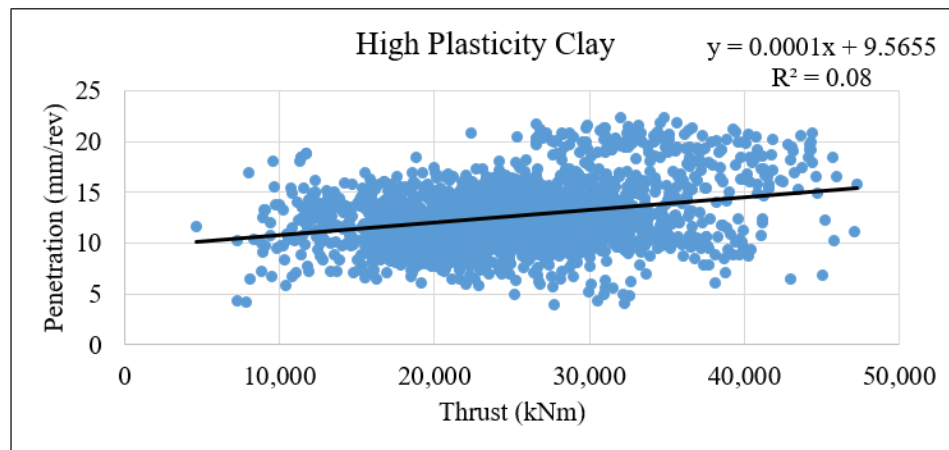


Figure 6.28. Relationship between Thrust Force and Penetration values in High plasticity clay.

According to Figure 6.29, in terms of medium-grained sand, there is a directly proportional and weak correlation between penetration value and thrust value based on the value of $R^2=0.26$ in comparison to other types of soil.

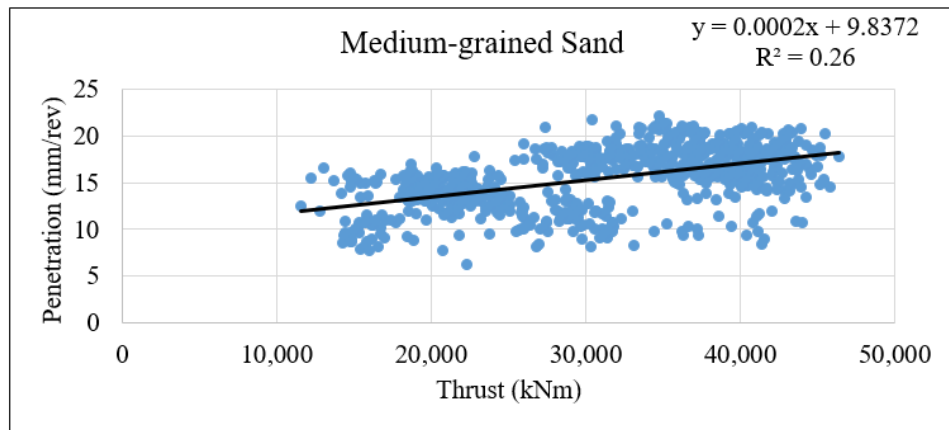


Figure 6.29. Relationship between Thrust Force and Penetration values in Medium-grained sand.

As seen in Figure 6.30, in terms of low plasticity clay, there is no correlation between penetration value and thrust value based on the value of $R^2=0.06$.

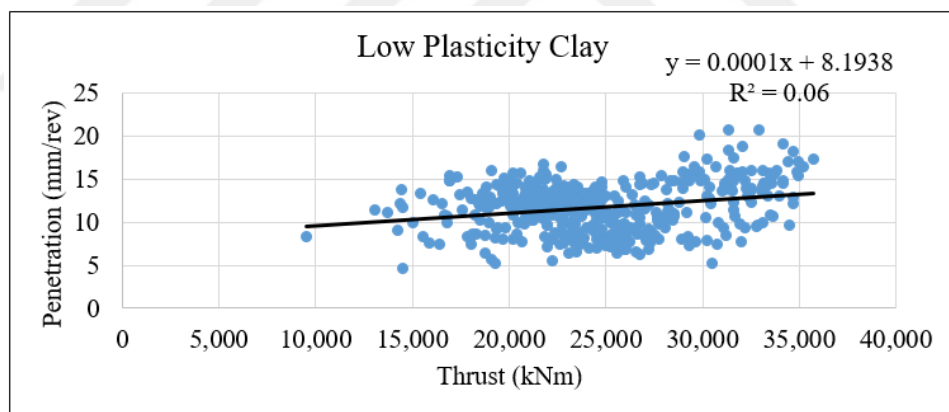


Figure 6.30. Relationship between Thrust Force and Penetration values in Low plasticity clay.

6.2.4. Comparison of the Penetration and Specific Energy

According to Figure 6.31, Figure 6.32 and Figure 6.33 in terms of high plasticity clay, medium-grained sand and low plasticity clay there is a weak relation between specific energy value and penetration value based on the value of $R^2=0.25$, $R^2=0.32$ and $R^2=0.22$ respectively.

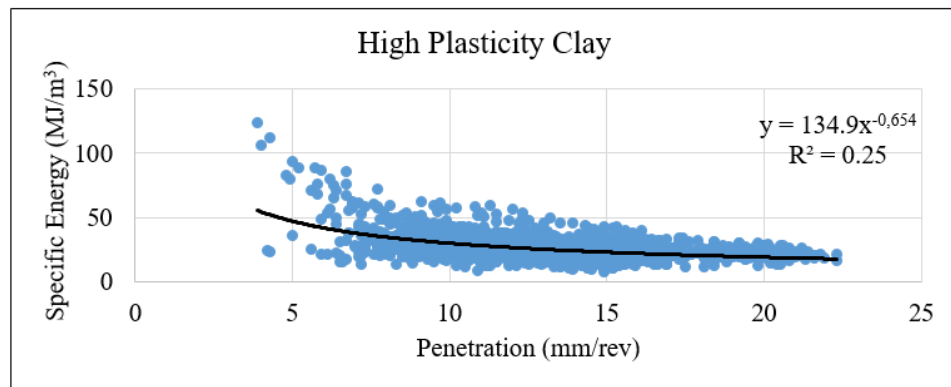


Figure 6.31. Relationship between Penetration and Specific Energy values in High plasticity clay.

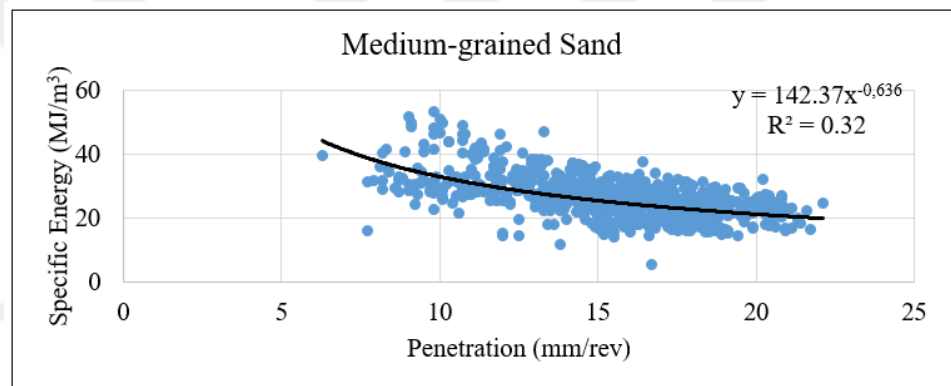


Figure 6.32. Relationship between Penetration and Specific Energy values in Medium-grained sand.

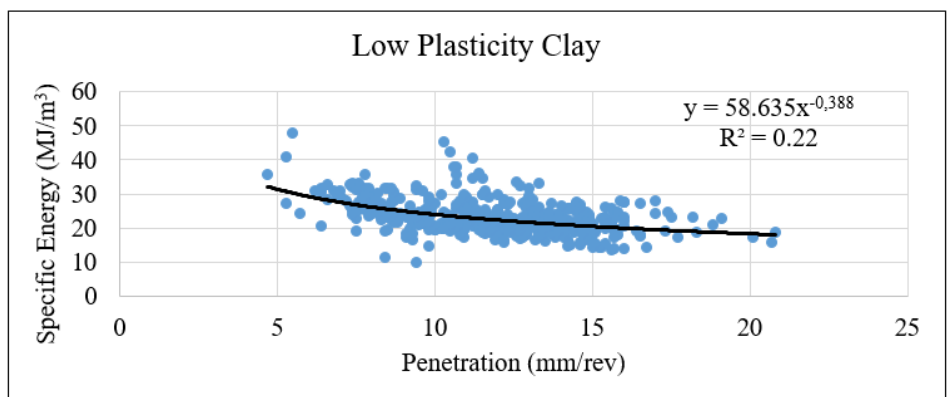


Figure 6.33. Relationship between Penetration and Specific Energy values in Low plasticity clay.

6.2.5. Comparison of the Consistency Index and Cutterhead Torque

Taking into account the entire line for all soil types, the variation of consistency index values according to cutterhead torque is shown in Figure 6.34. As can be seen there is a moderately strong relationship between consistency index and cutterhead torque, and the torque requirement increases with an increasing consistency index.

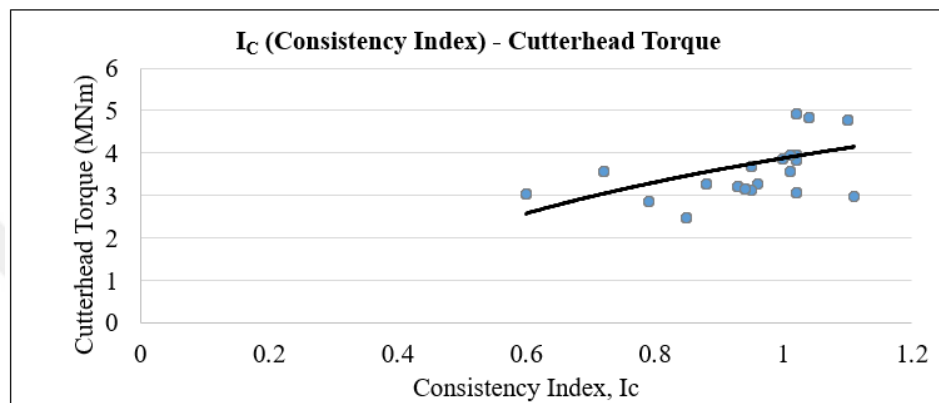


Figure 6.34. Relationship between Consistency Index and Cutterhead Torque.

6.2.6. Comparison of Instantaneous Cutting Rate and Plastic Limit

The relationship obtained between instantaneous cutting rate and plastic limit is represented in Figure 6.35. According to the results, a moderately strong relationship exists between the instantaneous cutting rate and plastic limit, and the instantaneous cutting rate decreases with an increasing plastic limit.

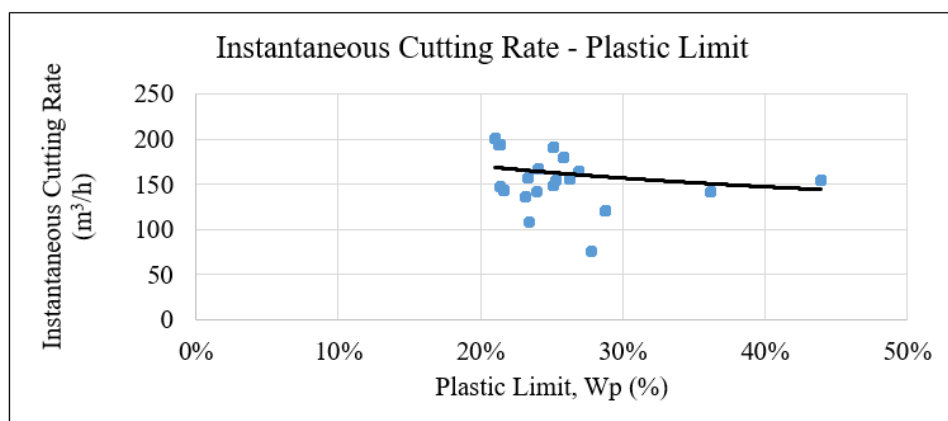


Figure 6.35. Relationship between Instantaneous Cutting Rate and Plastic Limit.

6.3. Variation of Performance Parameters Under Different Earth Pressures

The tunnel alignment was divided into 5 sections in terms of average earth pressure measured by earth pressure sensor no 1 (P1). In this classification, which is made in consideration of EPB pressure applied, change in various operational parameters, such as cutterhead torque, thrust force, instantaneous cutting rate and specific energy etc., is examined under determined pressures respectively by the type of soil. These pressure values ranged between (0.0-0.5) bar, (0.5-1.0) bar, (1.0-1.5) bar, (1.5-2.0) bar and (2.0-3.0) bar.

6.3.1. Effects of Observed Parameters Under (0.0-0.5) Bar Earth Pressure

As seen in Table 6.4, the results indicate that between 0.0 Bar and 0.5 Bar earth pressure section, the mean cutterhead torque, specific energy and instantaneous cutting rate values are higher, the thrust force value is lower are for high plasticity clays.

Table 6.4. Variations in EPB TBM operational parameters during excavation of (0.0-0.5) bar earth pressure section.

Mean Operational Parameters	High Plasticity Clay	Medium-grained sand	Low Plasticity Clay
Torque (Mnm)	3.31	2.20	1.77
Specific Energy (MJ/m ³)	31.1	21.7	21.9
Earth Pressure (Bar)	0.25	0.28	0.26
Thrust Force (kN)	14,190	20,300	15,690
ICR (m ³ /h)	107	97	103

Due to reason that the support pressure in the excavation chamber is generated by the thrusting the tunneling machine against the face, it is observed that there is directly proportional relationship with mean earth pressure and thrust force. The mean thrust force value increases with an increasing earth pressure. The field-specific energy for excavation of the high plasticity soil was greater than the values obtained

during excavation of the other soils. Also, the cutterhead torque requirement, which is a function of the consumed power, increases with an increasing specific energy for high plasticity clay and low plasticity clay.

The mean instantaneous cutting rate values for the soils high plasticity clay, medium-grained sand and low plasticity clay are $107 \text{ m}^3/\text{h}$, $97 \text{ m}^3/\text{h}$ and $103 \text{ m}^3/\text{h}$, respectively. The highest mean instantaneous cutting rate was achieved during excavation of the high plasticity clay soil at $107 \text{ m}^3/\text{h}$, while the lowest was achieved during excavation of the medium-grained sand at $97 \text{ m}^3/\text{h}$.

As seen in Figure 6.36, foam installation values ranged between 200 and 400. Under (0.0-0.5) bar earth pressure section, the mean foam installation value is 2771/min.

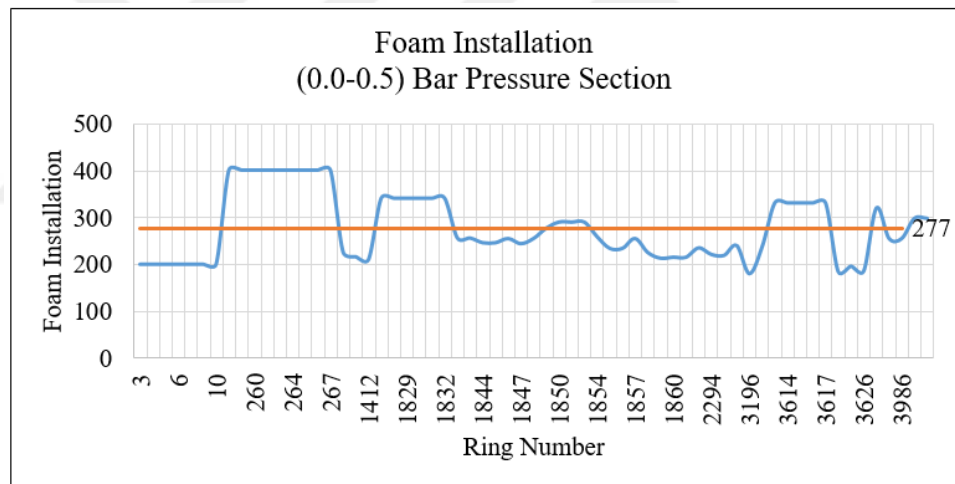


Figure 6.36. Foam Installation along the (0.0-0.5) Bar Pressure Section .

6.3.2. Effects of Observed Parameters Under (0.5-1.0) Bar Earth Pressure

As indicated in Table 6.5, the earth pressures between 0.5 Bar and 1.0 Bar the performance parameters, such as torque and specific energy are similar for high plasticity clay and low plasticity clay.

It is observed that there is directly proportional relationship with mean earth pressure and thrust force. The mean thrust force value increases with an increasing

earth pressure for low plasticity clay.

The mean instantaneous cutting rate values for the soils high plasticity clay, medium-grained sand and low plasticity clay are 128 m³/h, 184 m³/h and 147 m³/h, respectively. The highest mean instantaneous cutting rate was achieved during excavation of the medium-grained sand soil at 184 m³/h, while the lowest was achieved during excavation of the high plasticity clay at 128 m³/h.

Table 6.5. Variations in EPB TBM operational parameters during excavation of (0.5-1.0) bar earth pressure section.

Mean Operational Parameters	High Plasticity Clay	Medium-grained sand	Low Plasticity Clay
Torque (Mnm)	3.16	3.25	3.16
Specific Energy (MJ/m ³)	27.8	23.4	28.1
Earth Pressure (Bar)	0.77	0.76	0.86
Thrust Force (kN)	17,270	20,700	21,200
ICR (m ³ /h)	128	184	147

According to Figure 6.37, foam installation values ranged between 180 and 401. Under (0.5-1.0) bar earth pressure section, the mean foam installation value is 262 l/min.

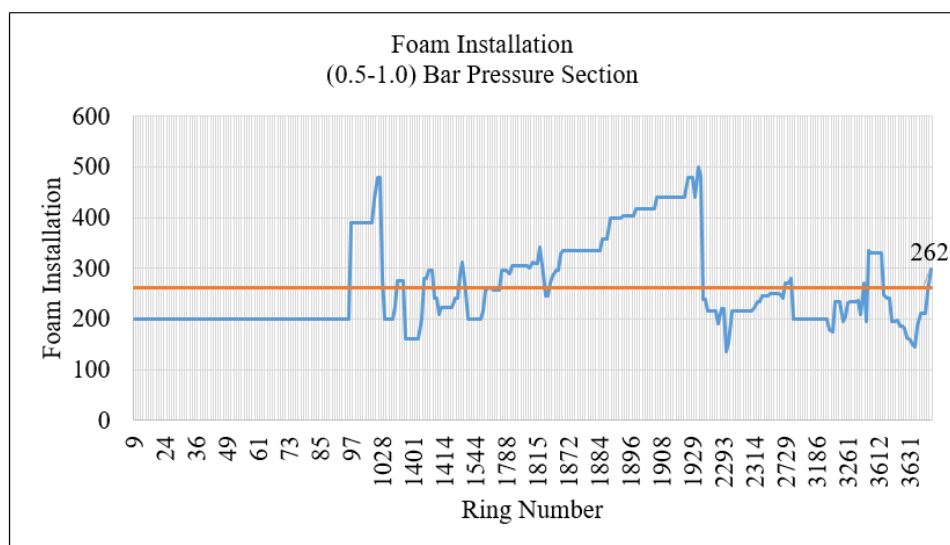


Figure 6.37. Foam Installation along the (0.5-1.0) Bar Pressure Section.

6.3.3. Effects of Observed Parameters Under (1.0-1.5) Bar Earth Pressure

As seen in Table 6.6, the results indicate that between 1.0 Bar and 0.5 Bar earth pressure section, the mean cutterhead torque and specific energy values are higher for medium-grained sand.

Due to reason that the support pressure in the excavation chamber is generated by the thrusting the tunneling machine against the face, it is observed that there is directly proportional relationship with mean earth pressure and thrust force. The mean thrust force value increases with an increasing earth pressure for low plasticity clay.

The field-specific energy is in parallel to the cutterhead torque requirement, which is a function of the consumed power.

The mean instantaneous cutting rate values for the soils high plasticity clay, medium-grained sand and low plasticity clay are 159 m³/h, 184 m³/h and 170 m³/h, respectively. The highest mean instantaneous cutting rate was achieved during excavation of the medium-grained sand soil at 184 m³/h, while the lowest was achieved during excavation of the high plasticity clay at 159 m³/h.

As seen in Figure 6.38, foam installation values ranged between 168 and 500. Between 0.0 Bar and 0.5 Bar earth pressure section, the mean foam installation value is 305 l/min.

Table 6.6. Variations in EPB TBM operational parameters during excavation of (1.0-1.5) bar earth pressure section.

Mean Operational Parameters	High Plasticity Clay	Medium-grained sand	Low Plasticity Clay
Torque (Mnm)	3.45	4.01	2.97
Specific Energy (MJ/m ³)	27.5	28.7	23.4
Earth Pressure (Bar)	1.28	1.22	1.30
Thrust Force (kN)	23,400	21,900	24,000
ICR (m ³ /h)	159	184	170

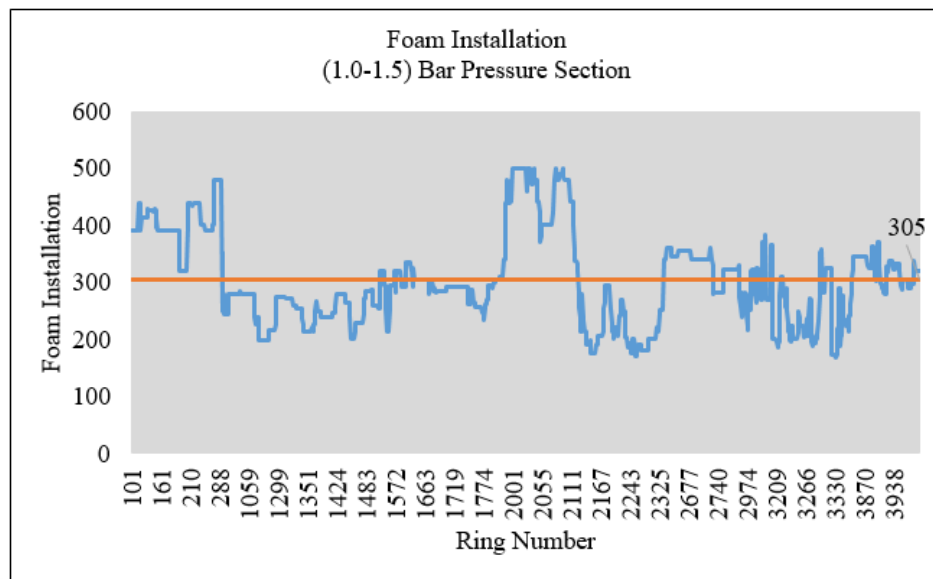


Figure 6.38. Foam Installation along the (1.0-1.5) Bar Pressure Section.

6.3.4. Effects of Observed Parameters Under (1.5-2.0) Bar Earth Pressure

According to Table 6.7, the results indicate that between 1.5 Bar and 2.0 Bar earth pressure section, the mean cutterhead torque, specific energy and thrust force values are higher, the instantaneous cutting rate value is lower are for medium-grained sands.

It is observed that there is directly proportional relationship with mean earth pressure and thrust force. The mean thrust force value increases with an increasing earth pressure for medium-grained sand.

In parallel to the cutterhead torque requirement, the field-specific energy for excavation of the high plasticity clay and medium-grained sand soil was very close for each other which is greater that of the values obtained during excavation of the low plasticity clay soils.

The mean instantaneous cutting rate values for the soils high plasticity clay, medium-grained sand and low plasticity clay are 177 m³/h, 146 m³/h and 179 m³/h,

respectively. The highest mean instantaneous cutting rate was achieved during excavation of the low plasticity clay soil at 179 m³/h, while the lowest was achieved during excavation of the medium-grained sand at 146 m³/h.

As seen in Figure 6.39, foam installation values ranged between 189 and 481. Between 1.5 Bar and 2.0 Bar earth pressure section, the mean foam installation value is 307 l/min.

Table 6.7. Variations in EPB TBM operational parameters during excavation of (1.5-2.0) bar earth pressure section

Mean Operational Parameters	High Plasticity Clay	Medium-grained sand	Low Plasticity Clay
Torque (Mnm)	3.81	3.95	2.96
Specific Energy (MJ/m ³)	27.4	27.5	22.4
Earth Pressure (Bar)	1.73	1.75	1.58
Thrust Force (kN)	27,400	29,800	24,200
ICR (m ³ /h)	177	146	179

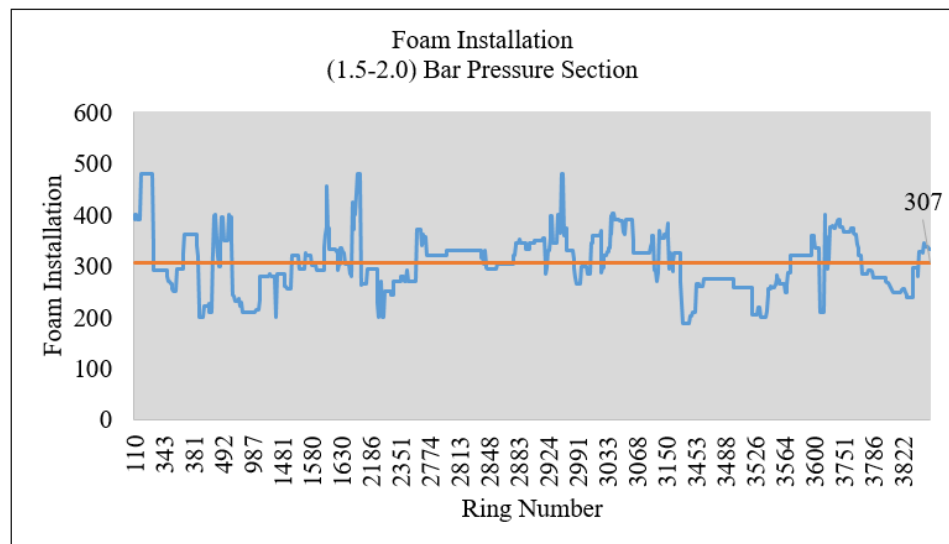


Figure 6.39. Foam Installation along the (1.5-2.0) Bar Pressure Section.

6.3.5. Effects of Observed Parameters Under (2.0-3.0) Bar Earth Pressure

As it is seen in Table 6.8, due to absence of low plasticity clay in the examined range, all the performance parameters showed as zero. As high plasticity clay and medium-grained sand soils are considered, the results show that between 2.0 Bar and 3.0 Bar earth pressure section, the mean cutterhead torque and thrust force values are higher, the specific energy and instantaneous cutting rate values are lower are for medium-grained sands.

It is observed that there is directly proportional relationship with mean earth pressure and thrust force. The mean thrust force value increases with an increasing earth pressure for medium-grained sand.

The field-specific energy value for high plasticity clay is greater than values obtained during excavation of the medium-grained sands.

The mean instantaneous cutting rate values for the soils high plasticity clay and medium-grained sand are $159 \text{ m}^3/\text{h}$, $157 \text{ m}^3/\text{h}$ respectively. Although the results were almost the same, the highest mean instantaneous cutting rate was achieved during excavation of the high plasticity clay soil at $159 \text{ m}^3/\text{h}$.

As seen in Figure 6.40, foam installation values ranged between 209 and 430. Between 2.0 Bar and 3.0 Bar earth pressure section, the mean foam installation value is $316 \text{ l}/\text{min}$.

Table 6.8. Variations in EPB TBM operational parameters during excavation of (2.0-3.0) bar earth pressure section.

Mean Operational Parameters	High Plasticity Clay	Medium-grained sand	Low Plasticity Clay
Torque (Mnm)	4.54	4.77	0.00
Specific Energy (MJ/m ³)	27.4	25.3	0.00
Earth Pressure (Bar)	2.18	2.30	0.00
Thrust Force (kN)	33,500	38,400	0.00
ICR (m ³ /h)	159	157	0.00

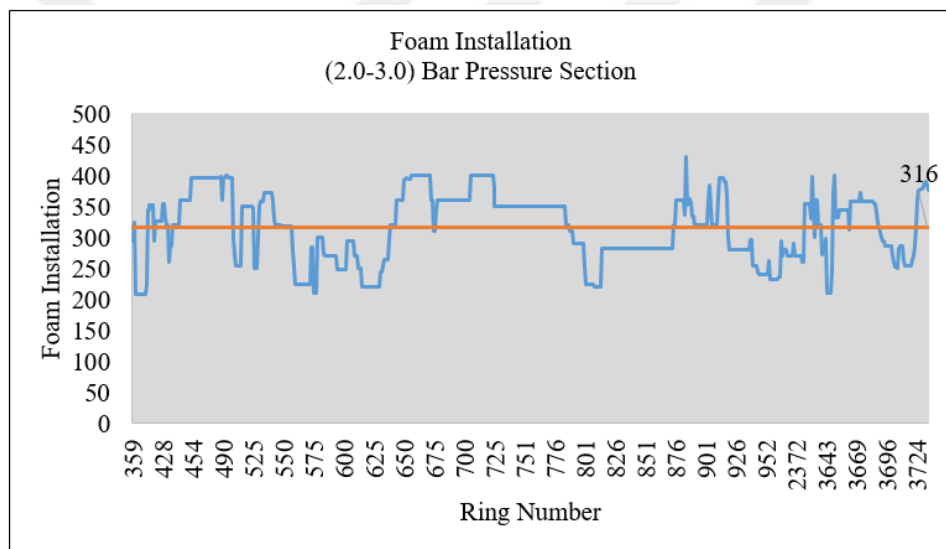


Figure 6.40. Foam Installation along the (2.0-3.0) Bar Pressure Section.

6.4. Assessment of TBM Advance Rates and Downtime Analysis

6.4.1. Achieved Advance Rates

As seen in Figure 6.41, the best advance rate (37.5 m/day) 73.1 mm/min was achieved during the excavation of low plasticity clay soil with 32,900 kN thrust force and 4.32 MNm cutterhead torque values. The lowest advance rate 6.7 mm/min was observed during the excavation of high plasticity clay, thrust force and cutterhead torque values were 7,860 kN and 1.17 MNm respectively.

A total of 3,996 rings were installed within 349 working days with the EPB TBM excavation throughout the line. Accordingly, the average daily advance rate was completed at 11.5 rings/day.

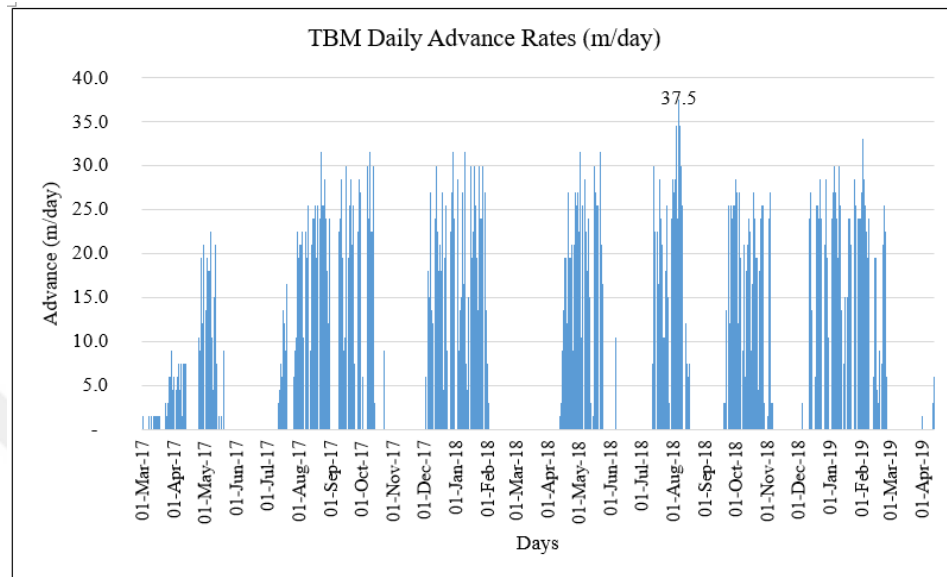


Figure 6.41. Daily Advance Rate of EPB TBM.

When the advance speed values on the entire line are examined according to the three soil types, it is seen in Table 6.9 that the values for high plasticity clay, medium grained sand and low plasticity clay were; 38.6 mm/min, 39.9 mm/min and 41.2 mm/min respectively.

Table 6.9. Average Advance Speed Values Depending on Soil Types

Average	High Plasticity Clay	Medium-grained sand	Low Plasticity Clay
Speed (mm/min)	38.6	39.9	41.2

6.4.2. Assessment of TBM Performance Measures and Downtime-Breakdown Analysis

Net excavation speed, machine utilization rate, reasons and length of downtimes are emphasized during assessment of TBM performance measures. TBM is operated

as 2 shifts each continued for 12 hours. Assessment of TBM performance measures was performed for 3,996 rings in total in a way to cover the entire line. TBM excavation commenced with the excavation of the section between the launching shaft and Station No.: 14 on 01/03/2017 and completed with the excavation between Station No.: 8 and exit shaft on 12/03/2019.

Machine utilization rate between the launching shaft and Station No.: 14 was 18.5%, and average advance speed was 28.9 mm/min. In terms of time-based distribution, total amount of time that passed for downtimes and failures was 62%, and total excavation time was 22%, and ring assembly time was 16%. 72% of total downtimes and failure times are comprised of planned downtimes, and 28% of the same are comprised of unplanned downtimes. Average excavation time per ring is 98 minutes, and average assembly time is 70 minutes.

Machine utilization rate between Station No.: 14 and Station No.: 12 was 33.4%, and average advance speed was 35.5 mm/min. In terms of time-based distribution, total amount of time that passed for downtimes and failures was 52%, and total excavation time was 26%, and ring assembly time was 22%. 48% of total downtimes and failure times are comprised of planned downtimes, and 52% of the same are comprised of unplanned downtimes. Average excavation time per ring is 45 minutes, and average assembly time is 37 minutes.

Machine utilization rate between Station No.: 12 and Station No.: 11 was 31.7%, and average advance speed was 42.7 mm/min. In terms of time-based distribution, total amount of time that passed for downtimes and failures was 50%, and total excavation time was 28%, and ring assembly time was 22%. 43% of total downtimes and failure times are comprised of planned downtimes, and 57% of the same are comprised of unplanned downtimes. Average excavation time per ring is 36 minutes, and average assembly time is 29 minutes.

Machine utilization rate between Station No.: 11 and Station No.: 10 was 29.6%, and average advance speed was 37.8 mm/min. In terms of time-based distribution, total

amount of time that passed for downtimes and failures was 58%, and total excavation time was 23%, and ring assembly time was 19%. 32% of total downtimes and failure times are comprised of planned downtimes, and 68% of the same are comprised of unplanned downtimes. Average excavation time per ring is 41 minutes, and average assembly time is 33 minutes.

Machine utilization rate between Station No.: 10 and Station No.: 9 was 27.7%, and average advance speed was 43,1 mm/min. In terms of time-based distribution, total amount of time that passed for downtimes and failures was 46%, and total excavation time was 29%, and ring assembly time was 25%. 31% of total downtimes and failure times are comprised of planned downtimes, and 69% of the same are comprised of unplanned downtimes. Average excavation time per ring is 37 minutes, and average assembly time is 33 minutes.

Machine utilization rate between Station No.: 9 and Station No.: 8 was 25.9%, and average advance speed was 44.3 mm/min. In terms of time-based distribution, total amount of time that passed for downtimes and failures was 54%, and total excavation time was 23%, and ring assembly time was 23%. 34% of total downtimes and failure times are comprised of planned downtimes, and 66% of the same are comprised of unplanned downtimes. Average excavation time per ring is 34 minutes, and average assembly time is 33 minutes.

Machine utilization rate between Station No.: 8 and the Exit Shaft was 25.8%, and average advance speed was 40.7 mm/min. In terms of time-based distribution, total amount of time that passed for downtimes and failures was 64%, and total excavation time was 21%, and ring assembly time was 15%. 33% of total downtimes and failure times are comprised of planned downtimes, and 67% of the same are comprised of unplanned downtimes. Average excavation time per ring is 37 minutes, and average assembly time is 26 minutes.

Along the entire line the machine utilization rate was 27.7% and average advance speed was 39.5 mm/min. In terms of time-based distribution, total amount of

time that passed for downtimes and failures was 56%, and total excavation time was 24%, and ring assembly time was 20%. 44% of total downtimes and failure times are comprised of planned downtimes, and 56% of the same are comprised of unplanned downtimes. Average excavation time per ring is 43 minutes, and average assembly time is 34 minutes.

The analysis of planned downtimes and unplanned downtimes is showed in Table 6.10 and Table 6.11.

Table 6.10. Unplanned TBM downtimes.

Unplanned TBM Downtimes	
Control and Maintenance of Tail Brush	5.8%
Control and Maintenance of Cutter Head	14.9%
Tunnel Conveyor Belt	6.5%
TBM Logistics	8.6%
Cleaning	5.7%
Muck Pit	4.9%
Segment Logistics	0.5%
TBM General and Occupational Safety Controls	1.1%
Waiting Period for Water	0.8%
Station Outlet Preparations	26.9%
Route Measurement	3.3%
Events, each of which cause a downtime of less than one hour	0.2%
Grout Plant	3.4%
Tunnel Conveyor Belt	9.1%
Segment Crane	0.9%
Injection Transfer Pump	0.9%
Erector	0.8%
OG Cable Failure	1.2%
MSV	1.2%
Other TBM Failures	2.7%
Tower Crane	0.6%

Table 6.11. Planned TBM downtimes.

Planned TBM Downtimes	
Shift Breaks and Holidays	35.6%
Losses Due to Single Shift	10.3%
Belt and OG Cable Splice	20.1%
Excavation Preparations	26.9%
Booster Installation	6.6%
Obligator Standstill due to Route	0.4%

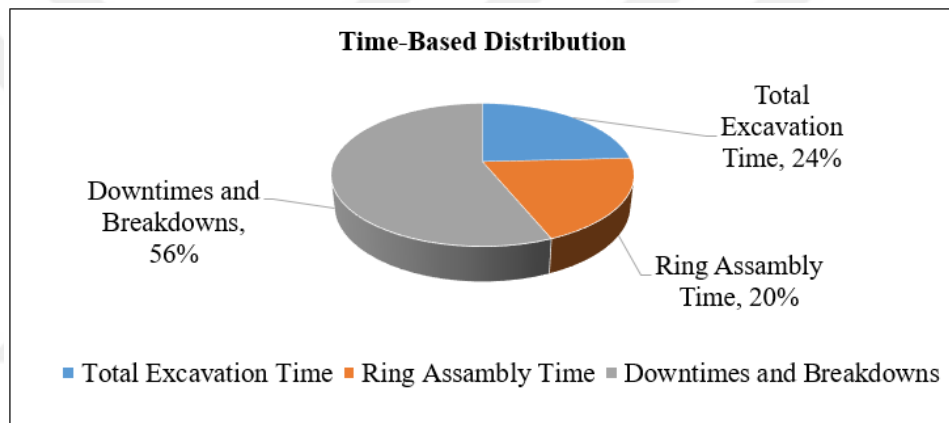


Figure 6.42. Distribution of Total Amount of TBM Working Time.

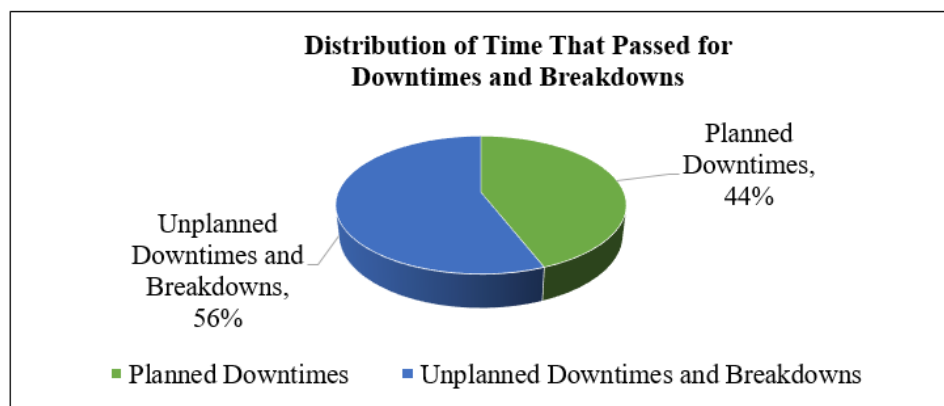


Figure 6.43. Distribution of Time for Downtimes and Breakdowns.

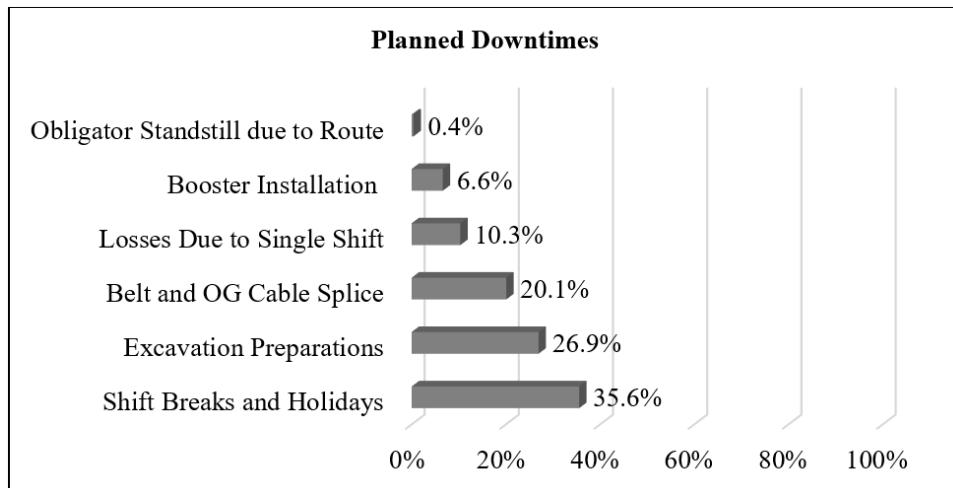


Figure 6.44. Distribution of Planned Downtimes.

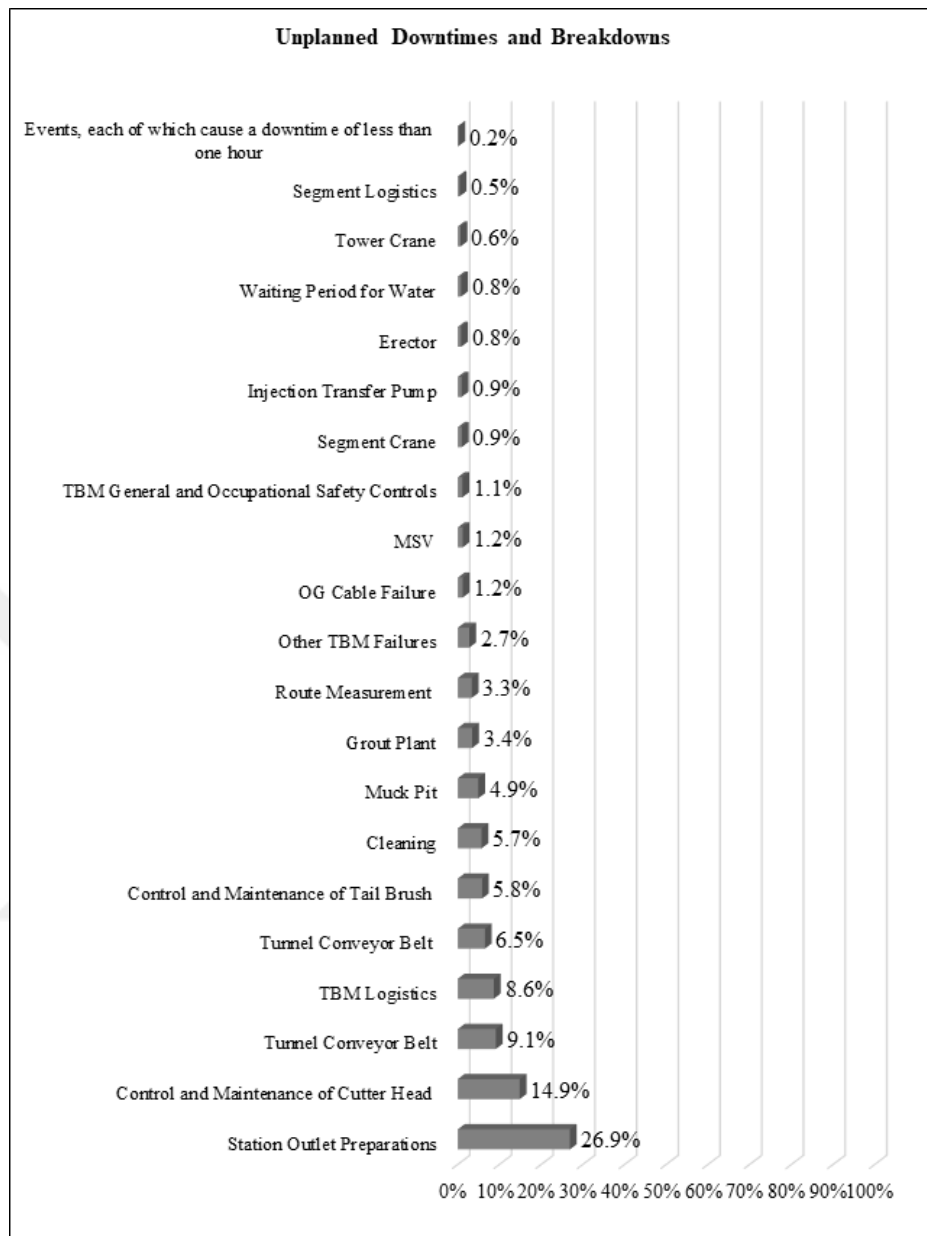


Figure 6.45. Distribution of Unplanned Downtimes.

7. CONCLUSIONS AND RECOMMENDATIONS

This study demonstrates the effect of soil type (cohesive or frictional) on the performance prediction of EPB TBM based on the data obtained during the construction of Sofia Metro Line-3 Project. This information may provide a potential tool for future initiatives to predict performance of TBM tunneling in soils.

Selection of TBM is very crucial in terms of success of the Project. The selection of a single shield earth pressure balance tunnel boring machine can be considered as a correct choice for the construction of Sofia Metro Line-3 Project. The main characteristic of the ground in Sofia is the presence of fine soils in combination with silty sand characterized by different grain size distribution. EPB TBMs are normally used for excavation of fine sand, silt and clay soils having low permeability, due to reason that they are not very effective in soils having fine materials less than 10% (Guglielmetti, (2008)).

With respect to geotechnical parameters, the studied tunnel section is divided into three zones as; high plasticity clay, medium-grained sand and low plasticity clay. The soil type effecting EPB TBM performance was investigated in terms of operational parameters, different correlations with two variable parameters and variations of operational parameters under specified earth pressures.

It was seen that, the highest cutterhead torque was needed during excavation of the high plasticity clay (7.43 MNm) whereas the lowest torque was needed for the excavation of medium-grained sand (1.02 MNm).

On the other hand, the highest mean thrust forces was measured during excavation of the medium-grained sand (47,300 kN), and the lowest thrust force was measured during excavation of the high plasticity clay (3,200 kN). The highest mean field specific energy value was measured during excavation of the high plasticity clay (124.0 MJ/m³), while the lowest was during excavation of the medium-grained sand (5.53 MJ/m³).

The highest mean instantaneous cutting rate was measured during excavation of the low plasticity clay (304.0 m³/h), while the lowest was during excavation of the high-plasticity clay (27.8 m³/h) in parallel to the advance speed rates. A summary of the main operational values along the tunnel is given in Table 7.1 filtered for the main soil types encountered along the route, namely High Plasticity Clay, Low Plasticity Clay and Medium Grained Sand.

Table 7.1. Main Operational Values Along the Tunnel Alignment.

Parameter	High Plasticity Clay	Low Plasticity Clay	Medium-grained sand
Mean Torque (MNm)	3.69	2.95	4.31
Mean Speed (mm/min)	38.6	41.2	39.9
Mean Power (kW)	1,185	1,080	1,191
Mean Specific Energy (MJ/m ³)	27.6	23.3	26.1
Mean Earth Pressure (Bar)	1.48	1.34	1.79
Mean Thrust Force (kN)	25,300	24,500	30,900
Mean ICR (m ³ /h)	160	171	166
Mean Foam Installation (l/min)	305	301	299

According to correlations between variable operational parameters, it is seen that there was a moderately proportional relationship between the thrust force and the cutterhead torque values for every soil type. Although thrust and torque have comparable curve forms, the thrust force is not an influencing factor of cutterhead torque, and both are determined by numerous excavation parameters.

The results indicated that the cutterhead torque increases with an increasing consistency index and instantaneous cutting rate decreases with an increasing plastic

limit.

It has been detected that cohesion has a pivotal effect on TBM performance. Highly cohesive clays show high liquid limits and high plasticity indexes. Therefore, owing to the swelling impact of clay particles, these kinds of soils tend to become very sticky on contact with water (Feng, 2004). Considering this, the mean foam installation for high plasticity clay, low plasticity clay and medium-grained sand are 305 l/min, 301 l/min and 299 l/min respectively. Since swelling increases with increasing plasticity, cohesive soils' foam installation rates are greater than frictional soil. According to the performance parameters under different earth pressures, the mean foam installation increases with an increasing pressure. For the specified pressure ranges (0.0-0.5) bar, (0.5-1.0) bar, (1.0-1.5) bar, (1.5-2.0) bar and (2.0-3.0) bar, foam installation values are 277 l/min, 262 l/min, 305 l/min, 307 l/min and 316 l/min respectively. In order to improve the excavation efficiency of fine-grained soils, the soil should be conditioned by using soil conditioning methods to have a less viscose form. Furthermore, it is noted during the excavation of clayey soil that the use of soil conditioning considerably reduced the thrust force and cutterhead torque. It was concluded that, not only different soil types had an effect on the performance, but also the operation parameters changed under different pressures. It is observed that the face pressures should be considered when estimating the EPB TBM excavation performance parameters. Earth pressure plays a decisive role in determining the cutterhead torque. (Wang *et al.* 2012) According to results, a considerable linear relation exist between applied earth pressure and cutterhead torque values.

Moreover, as indicated in Table 7.2, the downtime and breakdown times are greater than the sum of the excavation time and ring assembly time. Therefore, the downtime and breakdown effects the total duration significantly.

Table 7.2. Machine Utilization.

Machine Utilization	Duration (hour)
Excavation time	2835
Ring assembly time	2289
Downtimes and breakdowns	6588
Total	11713

Time spent during control/maintenance of cutterhead and station outlet preparations constitutes half of the unplanned downtimes and breakdowns.

REFERENCES

- “American Society for Testing and Materials”, *Classification of Soils for Engineering Purposes: Annual Book of ASTM Standards*, pp. 2487-83 1985.
- Avunduk E., H. Copur H., “Empirical Modeling for Predicting Excavation Performance of EPB TBM Based On Soil Properties Tunn”, *Space Technol*, Vol. 71, pp. 340-353, 2018.
- Avunduk E., H. Copur, *Effect of Clogging on EPB TBM Performance: A Case Study in Akfirat Wastewater Tunnel*, Turkey, 2019.
- Ball, R.P.A., D.J. Young, J. Isaacson, J. Champa, C. Gause, “Research in Soil Conditioning for EPB Tunnelling Through Difficult Soils”, *Proceeding*, pp. 320-333, 2009.
- Bardet, J.P., *Experimental Soil Mechanics*, Prentice Hall Increment, 1997.
- Barla G. and S. Pelizza, *TBM Tunneling In Difficult Ground Conditions*, Procedure GeoEng2000, Melbourne, 2000.
- Bilgin, N., H. Copur, C. Balci, *Mechanical Excavation in Mining and Civil Industries*, CRC Press, Taylor and Francis Group, London, 2014.
- Maidl, U., *Erweiterung der Einsatzbereiche der Erddruckschilde Durch odenkonditionierung met Schaum*, Ph.D Thesis, Ruhr Unvisersitat Bochum, Germany, 1995.
- Das, B.M., *Principles of Geotechnical Engineering*, CL Engineering, 2009
- “DAUB (German Committee for Underground Construction)”, Recommendations for Face Support Pressure Calculations for Shield Tunneling in Soft Ground (October 2016).

- EFNARC, “Specification and guidelines for the use of specialist products for mechanized tunneling (TBM) in soft ground and hard rock”, Recommendation of European Federation of Producers and Contractors of Specialist Products for Structures, 2005.
- Spagnoli, G.M., R. Feinendegen, M.V. Ernst, *Manipulations of The Sticky Clays Regarding EPB Tunnel Driving*, In: The 7th Geotechnical Aspects of Underground Construction in Soft Ground, 2011.
- Feng, Q., “Soil Conditioning for Modern EPBM Drives”, *Tunn Tunn Int*, vol. 36, pp. 18-20, 2004.
- Fernandez, E., *The Madrid Renewal Inner Ring Calle 30 with the Largest EPB Machines*, Fernandez, E., Planning and Results, Rapid Excavation and Tunneling Conference Proceedings, 2007.
- Fernandez-Steeger, T. M., C. Post, M. Feinendegen, K. Bappler, O. Zwick, R. Azzam, M. Ziegler, H. Staandjek, A. Peschard, “ane Pralle, Interfacial processes between mineral and tool surfaces-causes”, *problems and solution in mechanical tunnel driving. Geotechnologien Science Report*, Vol. 12, pp. 46-57, 2008.
- Guglielmetti, V., “Mechanized Tunnelling in urban areas: Design Methodology and Construction Control”, *Taylor and Francis*, 2008.
- Herrenknecht, M., Maidl, U., Applying foam for an EPB shield drive in Valencia. Tunnel 5 Vol. 95, pp. 10-19, 2015.
- Hollmann, F.S., Thewes, M., “Evaluation of the Tendency of Clogging and Separation of Fines on Shield Drives”, *Geomech Tunn*, Vol. 5, No. 5, pp. 574-580, 2012.
- Hollmann, F.S., M. Thewes, “Assessment Method for Clay Clogging And Disintegration of Fines In Mechanised Tunnelling”, *Tunner Undergr Space Technol*, Vol. 37, pp. 96-106, 2013.

- Japan Society of Civil Engineers (JSCE)*, Standard Specifications For Tunneling - Shield Tunnels, 2007.
- Maidl, B., L. Schmid, W. Ritz, and M. Herrenknecht, *Hardrock tunnel Boring Machines*, Ernst and Sohn, 2008.
- Marinos, P.G., M. Novack, M. Benissi, M. Panteliadou, D. Papouli, G. Stoumpos, V. Marinos, K. Korkaris, "Ground information and selection of TBM for the Thessaloniki Metro", *Greece Environmental and Engineering Geoscience XIV*, Vol. 1, pp. 17-30, 2008.
- O'Carrol, B.J., *A Guide to Planning, Constructing and Supervising Earth Pressure Balance TBM Tunneling*, Professional Associate Parsons Brinckerhof, April, 2005
- Rostami, J., L. Özdemir, and M.D. Neil, *Performance Prediction: A Key Issue in Mechanical Hard Rock Mining*, Mining Engineering, 1994.
- Schlick, G., *Adhasion im Boden-Werkzeug-System. Forschungsbericht des Instituts für Maschinenwesen im Baubetrieb*, Universität Karlsruhe, 1989.
- Spagnoli G., M. Feinendegen, R. Ernst, M. Weh, *Manipulations of the Sticky Clays Regarding EPB Tunnel Driving Geotechnical Aspects of Underground Construction in Soft Ground*, Natural Resource Solutions, 2011.
- Thewes, M., *Adhasion von Tonboden beim Tunnelvortrieb mit Flüssigkeitsschilden*, Bericht Nr. 21 Bergische Universität Gesamthochschule Wuppertal, 1999.
- Thewes, M., C. Budach, A. Bezuijen, "Foam Conditioning in EPB Tunnelling. In: The 7th Geotechnical Aspects of Underground" *Construction in Soft Ground*, pp. 9, 2010.
- Thewes, M., W. Burger, "Clogging Risks for TBM Drives in Clay", *Tunnel Introduction*, Vol. 6, pp. 28-31, 2004.

- Thewes M., “TBM Tunneling Challenges - Redefining the State of the Art”, *Key-Note Lecture ITA - AITES WTC 2007 Prague*, Tunel, pp. 13-27, 2007.
- Wang, L.T., G.F. Gong, H. Shi, “A new calculation model of cutterhead torque and investigation of its influencing factor”, *Science China Technical Science*, Vol. 55, pp. 1581- 588, 2012.
- Zumsteg, R., A.M. Puzrin, “Stickiness and Adhesion of Conditioned Clay Pastes”, *Tunnell Under Space Technol*, Vol. 31, pp. 86-96, 2012.
- Zumsteg, R., M. Plotze, A.M. Puzrin, “Reduction of the Clogging Potential of Clays: New Chemical Applications and Novel Quantification Approaches”, *Geotechnique*, Vol. 63, No. 4, pp. 276-286, 2013.